Adaptive Discontinuous Galerkin Methods for Interface Problems

Thesis submitted for the degree of

Doctor of Philosophy

at the

University of Leicester

by

Younis Sabawi

Department of Mathematics

University of Leicester

November 2016

Abstract

The aim of this thesis is to derive adaptive methods for discontinuous Galerkin approximations for both elliptic and parabolic interface problems. The derivation of adaptive method, is usually based on a posteriori error estimates. To this end, we present a residual-type a posteriori error estimator for interior penalty discontinuous Galerkin (dG) methods for an elliptic interface problem involving possibly curved interfaces, with flux-balancing interface conditions, e.g., modelling mass transfer of solutes through semi-permeable membranes. The method allows for extremely general curved element shapes employed to resolve the interface geometry exactly. Respective upper and lower bounds of the error in the respective dG-energy norm with respect to the estimator are proven. The a posteriori error bounds are subsequently used to prove a basic a priori convergence result. Moreover, a contraction property for a standard adaptive algorithm utilising these a posteriori bounds, with a bulk refinement criterion is also shown, thereby proving that the a posteriori bounds can lead to a convergent adaptive algorithm subject to some mesh restrictions. This work is also concerned with the derivation of a new $L_\infty(L_2)$-norm a posteriori error bound for the fully discrete adaptive approximation for non-linear interface parabolic problems. More specifically, the time discretization uses the backward Euler Galerkin method and the space discretization uses the interior penalty discontinuous Galerkin finite element method. The key idea in our analysis is to adapt the elliptic reconstruction technique, introduced by Makridakis and Nochetto [48], enabling us to use the a posteriori error estimators derived for elliptic interface models and to obtain optimal order in both $L_\infty(L_2)$ and $L_\infty(L_2) + L_2(H^1)$ norms. The effectiveness of all the error estimators and the proposed algorithms is confirmed through a series of numerical experiments.

Acknowledgements

First of all, I would like to thank Allah for the seeing me and keeping me strong through this PhD study. This thesis would not have been completed without him. It is a pleasure to acknowledge the help and support which I have received from many people during almost four years of student life at the University of Leicester. My deepest gratitude is to my supervisors, Professor Emmanuil Georgoulis and Dr. Andrea Cangiani, for their support, time and patient guidance during my study. I must thank them for all of their help, encouragement and suggestions. Furthermore, they have given me intersecting ideas for my research and have also proven valuable in my life. This thesis could not have been completed without drawing on their talents, knowledge and contribution.

I would also like to thank all of the staff in College House for their help and for making so many things easier. I am really thankful for all my friends at the Michael Atiyah Building: Ali, Mohammad Ali, Husan, Jehan, Anwar, Samira, Mohammad, Omer and Hoger. Special thanks go to Oliver, Sam, Peter and Stephen their support, help and time. It gives me the most pleasure to thank my family; in particular my parents and my parents-in-law sisters and brothers.

I would also like to express my great appreciation for the crucial role of my wife and daughters for their love, faith and support. Without their help, this thesis would not have been possible. I would like to acknowledge my thanks for to the Government of Kurdistan, Iraq, for giving me the opportunity to study in the UK to get a PhD degree. Last but not least, I could not have completed this without my friends in Iraq. A special thanks goes to assistant Professor Mohammad Shami Hasso for his help and support.

Contents

List of Figures

List of Tables

Chapter 1

Introduction

Interface conditions are used in the modelling of various engineering applications stemming from physical, chemical, and biological phenomena, in particular, ones involving multiple distinct materials with different diffusion, density, permeability or conductivity properties. Such interface conditions are typically used to close systems of partial differential equations (PDEs) posed on multi-compartment distinct material regions. As a result, these interface problems often produce solutions having jump discontinuities of the state variable and/or of some of its derivatives across the interface. In other words, their solutions may have higher regularity in individual material regions than in the entire physical domain. The analytical regularity theory for interface problems is far less advanced than for respective standard (one-compartment) initial/boundary-value problems. Therefore, the reliable and efficient numerical approximation of such problems is desirable. Furthermore, such a development has the potential to be used to inform on the underlying local analytical regularity properties, too.

A class of interface problems, which is still relatively unexplored, are problems with flux-balancing interface conditions, resulting in discontinuities in the state variable itself. This class of interface conditions model, among other things, the mass transfer of solutes through semi-permeable membranes in a number of engineering applications and biological processes; see, e.g., [19, 20] for more details on the modelling. The design of practical high-order numerical methods for this class of problems poses a number of challenges, most important being the discontinuity of the solution across the interface, and the geometric approximation of the, possibly curved, interface itself.

In the context of finite element methods (FEMs), when the interface is a general manifold of co-dimension one, the geometry cannot be described exactly by the mesh, as even isoparametric elements can only exactly resolve interfaces with polynomial level-sets. A number of methods to address this shortcoming have been proposed over the years, such as the unfitted FEM [37], immersed interface methods [45, 46, 54], fictitious domain methods [10, 15, 16], composite FEM [55], cut-cell techniques [49, 57, 14, 36], etc.

Many of the aforementioned works also provide a priori error analysis of the proposed methods and/or goal-oriented error estimation techniques and the lack of availability of rigorous a posteriori bounds may appear somewhat surprising at first sight. Observing, however, that, upon interface approximation, the exact solution is defined on a different domain to its finite element approximation, the standard approach of proving a posteriori bounds, i.e., using PDE stability results linking the error with the residual, becomes cumbersome. Few a posteriori bounds for curved domains exist, focusing on the related (but simpler) problem of proving a posteriori bounds for elliptic problems posed on (single-compartment) curved domains [27, 4].

Moreover, the topic of a convergence analysis of adaptive algorithms for elliptic problems is now relatively well understood for both conforming and nonconforming methods, see, e.g., [52, 42, 25, 11, 39, 40, 53]; no results in the context of elliptic interface problems exist.

To address the challenge of general curved interface geometry, in this work we present a *fitted* interior-penalty discontinuous Galerkin (dG) method for an elliptic interface problem involving elements with extremely general curved faces. This fitted approach avoids some of the aforementioned challenges for crucially, proving a posteriori error bounds, at the expense of extending standard approximation, inverse, and conforming-nonconforming recovery estimates (in the spirit of the seminal work [41]) to elements with curved faces, which are also derived. The latter results may be of independent interest. The elliptic interface problem considered here is posed on a multi-compartment domain with specific flux-balancing interface conditions modelling mass transfer through semi-permeable membranes [17, 19, 20]. Such interface problems, yielding discontinuous solutions across the interface, can be easily implemented within an existing dG code simply by modifying the interior penalty dG numerical fluxes accordingly [35, 20, 21].

Moreover, the extremely general element shapes allowed in the proposed method are able to resolve very general interface geometries exactly, up to quadrature errors. The optimal approximation of the finite element spaces and good conditioning of the respective stiffness matrices are ensured by the use of *physical coordinate* basis functions, as opposed to standard mapped ones from a reference element; this idea was utilised in [9, 18], where efficient techniques for the assembly step are presented. Furthermore, an alternative construction using *parametric maps* of reference elements with *extremely general reference element shapes* is also proposed. The latter may prove to be useful in the context of high-order finite element spaces.

Of course, the "fitted" approach proposed below may appear cumbersome at first sight particularly in view of spatial discretisation in the context of evolutionary PDEs involving moving interfaces. This is, in fact, not necessarily the case as the developments presented below appear to be generalisable, at least in principle, to a cut-cell-type setting, whereby a mesh is not subordinate to the interface location a priori. This is not done here, however, in the interest of simplicity of the presentation of the key ideas.

The choice the interior penalty dG method for interface problems is motivated by the following factors. First, due to the lack of any conformity requirements, it is possible to choose the local element bases freely, which is important when employing very general element shapes to ensure optimal approximation rates and well-conditioned stiffness matrices; this idea was utilised in [18], where efficient techniques for the assembly step where presented. Second, for interface problems yielding discontinuous solutions across the interface, such as the one considered below, the interface conditions can be easily implemented within an existing dG code simply by modifying the interior penalty dG numerical fluxes accordingly [35, 20, 21]

This thesis is also concerned with the development and analysis of numerical methods for a class of parabolic interface problems, modelling the mass transfer of solutes through semi-permeable membranes, closed by nonlinear interface conditions. We tackle the challenge of deriving a posteriori error bound for such problems by employing a nonstandard elliptic reconstruction. This is inspired by a classical elliptic projection construction of Douglas and Dupont for the treatment of nonlinear boundary conditions in the a priori error analysis setting [29]. A key aspect of our analysis is the use of elliptic reconstruction technique, introduced by

Makridakis and Nochetto [48, 44], and extended to dG methods in [33]. Here, we investigate adaptive algorithms for both elliptic and parabolic interface problems with a focus on addressing some challenges to derive estimators error for nonlinearity and the geometric approximation of the interface itself. To do this, different problems are presented below along with their respective challenges.

In Chapter 2, the model problems are introduced. The discontinuous Galerkin method, along with the admissible curve element shape, are given. Semi and fully discrete approximation scheme for nonlinear interface problem are shown. Some necessary lemmas and theorems which will be used throughout this work are also given. In Chapter 3, we present some necessary approximation, trace, inverse and continuity recovery. These are a key part of the error analysis which we use to derive a posterior error bounds in Chapter 4. Further, in Chapter 3, the coercivity and contiounty are also proven. Chapter 4 is devoted to the proof of reliable and efficient a posteriori error bounds in terms of the energy norm for the interior penalty discontinuous Galerkin method. An important attribute of this method is the use of *physical coordinate* basis functions, as opposed to standard mapped ones from a reference element. We stress that the developments presented in Chapter 4 also apply to the special case of elliptic problems with non-essential boundary conditions on a *single* non-polygonal/non-polyhedral domain. Using the derived a posteriori bounds, we also give a basic priori convergence result for the proposed method using the efficiency under minimal regularity assumptions, in the spirit of the seminal work [34]. We do so since of regularity theory for elliptic interface problems is far from being well developed. The theory presented is complemented by a series of numerical experiments.

The aim of Chapter 5 is to study the convergence analysis for the presented adaptive algorithm. We prove a basic error contraction result of an adaptive discontinuous Galerkin method for an elliptic interface problem. The adaptive algorithm is based on the residual-type a posteriori error estimator, with a bulk refinement criterion. The results here are inspired and influenced by [42, 11] in the context of elliptic problems. The derivation of the adaptive schemes to arrive to a contraction result poses a number of challenges. First, the treatment of the interface conditions. Second, the refinement of curved elements touching the interface boundary so that their angles remain uniformly bounded. The latter will introduce some mild mesh assumptions.

Chapter 6 deals with nonlinear parabolic interface problems. In particular, we

derive new posteriori error estimator for backward Euler time-stepping method combined with the spatial discontinuous Galerkin scheme from Chapter 4. The main challenge in the construction of such an error estimator is having to deal with a nonlinear error equation due to the interface modelling. This challenge can be handled with an elliptic reconstruction inspired by a nonstandard elliptic projection of Douglas and Dupont [29] for the treatment of nonlinear boundary conditions.

To the best of our knowledge, an a posteriori error estimator for an interface problem with linear conditions at the interface was only proven in [50] for *straight* interfaces. The main contribution of Chapter 6 is to provide an a posteriori error estimator for the backward Euler in time and *fitted* interior-penalty discontinuous Galerkin method in space applied to nonlinear interfaces problem. The presented a posteriori error analysis in terms of $L_\infty(L_2) + L_2(H^1)$ and $L_\infty(L_2)$-norms appear to be of optimal order. The derivation of the energy-norm bound is inspired and influenced by [22, 23]. For linear parabolic problems, there are many error estimators available in the literature [8, 26, 44, 47, 48, 6, 43]. Other posteriori error estimates for linear and nonlinear parabolic problems in the literature include [33, 59, 51, 2, 24, 58, 30, 56]. Numerical experiments are presented through an implementation based on the `deal.II` finite element library [7].

Finally, in Chapter 7 we summarise the results of this work and discuss ways in which this work could be extended.

Chapter 2

Interface problems and Discontinuous Galerkin methods

2.1 Introduction

The objective of this chapter is to introduce the elliptic and parabolic interface model problems, and the *fitted* interior-penalty discontinuous Galerkin (dG) scheme for their discretisation.

The dG method employs elements with, possibly, curved faces, able to resolve the interface geometry exactly. The method is closely related to the spatial discretization for parabolic interface problems introduced in [20], with the latter assuming exact interface resolution using standard (non-curved) simplicial or box-type elements only.

A key attribute of the proposed method is the use of physical frame basis functions, i.e., the elemental bases consist of polynomials on the elements themselves, rather than mapped polynomials through a mapping from a reference element. Crucially, the lack of conformity of the dG method allows for such physical frame polynomial basis functions to be used on very general element shapes. The implementation challenges arising from this non-standard choice will be discussed below.

Before introducing the model problems and their dG discretisation, some useful general definitions and basic inequalities that shall be used throughout this work are also given here.

2.1.1 Sobolev spaces

Let $\omega \subset \mathbb{R}^d, \quad d = 1, 2, 3$ be a bounded Lipschitz domain with boundary $\partial\omega$. The norm of $L_2(\omega) \equiv H^0(\omega)$, $\omega \subset \Omega$, will be denoted by $\|\cdot\|_\omega$, and is induced by the standard $L_2(\omega)$-inner product, denoted by $\langle\cdot,\cdot\rangle_\omega$; when $\omega = \Omega$, we shall use the abbreviations $\|\cdot\| \equiv \|\cdot\|_\Omega$ and $\langle\cdot,\cdot\rangle \equiv \langle\cdot,\cdot\rangle_\Omega$. For $1 \leq p \leq +\infty$, we define the L_p norms by

$$\|v\|_{L_p(\omega)} = \left(\int_\omega |v|^p \mathrm{dx}\right)^{1/p} \qquad \text{for some} \quad 1 \leq p \leq +\infty,$$
$$\|v\|_{L_p(\omega)} := ess\sup |v(x)| \qquad \text{for} \quad p = +\infty.$$

Note that $L_2(\omega)$ is a Hilbert space with an inner product given by $\langle\cdot,\cdot\rangle_\omega$. For $\alpha = (\alpha_1, \alpha_2, \ldots, \alpha_d)$ multi-index, the distributional derivative $D^\alpha v$ is denoted by

$$D^\alpha =: \frac{\partial^{|\alpha|}}{\partial x_1^{\alpha_1} \partial x_2^{\alpha_2} ... \partial x_d^{\alpha_d}}.$$

The Hilbertian Sobolev space of order $s \in \mathbb{N}$ is defined by

$$H^s(\omega) := \{v \in L_2(\omega) : D^\alpha v \in L_2(\omega),\ 0 \leq |\alpha| \leq s\},$$

with associated norm

$$\|v\|_{H^s(\omega)} := \left(\sum_{0 \leq |\alpha| \leq s} \|D^\alpha v\|_\omega^2\right)^{1/2},$$

and seminorm

$$|v|_{H^s(\omega)} := \left(\sum_{|\alpha| = s} \|D^\alpha v\|_\omega^2\right)^{1/2}.$$

It is also possible to define Sobolev spaces of fractional order based on function space interpolation, we refer to [1] for details. Whenever boundary values are used in this thesis, they are to be understood in the sense of traces. The space H_G^1 is defined as

$$H_G^1 := \left\{u \in H^1(\omega) : u|_{\Gamma_G} = 0\right\},$$

where $\Gamma_G \subset \partial\omega$. If $\Gamma_G = \partial\omega$, then the space will be denoted by $H_0^1(\omega)$. With $C^k(\omega)$ we denote the space of all functions u for which $D^\alpha u$ is continuous for all muliti-indices α with norm $|\alpha| \leq k$. Further, we Let $L_p(0, T; X)$ be the Bohner

space (where X is real Banach space equipped with norm $\|.\|_X$ which consist of all measurable functions $v : [0, T] \to X$) defined by

$$\begin{aligned} \|v\|_{L_p(0,T;X)} &= \left(\int_0^T \|v(t)\|_X^p \mathrm{d}t \right)^{1/p} < +\infty, \quad 1 \leq p < \infty, \\ \|v\|_{L_\infty(0,T;X)} &= ess\sup \|v(t)\|_X < +\infty, \quad p = +\infty. \end{aligned} \tag{2.1}$$

2.1.2 Useful inequalities

The purpose of this section is to introduce general results which will be utilized throughout the rest of this work.

Theorem 2.1 (Young's inequality)**.** *Let $a, b \in \mathbb{R}$, then for any $\varepsilon > 0$, we have*

$$ab \leq \frac{a^2\varepsilon}{2} + \frac{b^2}{2\varepsilon}.$$

Theorem 2.2 (Poincare–Friedrichs inequality)**.** *Let ω be a connected open polygonal/polyhedral domain in $\mathbb{R}^d$, $d = 2, 3$. Then, for all $u \in H_0^1(\omega)$, we have*

$$\|u\|_\omega^2 \leq C\|\nabla u\|_\omega^2.$$

Proof. See [12]. □

Theorem 2.3 (Trace inequality)**.** *Given $z \in H^1(\omega)$, for and open Lipschitz domain $\omega \subset \mathbb{R}^d$, $d = 2, 3$, the following bound holds*

$$\|z\|_\psi^2 \leq C_{trace}\big(\delta^{-1}\|z\|_\omega^2 + \delta\|\nabla z\|_\omega^2\big), \tag{2.2}$$

for all δ positive and for some positive constant C_{trace}, independent of z, where $\psi \subset \partial\omega$ of positive $(d-1)$-dimensional Hausdorff measure.

Proof. See [1] for a proof. □

Lemma 2.4 (Gronwall's inequilty)**.** *If a and b are non-negative constants and*

$$0 \leq u(t) \leq a + b\int_0^t u(s)ds, \quad \forall 0 \leq t < T, \tag{2.3}$$

then, we have

$$u(t) \leq a\mathrm{e}^{bt}. \tag{2.4}$$

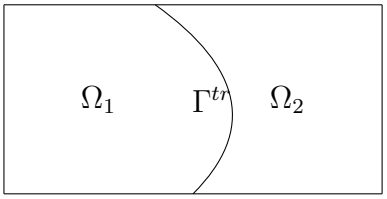

FIGURE 2.1: The Ω is subdivided into two sub-domains Ω_1 and Ω_2 by the interface $\Gamma^{tr} = \Omega \backslash (\Omega_1 \cup \Omega_2)$.

Proof. See [38]. □

2.2 A fitted dG method for interface problems

We shall consider two model problems: a linear interface problem for the Poisson equation and a nonlinear interface parabolic problem. The former will be used to introduce the basic idea of the *fitted* approach for the discretisation of the space variables. This framework is then applied to the latter problem, starting with the semi-discrete approximation using the fitted dG in space approximation and finishing with the fully discrete backward Euler in time fitted dG in space approximation.

2.2.1 Elliptic model problem

Let Ω be a bounded open polygonal/polyhedral domain with Lipschitz boundary $\partial\Omega$ in $\mathbb{R}^d$, $d = 2, 3$. Ω is split into two sub-domains Ω_1 and Ω_2, such that $\Omega = \Omega_1 \cup \Omega_2 \cup \Gamma^{tr}$, with $\Gamma^{tr} := (\partial\Omega_1 \cap \partial\Omega_2) \backslash \partial\Omega$ being also Lipschitz continuous with bounded curvature; see Figure 2.1 for an illustration.

We consider the model problem:

$$\begin{aligned} -\Delta u &= f, && \text{in } \Omega_1 \cup \Omega_2, \\ u &= 0, && \text{on } \partial\Omega, \\ \mathbf{n}^1 \cdot \nabla u_1 &= C_{tr}(u_2 - u_1)|_{\Omega_1} && \text{on } \bar{\Omega}_1 \cap \Gamma^{tr}, \\ \mathbf{n}^2 \cdot \nabla u_2 &= C_{tr}(u_1 - u_2)|_{\Omega_2} && \text{on } \bar{\Omega}_2 \cap \Gamma^{tr}, \end{aligned} \tag{2.5}$$

with $u_i = u|_{\bar{\Omega}_i}$, $i = 1, 2$, $C_{tr} > 0$ a given interface transmission (e.g., *permeability*) constant and $\mathbf{n}^i$, $i = 1, 2$ denoting the respective outward unit normal vectors.

This is a simplified model for mass transfer of a solute through a semi-permeable membrane through osmosis, but it is rich enough in highlighting the aforementioned challenges posed for the numerical analysis of this class of problems. Also, we set $\mathcal{H}^1 := H^1(\Omega_1 \cup \Omega_2)$, and

$$\mathcal{H}_0^1 := \{v \in \mathcal{H}^1 : v = 0 \text{ on } \partial\Omega\}.$$

Upon integrating by parts on each sub-domain and applying the interface condition, we arrive to (2.5) in weak form, which reads: find $u \in \mathcal{H}_0^1$ such that

$$D(u, v) := \int_{\Omega_1 \cup \Omega_2} \nabla u \cdot \nabla v dx + \int_{\Gamma^{tr}} C_{tr} [\![u]\!] \cdot [\![v]\!] ds = \int_{\Omega} f v dx, \tag{2.6}$$

for all $v \in \mathcal{H}_0^1$, where $[\![u]\!] := v_1|_K \mathbf{n}^1 + v_2|_K \mathbf{n}^2$ is the jump across the interface.

We shall now introduce the fitted interior penalty discontinuous Galerkin (dG) finite element method for the discretization of the elliptic interface problem (2.6).

2.2.2 The Mesh

Let $\mathcal{T} = \{K\}$ be a locally quasi-uniform subdivision of Ω, possibly containing regular hanging nodes, with K a generic, possibly curved, simplicial, box-type, or prismatic element of diameter h_K. More specifically, we shall assume that the mesh consists of triangular or quadrilateral elements when $d = 2$, and of tetrahedral or prismatic elements with triangular bases when $d = 3$. We stress that the prismatic elements considered here are *not* assumed to have parallel bases, in general.The mesh skeleton $\Gamma := \cup_{K \in \mathcal{T}} \partial K$ is subdivided into three disjoint subsets $\Gamma = \partial\Omega \cup \Gamma^{int} \cup \Gamma^{tr}$, where $\Gamma^{int} := \Gamma \backslash (\partial\Omega \cup \Gamma^{tr})$.

For simplicity of the presentation, we shall assume that elements with curved faces will be employed *only* to resolve the interface geometry, i.e., only elements $K \in \mathcal{T}$ such that $\partial K \cap \Gamma^{tr} \neq \emptyset$ are curved, see Figure 2.2 for an illustration. This is also realistic from a practical perspective, as the global use of curved elements is more computationally demanding (with no immediate advantage) during assembly. Nevertheless, the theory below can be easily modified to cover the case of curved elements away from the interface, if so desired.

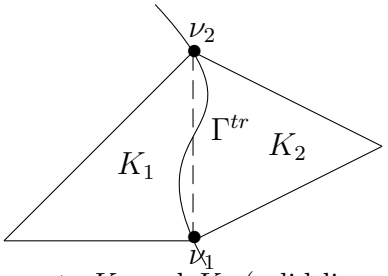

FIGURE 2.2: Curved elements K_1 and K_2 (solid lines/curves) from either side of the interface Γ^{tr}, resolving the geometry of Γ^{tr}.

2.2.3 Finite element space

We define the discontinuous finite element space S_h^p, subortinate to the mesh $\mathcal{T} = \{K\}$, by

$$S_h^p \equiv S_h^p(\mathcal{T}) = \{v \in L^2(\Omega) : v|_K \in \mathcal{P}_p(K), K \in \mathcal{T}\}, \tag{2.7}$$

where $\mathcal{P}_p(K)$ denotes the space of polynomials of *total* degree p on an element K.

For each element face $E \subset \Gamma^{int} \cup \Gamma^{tr}$, there are two elements K_1 and K_2 such that $E \subset \partial K_1 \cap \partial K_2$. The outward unit normal vectors on E of ∂K_1 and ∂K_2 are denoted by $\mathbf{n}_{K_1}$ and $\mathbf{n}_{K_2}$, respectively. For a function $v : \Omega \to \mathbb{R}$ that may be discontinuous across Γ, we set $v_i = v|_{K_i}$, and we define the jump $[\![v]\!]$ and the average $\{v\}$ of v across E by

$$[\![v]\!] = v|_{K_1}\mathbf{n}_{K_1} + v|_{K_2}\mathbf{n}_{K_2}, \quad \{v\} = \frac{1}{2}\left(v|_{K_1} + v|_{K_2}\right). \tag{2.8}$$

Similarly, for a vector valued function $\mathbf{w}$, piecewise smooth on $\mathcal{T}$ with $\mathbf{w}_i = \mathbf{w}|_{K_i}$, we define

$$[\![\mathbf{w}]\!] = \mathbf{w}|_{K_1} \cdot \mathbf{n}_{K_1} + \mathbf{w}|_{K_2} \cdot \mathbf{n}_{K_2}, \quad \{\mathbf{w}\} = \frac{1}{2}\left(\mathbf{w}|_{K_1} + \mathbf{w}|_{K_2}\right).$$

When $E \subset \partial\Omega$, we set $\{v\} = v$, $[\![v]\!] = v\mathbf{n}$ and $[\![\mathbf{w}]\!] = \mathbf{w} \cdot \mathbf{n}$ with $\mathbf{n}$ denoting the outward unit normal to the boundary $\partial\Omega$.

We introduce the meshsize function $\mathbf{h} : \Omega \to \mathbb{R}$, where $\mathbf{h}|_K = h_K$, $K \in \mathcal{T}$ and $\mathbf{h} = \{\mathbf{h}\}$ on each $(d-1)$-dimensional open face $E \subset \Gamma$. We also define $h_{\max} := \max_{x\in\Omega} \mathbf{h}$ and $h_{\min} := \min_{x\in\Omega} \mathbf{h}$. Without loss of generality, we shall assume that $h_{\max}$ remains uniformly bounded throughout this work, thus, avoiding having estimation constants dependent on $\max\{1, h_{\max}\}$.

2.2.4 dG method for the elliptic problem

To arrive the interior penalty discontinuous Galerkin method, we multiply (2.5) by a test function $v \in S_h^p + \mathcal{H}_0^1$ and, integrate over each subdomain, we have.

$$-\int_\Omega (\Delta u)\, v \mathrm{dx} = \int_\Omega f v \mathrm{dx}. \tag{2.9}$$

Next, we decompose the integrals into element contributions and integrate by parts:

$$\sum_{K\in\mathcal{T}} \int_K \nabla u \cdot \nabla v \mathrm{dx} - \sum_{K\in\mathcal{T}} \langle \mathbf{n}\cdot\nabla u, v\rangle_{\partial K} = \sum_{K\in\mathcal{T}} \int_K f v \mathrm{dx}. \tag{2.10}$$

The next step is to split the face integrals:

$$\begin{aligned}\sum_{K\in\mathcal{T}} \langle \mathbf{n}\cdot\nabla u, v\rangle_{\partial K} = &\sum_{E\in\Gamma\setminus\Gamma^{tr}} \Big(\langle \mathbf{n}\cdot\nabla u, v\rangle_{\partial K_1 \bigcap E} + \langle \mathbf{n}\cdot\nabla u, v\rangle_{\partial K_2 \bigcap E}\Big) \\ &+ \sum_{E\in\Gamma^{tr}} \Big(\langle \mathbf{n}\cdot\nabla u, v\rangle_{\partial \Omega_1 \bigcap E} + \langle \mathbf{n}\cdot\nabla u, v\rangle_{\partial \Omega_2 \bigcap E}\Big),\end{aligned} \tag{2.11}$$

where $K_1, K_2 \in \mathcal{T}$, for $E \in \partial K_1 \cap \partial K_2$, $\mathbf{n}$ is the a corresponding unit normal on E (exterior to K_2). We can see that

$$\begin{aligned}\sum_{E\in\Gamma\setminus\Gamma^{tr}} \Big(\langle \mathbf{n}\cdot\nabla u, v\rangle_{\partial K_1\cap E} + \langle \mathbf{n}\cdot\nabla u, v\rangle_{\partial K_2\cap E}\Big) = &\int_{\Gamma\setminus\Gamma^{tr}} \{\nabla u\}\cdot[\![v]\!] ds \\ &+ \int_{\Gamma^{int}\setminus\Gamma^{tr}} [\![\nabla u]\!]\cdot\{v\} ds.\end{aligned} \tag{2.12}$$

Applying the interface condition, gives

$$\sum_{E\in\Gamma^{tr}} \Big(\langle \mathbf{n}\cdot\nabla u, v\rangle_{\partial\Omega_1\bigcap E} + \langle \mathbf{n}\cdot\nabla u, v\rangle_{\partial\Omega_2\bigcap E}\Big) = \int_{\Gamma^{tr}} C_{tr}[\![u]\!]\cdot[\![v]\!] ds. \tag{2.13}$$

Collecting all these results together, we obtain

$$\begin{aligned}&\sum_{K\in\mathcal{T}} \int_K \nabla u\cdot\nabla v \mathrm{dx} - \int_{\Gamma\setminus\Gamma^{tr}} \{\nabla u\}\cdot[\![v]\!] ds - \int_{\Gamma^{int}\setminus\Gamma^{tr}} [\![\nabla u]\!]\cdot\{v\} ds \\ &+ \int_{\Gamma^{tr}} C_{tr}[\![u]\!]\cdot[\![v]\!] ds = \int_\Omega f v \mathrm{dx}.\end{aligned} \tag{2.14}$$

Assuming that the fluxes ∇u are continuous almost everywhere in Ω, we obtain

$$\int_{\Gamma^{int}\setminus\Gamma^{tr}} [\![\nabla u]\!]\cdot\{v\} ds = 0 \quad \forall u \in H^{\frac{3}{2}+\epsilon}(\Omega_1\cup\Omega_2) \quad \text{for } \epsilon > 0.$$

Also $[\![u]\!] = 0$. We obtain, for all $u, v \in H^{\frac{3}{2}+\epsilon}(\Omega_1 \cup \Omega_2), \quad \epsilon > 0,$

$$\sum_{K\in\mathcal{T}} \int_K \nabla u \cdot \nabla v ds - \int_{\Gamma\setminus\Gamma^{tr}} (\{\nabla u\} \cdot [\![v]\!] + \{\nabla v\} \cdot [\![u]\!])\, ds + \int_{\Gamma\setminus\Gamma^{tr}} \frac{\gamma_0}{\mathbf{h}} [\![u]\!] \cdot [\![v]\!] ds$$
$$+ \int_{\Gamma^{tr}} C_{tr} [\![u]\!] \cdot [\![v]\!] ds = \int_\Omega f v \mathrm{dx}.$$

The above suggest the following interior penalty discontinuous Galerkin method : find $u_h \in S_h^p$ such that

$$D_h(u_h, v_h) = \langle f, v_h \rangle, \qquad \text{for all } v_h \in S_h^p, \tag{2.15}$$

where

$$\begin{aligned} D_h(u_h, v_h) = \sum_{K\in\mathcal{T}} \int_K \nabla u_h \cdot \nabla v_h dx - \int_{\Gamma\setminus\Gamma^{tr}} (\{\nabla u_h\} \cdot [\![v_h]\!] + \{\nabla v_h\} \cdot [\![u_h]\!]) ds \\ + \int_{\Gamma\setminus\Gamma^{tr}} \frac{\gamma_0}{\mathbf{h}} [\![u_h]\!] \cdot [\![v_h]\!] ds + \int_{\Gamma^{tr}} C_{tr} [\![u_h]\!] \cdot [\![v_h]\!] ds; \end{aligned} \tag{2.16}$$

here $\gamma_0 > 0$ is the discontinuity-penalization function (to be defined precisely in the next Chapters,) and $C_{tr} > 0$ is the permeability coefficient. We note carefully that there is *no* discontinuity penalization on the interface. As we shall see below, the penalty parameter has to be chosen large enough in order to ensure the stability of the discontinuous Galerkin discretization; cf., also, e.g., [20].

2.2.5 Parabolic model problem

We consider a parabolic interface model problem, modelling the mass transfer of solutes through semi-permeable membranes, closed by nonlinear interface conditions. To begin with, we define the permeability $p : \mathbb{R}^{2n} \longrightarrow \mathbb{R}^n$ as a function of the traces of u from both sides of the interface, with $\mathcal{P}(u) = p(u_1, u_2)$, we have

$$\begin{aligned} u_t - \Delta u &= f, && \text{in } \Omega_1 \cup \Omega_2 \cup [0,T], \\ u &= 0, && \text{on } \partial\Omega, \\ u(0,x) &= u_0(x), && \text{on } \{0\} \times \Omega, \\ \mathbf{n}^1 \cdot \nabla u_1 &= \mathcal{P}(u)(u_2 - u_1)|_{\Omega_1} && \text{on } \bar{\Omega}_1 \cap \Gamma^{tr}, \\ \mathbf{n}^2 \cdot \nabla u_2 &= \mathcal{P}(u)(u_1 - u_2)|_{\Omega_2} && \text{on } \bar{\Omega}_2 \cap \Gamma^{tr}, \end{aligned} \tag{2.17}$$

where $u_i = u|_{\bar{\Omega}_i \cap \Gamma^{tr}}$, $i = 1, 2$, and $\mathbf{n}^i$, $i = 1, 2$ denoting the respective outward unit normal vectors. Let $\tilde{p} : \mathbb{R}^{2n} \longrightarrow \mathbb{R}^n$ denote the function describing the diffusive flux across the interface Γ^{tr}, that is

$$\tilde{p}(x_1, x_2) = \mathcal{P}(x_1, x_2)(x_1 - x_2) \quad \forall x_1, x_2 \in \mathbb{R}^{2n}, \tag{2.18}$$

and assume that $\tilde{p} \in C^{1,1}(\mathbb{R}^{2n})$ and that its Jacobian $\tilde{p}'$ is bounded. Upon integrating by parts on each sub-domain and applying the interface condition, we arrive to (2.17) in weak form, which reads: find $u \in L_2(0, T, \mathcal{H}_0^1) \cap \mathcal{H}_0^1(0, T, L_2(\Omega_1 \cup \Omega_2))$ such that, for almost every $t \in (0, T]$, we have

$$\int_\Omega \frac{\partial u}{\partial t} v dx + D\left(t; u, v\right) + \mathcal{M}\left(u, v\right) = \int_\Omega f v dx, \tag{2.19}$$

for all $v \in \mathcal{H}_0^1$. Here,

$$D\left(t; u, v\right) = \int_{\Omega_1 \cup \Omega_2} \nabla u \cdot \nabla v dx, \qquad \mathcal{M}\left(u, v\right) = \int_{\Gamma^{tr}} \mathcal{P}(u) [\![u]\!] \cdot [\![v]\!] ds. \tag{2.20}$$

In the remaining of the chapter we present the semi-discrete and fully-discrete formulations of the model problem (2.17).

2.2.6 Semi-discrete formulation

We consider the semi-discrete interior penalty discontinuous Galerkin method for (2.17) as $\tilde{D}_h : S_h^p \times S_h^p \to \mathbb{R}$ of the bilinear form $\tilde{D}_h$, given by

$$\langle \frac{\partial u_h}{\partial t}, v_h \rangle + \tilde{D}_h(t; u_h, v_h) + \mathcal{M}(u_h, v_h) = \langle f, v_h \rangle, \qquad \text{for all } v_h \in S_h^p, \tag{2.21}$$

where

$$\begin{aligned} \tilde{D}_h(t; u_h, v_h) = \sum_{K \in \mathcal{T}} \int_K \nabla u_h \cdot \nabla v_h dx - \int_{\Gamma \setminus \Gamma^{tr}} (\{\nabla u_h\} \cdot [\![v_h]\!] + \{\nabla v_h\} \cdot [\![u_h]\!]) ds \\ + \int_{\Gamma \setminus \Gamma^{tr}} \frac{\gamma_0}{\mathbf{h}} [\![u_h]\!] \cdot [\![v_h]\!] ds; \end{aligned} \tag{2.22}$$

where the dependence on time has been made explicit in $\tilde{D}_h$ and $\mathcal{M}$ as in (2.20). Note that $\tilde{D}_h$ differs from D_h defined in (2.16), in that it does *not* include the interface term.

2.2.7 Fully discrete formulation

We consider a fully discrete scheme consisting of the fitted interior penalty discontinuous Galerkin method in space, together with backward Euler Galerkin time-stepping. To this end, we will discretise the time interval $[0, T]$ into subintervals $(t_{n-1}, t_n]$, $n = 1, ..., N$ with $t^0 = 0$ and $t_N = T$, and we denote by $k^n = t_n - t_{n-1}$ the local time step. We associate to each time-step t_N a spatial mesh $\mathcal{T}^n$ and the respective finite element space $S^n := S_h^p(\mathcal{T}^n)$. The fully discrete scheme is defined as follows. Set u_h^0 to be a projection of u_0 onto some space S^0 subordinate to a mesh $\mathcal{T}^0$ employed for the discretisation of the initial condition. For $k = 1, ..., n$, find $u_h^n \in S^n$ such that

$$\langle \frac{u_h^n - u_h^{n-1}}{k^n}, v^n \rangle + D_h^n \left(u_h^n, v^n\right) + \mathcal{M}\left(u_h^n, v^n\right) = \langle f^n, v^n \rangle \quad \forall v^n \in S^n, \tag{2.23}$$

where $D_h^n(\cdot, \cdot) = D_h(t_n, \cdot, \cdot)$ denotes the dG bilinear form defined on the mesh $\mathcal{T}^n$.

Chapter 3

Approximation and recovery on curved elements

3.1 Introduction

This chapter aims to present some useful approximation, trace, inverse estimates and recovery operator, which will be used in the derivation of the a posteriori error bound below. The coercivity and continuity of the bilinear form are also proven.

3.2 Mesh assumptions

We make some further assumptions on the admissible meshes near the (curved) interface. We assume that *no* interior point of an element $K \in \mathcal{T}$ (which we recall is an open set) can have a non-trivial intersection with the interface Γ^{tr}. Moreover, for simplicity (and with no essential loss of generality,) we assume that the set $\partial K \cap \Gamma^{tr} \neq \emptyset$ is one whole face of K, or one vertex of K only. Hence, when $d = 3$, we shall only consider (possibly curved) tetrahedral or prismatic elements with triangular bases $K \in \mathcal{T}$ such that $\partial K \cap \Gamma^{tr} \neq \emptyset$, so that a unique cut plane passes through the 3 vertices of K lying on Γ^{tr}. Elsewhere in the mesh, box-type elements when $d = 3$ are also allowed. Moreover, we assume that the mesh is constructed in such a way that each element K is a Lipschitz domain.

Assumption 3.1. For all elements $K \in \mathcal{T}^{tr}$, we assume that:

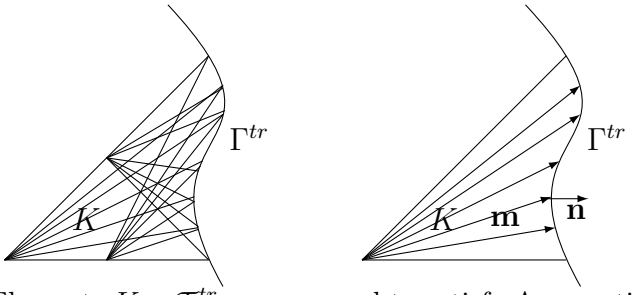

FIGURE 3.1: Elements $K \in \mathcal{T}^{tr}$ are assumed to satisfy Assumption 3.1 a) (left) and b) (right)

a) *(star-shapedness)* each element $K \in \mathcal{T}^{tr}$, having the face $E \subset \Gamma^{tr}$, is star-shaped with respect to all vertices opposite this face E; note that we have one such vertex when K is simplicial, or more than one such vertices when K is box-type or prismatic. Furthermore, we assume that each element $K \in \mathcal{T}^{tr}$ is also star-shaped with respect to all the midpoints of the edges sharing a common vertex with the face $E \subset \Gamma^{tr}$ and are not (edges of) $E \subset \Gamma^{tr}$ itself; we refer to Figure 3.1 for an illustration for $d = 2$.

b) *(shape-regularity)* we have $\mathbf{m}(\mathbf{x}) \cdot \mathbf{n}(\mathbf{x}) \geq c|\mathbf{m}(\mathbf{x})|$ uniformly across the mesh, for every vector $\mathbf{m}(\mathbf{x}) = \mathbf{x} - \mathbf{x_0}$, with $\mathbf{x} \in E$ and $\mathbf{x}_0$ any vertex opposite $E \in \Gamma$, and $\mathbf{n}(\mathbf{x})$ the respective unit outward normal vector to E at $\mathbf{x}$. Moreover, we assume that $|\mathbf{m}(\mathbf{x})| \sim h_K$ uniformly.

Note that Assumption 3.1 b) is trivially satisfied by shape-regular elements K with straight faces. It is a natural condition in view of proving trace estimates, cf. Lemma 3.3 below (see also [3, Theorem 3.10] and [31, Section 3] for illuminating expositions). Assumption 3.1 a) can always be fulfilled on sufficiently fine meshes, given that the curvature of Γ^{tr} is bounded.

We denote the set of, possibly curved, *interface elements* by

$$\mathcal{T}^{tr} := \{K \in \mathcal{T} : \text{meas}_{d-1}(\partial K \cap \Gamma^{tr}) > 0\};$$

with $\text{meas}_r(\omega)$ denoting the r-dimensional Hausdorff measure of a set $\omega \subset \mathbb{R}^d$; see Figure 2.2 for an illustration of such elements. Note that elements having just one vertex on Γ^{tr} do *not* belong to $\mathcal{T}^{tr}$.

Definition 3.2. For each $K \in \mathcal{T}^{tr}$, we define the simplicial or box-type *related element* $\tilde{K}$ to be the element with straight/planar faces having the same vertices as K. Let also $\underline{K} \subset K$ be the largest sub-element with straight/planar faces and all faces parallel to the faces of the related element $\tilde{K}$.

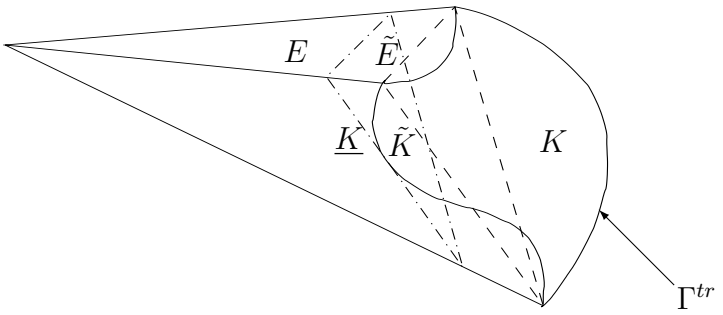

FIGURE 3.2: A three-dimensional curved element $K \in \mathcal{T}^{tr}$ (enclosed by the solid lines and curve), its related elements $\tilde{K}$ having the same vertices as K and straight faces (two same faces and the third depicted by a dashed line,) and $\underline{K}$ (having two same faces and the third depicted by a dashed-dotted line.) Although it does not belong to Γ^{tr}, the face E (enclosed by the solid lines and curve,) has a curved edge while the related face $\tilde{E}$ (two same faces and the third depicted by a dashed line,) is a straight triangle.

For two adjacent elements $K, K' \in \mathcal{T}^{tr}$ sharing a common face $E \in \Gamma^{int} \cup \Gamma^{tr}$, we shall denote by $\tilde{E} := \partial\tilde{K} \cap \partial\tilde{K}'$ the related common face of the two (also adjacent) related simplicial or prismatic elements $\tilde{K}, \tilde{K}'$.

Notice that in general, $K \neq \tilde{K}$ when $\partial K \cap \Gamma^{tr}$ is curved; see Figure 3.2 for an illustration.

Next, we define

$$\Gamma^{int}_{tr} := \{E \in \Gamma^{int} : E \neq \tilde{E}\},$$

i.e., the subset of Γ^{int} containing all the faces $E \in \Gamma^{int}$ with different related faces $\tilde{E}$; see again Figure 3.2 for an illustration. Notice that $E \neq \tilde{E}$ is possible only when $d = 3$.

The above star-shapedness assumptions effectively imply that the angles between the faces $E \subset \Gamma^{tr}$ and those faces in Γ^{int}_{tr} cannot be arbitrarily small and that the Jacobian of the function parametrising $E \subset \Gamma^{tr}$ on a local coordinate system, as defined above, cannot be very large. Satisfying these assumptions may require a small number of refinements of the elements $K \in \mathcal{T}^{tr}$ of a given initial mesh.

3.3 Approximation, trace, and inverse estimates

For the proof of upper and lower a posteriori error bounds, we shall require approximation, trace, and inverse estimates for the elements with curved boundaries $K \in \mathcal{T}^{tr}$, with uniform constants, i.e., constants that are independent of the particular shape of K. We begin by extending the standard trace estimate (2.2) to

elements with curved faces in which the constant independent of the shape and size of K and of v.

Lemma 3.3. *Let $v \in H^1(K)$ and $K \in \mathcal{T}^{tr}$. Then, under the above assumptions on the mesh, we have*

$$\|v\|_{\partial K \cap \Gamma^{tr}} \leq C \left(h_K^{-1} \|v\|_K^2 + h_K \|\nabla v\|_K^2 \right), \tag{3.1}$$

with $C > 0$, independent of the shape and size of K and of v.

Proof. Since $K \in \mathcal{T}^{tr}$ is star-shaped with respect to any given vertex $\nu_{E_{tr}}$ opposite the face $E_{tr} = \partial K \cap \Gamma^{tr}$, let $\mathbf{m}(s)$ be the vector pointing from the vertex $\nu_{E_{tr}}$ to all points $s \in K$, thereby defining $\mathbf{m} : K \to \mathbb{R}^d$, cf. Figure 3.1 (right). Without loss of generality, we assume that $K \in \mathcal{T}^{tr}$ is simplicial. Indeed, if $K \in \mathcal{T}^{tr}$ is prismatic, let $K_0 \subset K$ to be the (curved) simplex defined by $\nu_{E_{tr}}$ and E_{tr} and follow the argument presented below for K_0 instead.

Defining the vector field $F = \mathbf{m}v^2$, the divergence theorem implies

$$\int_{E_{tr}} (\mathbf{m} \cdot \mathbf{n}) v^2 \, ds = \int_{\partial K} F \cdot \mathbf{n} \, ds = \int_K \nabla \cdot F \, dx = \int_K (\nabla \cdot \mathbf{m}) v^2 \, dx + 2 \int_K v \nabla v \cdot \mathbf{m} \, dx,$$

noting that $\mathbf{m}(s) \cdot \mathbf{n}(s) = 0$ for all $s \in \partial K \backslash E_{tr}$, which, in turn, yields

$$\min_{E_{tr}} |\mathbf{m} \cdot \mathbf{n}| \|v\|_{E_{tr}}^2 \leq d \|v\|_K^2 + h_K \|v\|_K \|\nabla v\|_K, \tag{3.2}$$

noting that $\|\nabla \cdot \mathbf{m}\|_{L_\infty(K)} = d$ and $\| \, |\mathbf{m}| \, \|_{L_\infty(K)} \leq h_K$. The result already follows by Assumption 3.1 b). □

Next, let $\Pi_0 : L^2(\Omega) \to S_h^0$ denote the orthogonal L^2-projection operator onto the element-wise constant functions, given by

$$\Pi_0 v|_K := |K|^{-1} \int_K v dx, \qquad \text{for } K \in \mathcal{T},$$

with $|\cdot| \equiv \text{meas}_d(\cdot)$ denoting the volume. We have the following approximation result.

Lemma 3.4. *Given the assumptions on the mesh, for each $v \in H^1(K)$, $K \in \mathcal{T}$, we have the bounds*

$$\|v - \Pi_0 v\|_K \leq C h_K \|\nabla v\|_K, \tag{3.3}$$

and

$$\|v - \Pi_0 v\|_{\partial K} \leq C\sqrt{h_K}\|\nabla v\|_K, \tag{3.4}$$

with $C > 0$ constant independent of the shape of $K \in \mathcal{T}$, on v and on h_K.

Proof. Due to the general, possibly curved, shape of the elements $K \in \mathcal{T}^{tr}$, a simple application of a standard Bramble-Hilbert type result (cf., e.g., [13]) and scaling is *not* sufficient to provide uniform constant C with respect to the shape of K. Instead, we work as follows. For $K \in \mathcal{T}\backslash\mathcal{T}^{tr}$, the results are well-known. For $K \in \mathcal{T}^{tr}$, the Friedrichs-type inequality proven in [61, Theorem 3.2], with explicit constant with respect to the domain, along with shape-regularity, yields (3.3). The bound (3.4) follows by combining (3.1) with (3.3). □

For each $K \in \mathcal{T}^{tr}$, we shall require special sub-simplices contained in K, with certain properties, having, in particular, straight/planar faces.

Lemma 3.5. *Let $K \in \mathcal{T}^{tr}$. For each $v \in \mathcal{P}_p(K)$, there exists a simplex $K_\flat(v) \subset K$ with straight/planar faces such that*

$$|K| \leq C_\flat |K_\flat(v)| \qquad \textit{with} \qquad \|v\|_{L^\infty(K)} = \|v\|_{L^\infty(K_\flat(v))},$$

where the positive constant $C_\flat$ is independent of v, h_K, and p, but depends, however, on the shape-regularity constant of K.

Proof. Let $K \in \mathcal{T}^{tr}$ and fix $v \in \mathcal{P}(K)$. Define $\mathbf{x}_K \in K$ to be a point where the maximum of v in K is attained, viz.,

$$\|v\|_{L^\infty(K)} = |v(\mathbf{x}_K)|.$$

To prove the result, it is sufficient to show that there exists a simplex $K_\flat(v) \subset K$ with straight/planar faces containing $\mathbf{x}_K \in K$ such that $|K| \leq C_\flat |K_\flat(v)|$. Recalling Definition 3.2, we observe that, for $\underline{K}$, we have $|\underline{K}| \sim |\tilde{K}|$ from shape-regularity. If $\mathbf{x}_K \in \underline{K}$, then we can take $K_\flat(v) := \underline{K}$. If $\mathbf{x}_K \in K\backslash\underline{K}$, the star-shapedness of K with respect to the midpoints of the faces (when $d = 2$) or the edges (when $d = 3$) allows for the construction of a simplex $K_\flat(v)$ with faces (when $d = 2$) or edges (when $d = 3$) defined by the line-segments connecting $\mathbf{x}_K$ with these midpoints. Given that the distance between $\mathbf{x}_K$ and these midpoints equivalent to $h_{\underline{K}}/2$, the result follows. Since we have established that exists at least one $K_\flat(v)$ per element, we may define $K_\flat(v)$ as the one with the maximum area, to minimize the constant

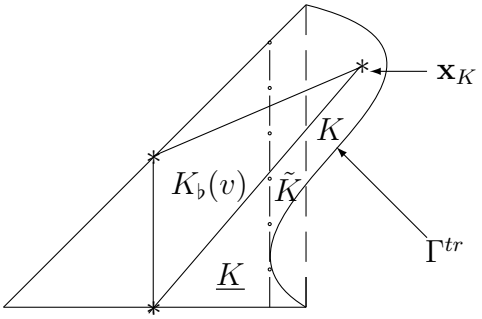

FIGURE 3.3: A curved element $K \in \mathcal{T}^{tr}$ (enclosed by the solid lines and curve,) its related element $\tilde{K}$ having the same vertices as K and straight faces (two same faces and the third depicted by a dashed line,) $\underline{K}$ (having two same faces and the third depicted by a dashed-dotted line,) and $K_\flat(v)$ for some $v \in \mathcal{P}_p(K)$ (enclosed by the solid lines with endpoints denoted by $*$.) Here, $\mathbf{x}_K$ is the point where the maximum of v in K is attained.

$C_\flat$. Notice that $C_\flat$ can be taken independent of the polynomial v, as the area of $K_\flat(v)$ is always bounded from below by a multiple of h_K^2 and K is compact. □

We refer to Figure 3.3 for an illustration of the elements $K, \tilde{K}, \underline{K}$, and $K_\flat(v)$, for some $v \in \mathcal{P}_p(K)$. Notice that we have $K = \tilde{K} = \underline{K} = K_\flat(v)$, for all $v \in \mathcal{P}_p(K)$, when the face $E \subset \Gamma^{tr}$ of a $K \in \mathcal{T}^{tr}$ is *not* curved.

The above result is required to show the following crucial inverse-type estimates between L^2-norms of polynomials on curved elements $K \in \mathcal{T}^{tr}$ and their related elements $\tilde{K}$.

Lemma 3.6. *Let $K \in \mathcal{T}^{tr}$ and assume that the related element $\tilde{K}$ is such that*

$$c_{inv} C_\flat p^{2d} |K \backslash \tilde{K}| < |K|, \tag{3.5}$$

with $c_{inv} > 0$ the constant of the inverse estimate $\|v\|^2_{L_\infty(\tilde{K})} \leq c_{inv} p^{2d} |\tilde{K}|^{-1} \|v\|^2_{\tilde{K}}$, for all $v \in \mathcal{P}_p(K)$. Then, the following estimate holds

$$\|v\|^2_K \leq \theta_{inv}(K) \|v\|^2_{K \cap \tilde{K}},$$

where $\theta_{inv}(K) := |K| / \big(|K| - c_{inv} C_\flat p^{2d} |K \backslash \tilde{K}|\big)$.

Proof. Let $v \in \mathcal{P}_p(K)$. We have, respectively,

$$\begin{aligned}\|v\|_K^2 &= \|v\|_{K\cap\tilde{K}}^2 + \|v\|_{K\setminus\tilde{K}}^2 \\ &\leq \|v\|_{K\cap\tilde{K}}^2 + |K\setminus\tilde{K}|\|v\|_{L_\infty(K\setminus\tilde{K})}^2 \\ &\leq \|v\|_{K\cap\tilde{K}}^2 + |K\setminus\tilde{K}|\|v\|_{L_\infty(K_\flat(v))}^2 \\ &\leq \|v\|_{K\cap\tilde{K}}^2 + c_{inv}p^{2d}|K_\flat(v)|^{-1}|K\setminus\tilde{K}|\|v\|_{K_\flat(v)}^2 \\ &\leq \|v\|_{K\cap\tilde{K}}^2 + c_{inv}C_\flat p^{2d}|K|^{-1}|K\setminus\tilde{K}|\|v\|_K^2,\end{aligned}$$

as $K_\flat(v) \subset K$, using Lemma 3.5; the result follows. □

Lemma 3.7. *Let $K \in \mathcal{T}^{tr}$ and let $\underline{K} \subset K$ and $\tilde{K}$ as in Definition 3.2 be such that*

$$c_{inv}p^{2d}|\tilde{K}\setminus\underline{K}| < |\tilde{K}|, \tag{3.6}$$

for $c_{inv} > 0$ as in Lemma 3.6. Then, for each $v \in \mathcal{P}_p(K)$, the following estimate holds

$$\|v\|_{\tilde{K}}^2 \leq \eta_{inv}(K)\|v\|_{\underline{K}}^2,$$

where $\eta_{inv}(K) := |\tilde{K}|/\big(|\tilde{K}| - c_{inv}p^{2d}|\tilde{K}\setminus\underline{K}|\big)$.

Proof. Let $v \in \mathcal{P}_p(K)$. We have, respectively

$$\begin{aligned}\|v\|_{\tilde{K}}^2 &= \|v\|_{\underline{K}}^2 + \|v\|_{\tilde{K}\setminus\underline{K}}^2 \leq \|v\|_{\underline{K}}^2 + |\tilde{K}\setminus\underline{K}|\|v\|_{L_\infty(\tilde{K}\setminus\underline{K})}^2 \\ &\leq \|v\|_{\underline{K}}^2 + |\tilde{K}\setminus\underline{K}|\|v\|_{L_\infty(\tilde{K})}^2 \leq \|v\|_{\underline{K}}^2 + c_{inv}p^{2d}|\tilde{K}|^{-1}|\tilde{K}\setminus\underline{K}|\|v\|_{\tilde{K}}^2,\end{aligned}$$

which implies the result. □

Notice that, when $K \in \mathcal{T}^{tr}$ is convex, we have $\tilde{K} = \underline{K}$ and, thus, $\eta_{inv}(K) = 1$. Also, when $K \in \mathcal{T}^{tr}$ is not curved, we have $K = \tilde{K} = \underline{K}$ and, therefore, $\theta_{inv}(K) = 1 = \eta_{inv}(K)$.

Remark 3.8. It is possible to extend the applicability of the above estimates by replacing p^{2d} by p^2 in (3.6) at the expense of a, more involved to estimate, constant c_{inv}. We refer to [32, Lemma 3.7] for a similar construction. This remark also applies to (3.5) for the case where $K_\flat(v)$ and K have parallel faces.

Remark 3.9. A close inspection of the proof of Lemma 3.5 reveals that the shape-regularity assumption of K can be relaxed to requiring that there exists a, uniform across the mesh, constant $c_{alt} > 0$ such that $|\tilde{K}| \leq c_{alt}|\underline{K}|$. The constant $C_\flat$ will then depend on c_{alt} instead of the shape-regularity constant of K as stated in Lemma 3.5. This, in turn, implies the validity of the inverse estimates in Lemmata 3.6 and 3.7 in this setting also.

For the remaining of this work, we shall require the above inverse-type estimates, hence we make the following saturation assumption which can always be satisfied after a finite number of refinements of an original coarse mesh.

Assumption 3.10. We assume that the conditions (3.5) and (3.6) are satisfied for all elements $K \in \mathcal{T}^{tr}$.

We continue with a generalization of the standard inverse-type estimate from a face of an element to the element itself; here the face is allowed to be curved.

Lemma 3.11. *Let $K \in \mathcal{T}^{tr}$ such that a whole face of K, say E_{tr}, is contained in Γ^{tr}, and is, in general, curved. Then, for each $v \in \mathcal{P}_p(K)$, the inverse estimate*

$$\|v\|^2_{E_{tr}} \leq C\frac{p^2}{h_K}\|v\|^2_K,$$

with $C > 0$ constant, independent of v, p, h_K and K, but dependent on the shape-regularity constant of K.

Proof. We partition E_{tr} into m $(d-1)$-dimensional pieces of equal measure, denoted by E_j, $j = 1, \ldots, m$. Further, we construct a partition of K into (curved) sub-elements K_j, by considering the simplices with one face E_j and the remaining vertex being the vertex of K opposite E_{tr}, when K is simplicial or by considering the prismatic elements obtained by extrusion of E_j orthogonally to the face of K opposite E_{tr}, when K is prismatic. We refer to Figure 3.4 for an illustration when $d = 2$.

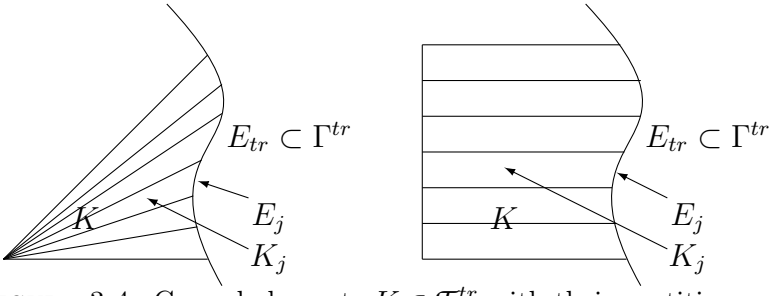

FIGURE 3.4: Curved elements $K \in \mathcal{T}^{tr}$ with their partitions.

Denoting by $\tilde{E}_j$ the straight/planar face of the related element $\tilde{K}_j$ approximating E_j, we have

$$\|v\|^2_{\tilde{E}_j} \leq Cp^2\frac{|\tilde{E}_j|}{|\tilde{K}_j|}\|v\|^2_{\tilde{K}_j} \leq C\frac{p^2}{h_K}\|v\|^2_{\tilde{K}_j} \leq C\eta_{inv}(K_j)\frac{p^2}{h_K}\|v\|^2_{K_j}, \tag{3.7}$$

as, in view of Remark 3.9, it is possible to apply Lemma 3.7 on each K_j (for sufficiently large m.)

As $m \to \infty$, K_j becomes infinitesimal in $(d-1)$-dimensions, and so, approximating K_j by $\tilde{K}_j$ produces arbitrarily small error in the geometry, resulting to $\eta_{inv}(K_j) \to 1$. Moreover, since E_{tr} admits a differentiable parametrization, we have $\lim_{m\to\infty} \sum_{j=1}^{m} \|v\|^2_{\tilde{E}_j} = \|v\|^2_{E_{tr}}$. Therefore, summing (3.7) over j and taking $m \to \infty$, we arrive at the required result. □

Lemma 3.12. *Let $K \in \mathcal{T}^{tr}$ and let E a face of K, such that $E \subset \partial K \backslash \Gamma^{tr}$. Then, for each $v \in \mathcal{P}_p(K)$, the inverse estimate*

$$\|v\|^2_E \leq C \frac{p^2}{h_K} \|v\|^2_K,$$

with $C > 0$ constant, independent of v, p, h_K and K, but dependent on the shape-regularity constant of K.

Proof. Fix $K \in \mathcal{T}^{tr}$ and a face $E_* \subset \partial K \backslash \Gamma^{tr}$. For $d = 2$, the star-shapedness with respect to the midpoints of the faces $E \subset \partial K \backslash \Gamma^{tr}$, allows for the existence of a straight-edged triangle $K_* \subset K$ having E_* as one face and as remaining vertex the midpoint of the other face $E \subset \partial K \backslash \Gamma^{tr}$ opposite to E_*. From the shape-regularity of K, we infer that $|K| \sim |K_*|$. On this triangle K_*, we can apply the standard inverse inequality to deduce

$$\|v\|^2_{E_*} \leq C \frac{p^2}{h_{K_*}} \|v\|^2_{K_*} \leq C \frac{p^2}{h_K} \|v\|^2_K,$$

as required.

For $d = 3$ and K with $\text{meas}_2(\partial K \cap \Gamma^{tr}) > 0$, we approximate $E_* \subset \partial K \backslash \Gamma^{tr}$ by a quasiuniform triangulation consisting of m triangles, denoted by $\tilde{E}_j$, $j = 1, \ldots, m$. Let x_{E_*} be the midpoint of an edge of K which is not an edge of E_* and consider the straight-faced pyramids $\tilde{K}_j$, $j = 1, \ldots, m$, having $\tilde{E}_j$ as one base and x_{E_*} as remaining vertex. On each $\tilde{K}_j$, we can apply the standard inverse estimate

$$\sum_{j=1}^{m} \|v\|^2_{\tilde{E}_j} \leq Cp^2 \sum_{j=1}^{m} \frac{|\tilde{E}_j|}{|\tilde{K}_j|} \|v\|^2_{\tilde{K}_j} \leq C \frac{p^2}{h_K} \sum_{j=1}^{m} \|v\|^2_{\tilde{K}_j} \leq C \eta_{inv}(K_j) \frac{p^2}{h_K} \sum_{j=1}^{m} \|v\|^2_{K_j},$$

working as before. Taking $m \to \infty$ gives the result. □

3.4 Recovery operator

An important tool for the a posteriori analysis will be a conforming recovery operator in the spirit of the original construction by Karakashian and Pascal [41]. In particular, we shall modify the construction from [41] to allow for discontinuous functions across Γ^{tr} and for curved elemental faces and edges on Γ^{tr}, under the following assumption.

Assumption 3.13. We define the positive function $\theta : L_2(\Omega_1 \cup \Omega_2) \to \mathbb{R}$ with $\theta|_K := \theta_{inv}(K)$, for $K \in \mathcal{T}^{tr}$, $\theta|_K := 1$, for $K \in \mathcal{T}\backslash\mathcal{T}^{tr}$, and $\theta := \{\theta\}$ on $\Gamma\backslash\Gamma^{tr}$. We also define the positive function $\eta : L_2(\Gamma\backslash\Gamma^{tr}) \to \mathbb{R}$ with $\eta|_E := \{\eta_{inv}\}$, for $E \in \Gamma\backslash\Gamma^{tr}$. For the remaining of this work, we shall assume that θ and η are locally quasi-uniform.

Lemma 3.14. *Given the above mesh assumptions, there exists a recovery operator* $\mathcal{E} : S_h^p \to \mathcal{H}_0^1$, *such that*

$$\sum_{K\in\mathcal{T}} \|\nabla^\alpha(v_h - \mathcal{E}(v_h))\|_K^2 \leq C_\alpha \sum_{E\subset\Gamma\backslash\Gamma^{tr}} \|\sqrt{\theta\eta}\mathbf{h}^{1/2-\alpha}[\![v_h]\!]\|_E^2, \tag{3.8}$$

for all $v_h \in S_h^p$, $C_\alpha > 0$, $\alpha = 0, 1$, *independent of* v_h, θ *and* $\mathbf{h}$.

Proof. The proof is based on the one of [41, Theorem 2.2]; particular care is given in dealing with the additional challenges posed by the, possibly curved, interface elements. Without loss of generality, we assume that the mesh is conforming on each Ω_i, $i = 1, 2$, i.e., no hanging nodes are present; for, otherwise, we perform a finite number of 'green' refinements to remove the hanging nodes, and we consider the new refined mesh in the place of the original $\mathcal{T}$ in what follows.

We begin by choosing a Lagrange basis for S_h^p. For each $K \in \mathcal{T}\backslash\mathcal{T}^{tr}$, we consider the standard Lagrange degrees of freedom. For each $K \in \mathcal{T}^{tr}$, we choose respective the Lagrange basis of $\tilde{K}$. Let $\mathcal{N}$ denote the set of all Lagrange nodes of S_h^p, and we define five of its subsets:

- $\mathcal{N}_0$ the set of all internal elemental nodes;
- $\mathcal{N}_{int}$ the set of all nodes situated on Γ^{int};
- $\mathcal{N}_{\partial\Omega}$ the set of all nodes situated on $\partial\Omega$;
- $\mathcal{N}_{tr}$ the set of all nodes situated on Γ^{tr};

- $\mathcal{N}_{out}$ the set of nodes belonging to each element $K \in \mathcal{T}^{tr}$, situated *outside* K. (E.g., the node of K_1 situated at the midpoint of the linear segment $\nu_1\nu_2$ in Figure 3.5.)

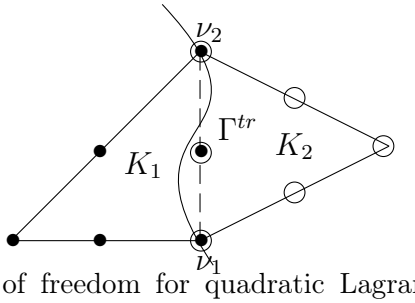

FIGURE 3.5: Degrees of freedom for quadratic Lagrange interface elements $K_1, K_2 \in \mathcal{T}^{tr}$, denoted by $\bullet$ and $\circ$, respectively. Note that one degree of freedom of K_1 is situated *outside* K_1 (i.e., in $\bar{\tilde{K}}_1 \backslash \bar{K}_1$,) at the midpoint of the linear segment $\nu_1\nu_2$.

Evidently, we have $\mathcal{N} = \mathcal{N}_0 \cup \mathcal{N}_{int} \cup \mathcal{N}_{\partial\Omega} \cup \mathcal{N}_{tr} \cup \mathcal{N}_{out}$. Note, however, that, $\mathcal{N}_{out} \cap \mathcal{N}_0 \neq \emptyset$, in general; for an illustration consider the node ν situated at the midpoint of the linear segment $\nu_1\nu_2$ in Figure 3.5: ν viewed as a node for K_2 implies $\nu \in \mathcal{N}_0$ and viewed as a node for K_1 implies $\nu \in \mathcal{N}_{out}$.

Further, let $\mathcal{N}_{tr}^i$ and $\mathcal{N}_{out}^i$ denote the two subsets of the interface nodes $\mathcal{N}_{tr}$, and the 'outer' nodes $\mathcal{N}_{out}$ associated with the Lagrange basis functions from the respective elements belonging to Ω_1 and Ω_2 only, respectively. Note that if non-matching grids are used across the interface Γ^{tr}, $\mathcal{N}_{tr}^1$ and $\mathcal{N}_{tr}^2$ are, in general different and strict subsets of $\mathcal{N}_{tr}$; if, on the other hand, there are no hanging nodes on the interface, the $\mathcal{N}_{tr}^i$, $i = 1, 2$, are each a copy of $\mathcal{N}_{tr}$. Completely analogous properties characterise $\mathcal{N}_{out}^i$, $i = 1, 2$ also.

For each node $\nu \in \mathcal{N} \backslash (\mathcal{N}_{tr} \cup \mathcal{N}_{out})$, we define its element-neighbourhood

$$\omega_\nu := \{K \in \mathcal{T} : \nu \in \bar{K}\},$$

along with its cardinality $|\omega_\nu|$. Note that, when $\nu \in \mathcal{N}_0$, we have $|\omega_\nu| = 1$. Also, for each node $\nu \in \mathcal{N}_{tr}^i$, $i = 1, 2$, we define its 'one-sided' element neighbourhood

$$\omega_\nu^i := \{K \in \mathcal{T} : K \subset \Omega_i,\, \nu \in \bar{K}\}, \qquad i = 1, 2,$$

along with its cardinality $|\omega_\nu^i|$, $i = 1, 2$, while for each node $\nu \in \mathcal{N}_{out}$, we define its 'one-sided' element neighbourhood

$$\omega_\nu^i := \{K \in \mathcal{T}^{tr} : K \subset \Omega_i,\, \nu \in \bar{\tilde{K}}\}, \qquad i = 1, 2,$$

along with its cardinality $|\omega_\nu^i|$. Finally, for each $K \in \mathcal{T}$, let $\mathcal{N}_K := \{\nu : \nu \in \bar{\tilde{K}}\}$, the set of Lagrange nodes of K.

The recovery operator $\mathcal{E} : S_h^p \to \mathcal{H}_0^1$ is defined by determining its nodal values N_ν at each of the Lagrange nodes $\nu \in \mathcal{N}$:

$$N_\nu(\mathcal{E}(v_h)) := \begin{cases} 0, & \text{if } \nu \in \mathcal{N}_{\partial\Omega}; \\ \dfrac{1}{|\omega_\nu|} \displaystyle\sum_{K \in \omega_\nu} N_\nu(v_h|_K), & \text{if } \nu \in \mathcal{N}_{int} \cup \mathcal{N}_0; \\ \dfrac{1}{|\omega_\nu^i|} \displaystyle\sum_{K \in \omega_\nu^i} N_\nu(v_h|_K), & \text{if } \nu \in \mathcal{N}_{tr}^i \cup \mathcal{N}_{out}^i,\ i = 1, 2. \end{cases} \tag{3.9}$$

Note that $\mathcal{E}(v_h)$ will be, in general, discontinuous across Γ^{tr}. Therefore, denoting by ϕ_ν the conforming Lagrange basis function at the node ν, (which may, nonetheless, be discontinuous across Γ^{tr},) we have

$$\mathcal{E}(v_h) = \sum_{\nu \in \mathcal{N}} N_\nu(\mathcal{E}(v_h))\phi_\nu, \tag{3.10}$$

allowing for the regular nodes on $\nu \in \mathcal{N}_{tr}$ to be counted twice in the summation, i.e., once for each $i = 1, 2$; here we have used the convention that ϕ_ν signifies its *restriction* onto the respective element K for all nodes $\nu \in \mathcal{N}_{out}$. Hence, we have $\mathcal{E}(v_h) \in \mathcal{H}_0^1$.

From this, we deduce, respectively,

$$\begin{aligned} \sum_{K \in \mathcal{T}} \|\nabla(v_h - \mathcal{E}(v_h))\|_K^2 &\le \sum_{K \in \mathcal{T}} \theta_{inv}(K) \|\nabla(v_h - \mathcal{E}(v_h))\|_{K \cap \tilde{K}}^2 \\ &\le \sum_{K \in \mathcal{T}} \sum_{\nu \in \mathcal{N}_K} \theta_{inv}(K) \big| N_\nu(v_h|_K) - N_\nu(\mathcal{E}(v_h)) \big|^2 \|\nabla \phi_\nu\|_{K \cap \tilde{K}}^2 \\ &\le C(p) \sum_{\nu \in \mathcal{N} \setminus \mathcal{N}_0} \theta(\nu) \mathbf{h}^{d-2}(\nu) \sum_{K : \nu \in \mathcal{N}_K} \big| N_\nu(v_h|_K) - N_\nu(\mathcal{E}(v_h)) \big|^2 \\ &=: C(p) \sum_{\nu \in \mathcal{N} \setminus \mathcal{N}_0} I_\nu, \end{aligned}$$

using the standard bound $\|\nabla \phi_\nu\|_{K \cap \tilde{K}}^2 \le \|\nabla \phi_\nu\|_{\tilde{K}}^2 \le C h_{\tilde{K}}^{d-2}$, where $\mathbf{h}(\nu)$ and $\theta(\nu)$ are given by extending the definitions of the functions $\mathbf{h}$ and θ (to include the

mesh nodes also)

$$\mathbf{h}(\nu) := \begin{cases} \dfrac{1}{|\omega_\nu|}\displaystyle\sum_{K\in\omega_\nu} h_K, & \text{if } \nu \in \mathcal{N}_{int}\cup\mathcal{N}_{\partial\Omega}; \\ \dfrac{1}{|\omega_\nu^i|}\displaystyle\sum_{K\in\omega_\nu^i} h_{\tilde{K}}, & \text{if } \nu \in \mathcal{N}_{tr}^i\cup\mathcal{N}_{out}^i,\ i=1,2, \end{cases}$$

and $\theta(\nu) := 1$, if $\nu \in \mathcal{N}_{int}\cup\mathcal{N}_{\partial\Omega}$, while $\theta(\nu) := \frac{1}{|\omega_\nu^i|}\sum_{K\in\omega_\nu^i}\theta_{inv}(K)$, if $\nu \in \mathcal{N}_{tr}^i\cup\mathcal{N}_{out}^i$, $i=1,2$. We have

$$\sum_{\nu\in\mathcal{N}_{\partial\Omega}} I_\nu = \sum_{\nu\in\mathcal{N}_{\partial\Omega}} \theta(\nu)\mathbf{h}^{d-2}(\nu) \sum_{K:\nu\in\mathcal{N}_K} \left|N_\nu(v_h|_K)\right|^2 \le C \sum_{E\subset\partial\Omega} \|\sqrt{\theta}\mathbf{h}^{\frac{d-2}{2}} v_h\|^2_{L_\infty(E)}.$$

Also,

$$\begin{aligned} \sum_{\nu\in\mathcal{N}_{int}\cup\mathcal{N}_{tr}\cup\mathcal{N}_{out}} I_\nu &\le C \sum_{E\subset\Gamma^{int}} \sum_{\nu\in\tilde{E}} \theta(\nu)\mathbf{h}^{d-2}(\nu)\left|N_\nu(v_h|_{K_1}) - N_\nu(v_h|_{K_2})\right|^2 \\ &\le C \sum_{E\subset\Gamma^{int}} \|\sqrt{\theta}\mathbf{h}^{\frac{d-2}{2}}[\![v_h]\!]\|^2_{L_\infty(\tilde{E})}, \end{aligned}$$

with $\tilde{E} := E$ when $E \notin \Gamma_{tr}^{int}$. Note that $\tilde{E} \neq E$ is possible only for $d=3$. The first inequality follows from applying the crucial [41, Lemma 2.2] and working as in the proof of [41, Theorem 2.2], while the last inequality follows from the shape-regularity property. We remark that, for $d=2$, we have $\left|N_\nu(v_h|_K) - N_\nu(\mathcal{E}(v_h))\right| = 0$ as $|\omega_\nu^i| = 1$ when $\nu \in \mathcal{N}_{out}^i$, $i=1,2$, while for $d=3$ and for $p=1$, we have $\mathcal{N}_{out} = \emptyset$. For $d=3$, and $p \ge 2$, we may have $|\omega_\nu^i| > 1$ and, thus, the above calculation is non-trivial for $\nu \in \mathcal{N}_{out}$.

Combining the above bounds, we arrive at

$$\sum_{K\in\mathcal{T}} \|\nabla(v_h - \mathcal{E}(v_h))\|_K^2 \le C \sum_{E\subset\Gamma\setminus\Gamma^{tr}} \|\sqrt{\theta}\mathbf{h}^{\frac{d-2}{2}}[\![v_h]\!]\|^2_{L_\infty(\tilde{E})}.$$

Finally, applying the standard inverse estimate

$$\|v\|^2_{L_\infty(\tilde{E})} \le C(p) h_K^{-d+1}\|v\|^2_{\tilde{E}},$$

for all polynomials $v \in \mathcal{P}_p(\tilde{E})$, and using Lemma 3.7 with $K = E$, we deduce

$$\|v\|^2_{\tilde{E}} \le \eta_{inv}(E)\|v\|^2_E.$$

Hence, we obtain the required bound for $\alpha = 1$. The proof for $\alpha = 0$ is completely analogous. □

Remark 3.15. When Γ^{tr} is not curved, i.e., when the mesh $\mathcal{T}$ does *not* contain any elements with curved faces, we have $\theta = 1 = \eta$ on $\Gamma \backslash \Gamma^{tr}$ in (3.8), thereby retrieving the known bound of Karakashian and Pascal [41, Theorem 2.2].

Next, we shall modified the trace estimate defined for straight line to case the curved boundary for functions in $S_h^p + \mathcal{H}_0^1$; see Karakashian and Pascal [41] and [20, Lemma 3.1].

Lemma 3.16. *Suppose that the mesh $\mathcal{T}$ is both shape-regular and locally quasi-uniform. Then for $v \in S_h^p + \mathcal{H}_0^1$, the following trace estimate holds*

$$\sum_{j=1}^{2} \|v|_{\Omega_j}\|_{\Gamma^{tr}}^2 \leq C_{trace}\Big(\varepsilon^{-1}\|v\|^2 + \varepsilon\big(\sum_{K\in\mathcal{T}} \|\nabla v\|_K^2 + \|\sqrt{\theta\eta/\mathbf{h}}[\![v]\!]\|_{\Gamma^{int}}^2\big)\Big). \tag{3.11}$$

for any $\varepsilon > h_{\max}$, and constants $C_{trace} > 0$ independent of the shape and size of K and of v.

Proof. Let decompose the function $v \in S_h^p + \mathcal{H}_0^1$ into a conforming part $\mathcal{E}(v)$ and a nonconforming part $v - \mathcal{E}(v) \in S_h^p$. Using Lemma 3.14, there exists a $\mathcal{E}(v) \in \mathcal{H}_0^1, \quad i = 1, 2$, such that

$$\sum_{K\in\mathcal{T}} \|\nabla^\alpha(v - \mathcal{E}(v))\|_K^2 \leq C_\alpha \|\sqrt{\theta\eta}\mathbf{h}^{1/2-\alpha}[\![v]\!]\|_{\Gamma^{int}}^2. \tag{3.12}$$

Applying triangle inequality i.e $v = c + v - \mathcal{E}(v)$, gives

$$\sum_{j=1}^{2} \|v|_{\Omega_j}\|_{\Gamma^{tr}}^2 \leq 2\sum_{j=1}^{2} \big(\|\mathcal{E}(v)|_{\Omega_j}\|_{\Gamma^{tr}}^2 + \|(v - \mathcal{E}(v)|_{\Omega_j}\|_{\Gamma^{tr}}^2\big). \tag{3.13}$$

Now, to bound the first term on the right-hand side of the (3.13), we note that $\mathcal{E}(v) \in \mathcal{H}_0^1$, giving

$$\sum_{j=1}^{2} \|\mathcal{E}(v)|_{\Omega_j}\|_{\Gamma^{tr}}^2 \leq C\left(\varepsilon^{-1}\|\mathcal{E}(v)\|^2 + \varepsilon\|\nabla\mathcal{E}(v)\|^2\right), \tag{3.14}$$

for any $\varepsilon > 0$ sufficiently small. Now, applying triangle inequality for each term, given

$$\|\mathcal{E}(v)\| \leq \|v - \mathcal{E}(v)\| + \|v\|, \quad \|\nabla\mathcal{E}(v)\|^2 \leq 2\sum_{K\in\mathcal{T}} \big(\|\nabla(v-\mathcal{E}(v))\|_K^2 + \|\nabla v\|_K^2\big).$$

From (3.12), we have

$$\begin{aligned}\sum_{j=1}^{2} \|\mathcal{E}(v)|_{\Omega_j}\|_{\Gamma^{tr}}^2 &\leq C_{trace}\Bigg(\varepsilon^{-1}C_0\|\sqrt{\theta\eta}\mathbf{h}^{1/2}[\![v]\!]\|_{\Gamma^{int}}^2 + \varepsilon^{-1}\|v\|^2 \\ &\quad + C_1\varepsilon\|\sqrt{\theta\eta}\mathbf{h}^{-1/2}[\![v]\!]\|_{\Gamma^{int}}^2 + \varepsilon\sum_{K\in\mathcal{T}}\|\nabla v\|_K^2\Bigg) \\ &\leq C_{trace}\Bigg(\varepsilon^{-1}\|v\|^2 + \varepsilon\sum_{K\in\mathcal{T}}\|\nabla v\|_K^2 + \varepsilon\|\sqrt{\theta\eta}\mathbf{h}^{-1/2}[\![v]\!]\|_{\Gamma^{int}}^2\Bigg),\end{aligned} \tag{3.15}$$

using the assumption that $\varepsilon > h_{\max}$. Now, it remains to bound the second term on the right-hand side of (3.13). To do this, applying trace estimate in Lemma 3.3 on each element, we obtain

$$\begin{aligned}\sum_{j=1}^{2} \|(v-\mathcal{E}(v))|_{\Omega_j}\|_{\Gamma^{tr}}^2 &\leq C_{trace}\sum_{K\in\mathcal{T}}\Bigg(\|\sqrt{1/\mathbf{h}}(v-\mathcal{E}(v))\|_K^2 + \|\sqrt{\mathbf{h}}\nabla(v-\mathcal{E}(v))\|_K^2\Bigg). \\ &\leq C_{trace}\|\sqrt{\theta\eta}[\![v]\!]\|_{\Gamma^{int}},\end{aligned} \tag{3.16}$$

using the assumption that $\varepsilon > h_{\max}$. Now, inserting (3.15) and (3.16) in (3.13) the proof is finished. □

Lemma 3.17. *For each $v_h \in \mathcal{H}_0^1$, $w, v \in \mathcal{H}_0^1 + S_h^p$, we have*

$$D_h(v_h, v_h) \geq \frac{1}{2}|||v_h|||^2 \tag{3.17}$$

$$\hat{D}_h(w, v) \leq C|||w|||\,|||v|||, \tag{3.18}$$

for $\gamma_0 > 0$ large enough, where D_h is given in (2.16), $\hat{D}_h$ is an (inconsistent) extension $\hat{D}_h : (\mathcal{H}_0^1 + S_h^p) \times (\mathcal{H}_0^1 + S_h^p) \to \mathbb{R}$ of the bilinear form D_h, given by

$$\begin{aligned}\hat{D}_h(w, v) = &\sum_{K\in\mathcal{T}}\int_K \nabla w\cdot\nabla v\,dx - \int_{\Gamma\setminus\Gamma^{tr}}(\{\nabla\Pi w\}\cdot[\![v]\!] + \{\nabla\Pi v\}\cdot[\![w]\!])ds \\ &+ \int_{\Gamma\setminus\Gamma^{tr}}\frac{\gamma_0}{\mathbf{h}}[\![w]\!]\cdot[\![v]\!]ds + \int_{\Gamma^{tr}} C_{tr}[\![w]\!]\cdot[\![v]\!]ds.\end{aligned} \tag{3.19}$$

and

$$|||v_h||| := \Big(\sum_{K\in\mathcal{T}} \|\nabla v_h\|_K^2 + \|\sqrt{\gamma_0/\mathbf{h}}[\![v_h]\!]\|_{\Gamma\setminus\Gamma^{tr}}^2 + C_{tr}\|[\![v_h]\!]\|_{\Gamma^{tr}}^2 \Big)^{\frac{1}{2}}. \tag{3.20}$$

Proof. We begin by assessing the coercivity of the dG bilinear form D_h on $S_h^p \times S_h^p$, thereby further determining the discontinuity-penalization parameter γ_0. To this end, we have

$$\begin{aligned} D_h(v_h, v_h) = \sum_{K\in\mathcal{T}} \int_K (\nabla v_h)^2 dx - 2\int_{\Gamma\setminus\Gamma^{tr}} \{\nabla v_h\}\cdot[\![v_h]\!] ds + \int_{\Gamma\setminus\Gamma^{tr}} \frac{\gamma_0}{\mathbf{h}}[\![v_h]\!]^2 ds \\ + \int_{\Gamma^{tr}} C_{tr}[\![v_h]\!]^2 ds. \end{aligned}$$

To bound the second term in the above equation. Using the Cauchy-Schwartz inequality and Lemma 3.12, we obtain

$$\begin{aligned} 2\int_{\Gamma\setminus\Gamma^{tr}} \{\nabla v_h\}\cdot[\![v_h]\!]\, ds &\le \Big(\sum_{E\subset\Gamma\setminus\Gamma^{tr}} \|\sqrt{\mathbf{h}/\gamma_0}\{\nabla v_h\}\|_E^2 \Big)^{\frac{1}{2}} \|\sqrt{\gamma_0/\mathbf{h}}[\![v_h]\!]\|_{\Gamma\setminus\Gamma^{tr}} \\ &\le C\Big(\sum_{E\subset\partial K, E\subset\Gamma\setminus\Gamma^{tr}} \|\sqrt{\mathbf{h}/\gamma_0}\nabla v_h\|_{E\cap\partial K}^2 \Big)^{\frac{1}{2}} \|\sqrt{\gamma_0/\mathbf{h}}[\![v_h]\!]\|_{\Gamma\setminus\Gamma^{tr}} \\ &\le C\Big(\sum_{K\in\mathcal{T}} \|\gamma_0^{-1/2}\nabla v_h\|_K^2 \Big)^{\frac{1}{2}} \|\sqrt{\gamma_0/\mathbf{h}}[\![v_h]\!]\|_{\Gamma\setminus\Gamma^{tr}}. \\ &\le \frac{C}{2}\sum_{K\in\mathcal{T}} \|\gamma_0^{-1/2}\nabla v_h\|_K^2 + \frac{1}{2}\|\sqrt{\gamma_0/\mathbf{h}}[\![v_h]\!]\|_{\Gamma\setminus\Gamma^{tr}}^2. \end{aligned} \tag{3.21}$$

Choosing $\gamma_0 > C$, we obtain

$$2\int_{\Gamma\setminus\Gamma^{tr}} \{\nabla v_h\}\cdot[\![v_h]\!]\, ds \le \frac{1}{2}\sum_{K\in\mathcal{T}} \|\nabla v_h\|_K^2 + \frac{1}{2}\|\sqrt{\gamma_0/\mathbf{h}}[\![v_h]\!]\|_{\Gamma\setminus\Gamma^{tr}}^2.$$

The continuity property follows analogously to (3.21), giving

$$\begin{aligned} \int_{\Gamma\setminus\Gamma^{tr}} \{\nabla \Pi w\}\cdot[\![v]\!]\, ds &\le \Big(\sum_{E\subset\Gamma\setminus\Gamma^{tr}} \|\sqrt{\mathbf{h}/\gamma_0}\nabla\Pi w\|_E^2 \Big)^{\frac{1}{2}} \|\sqrt{\gamma_0/\mathbf{h}}[\![v]\!]\|_{\Gamma\setminus\Gamma^{tr}} \\ &\le C\Big(\sum_{E\subset\partial K, E\subset\Gamma\setminus\Gamma^{tr}} \|\sqrt{\mathbf{h}/\gamma_0}\nabla\Pi w\|_{E\cap\partial K}^2 \Big)^{\frac{1}{2}} \|\sqrt{\gamma_0/\mathbf{h}}[\![v]\!]\|_{\Gamma\setminus\Gamma^{tr}} \\ &\le \Big(\sum_{K\in\mathcal{T}} \|\nabla w\|_K^2 \Big)^{\frac{1}{2}} \|\sqrt{\gamma_0/\mathbf{h}}[\![v]\!]\|_{\Gamma\setminus\Gamma^{tr}}, \end{aligned} \tag{3.22}$$

and similarly,

$$\begin{aligned}\int_{\Gamma\setminus\Gamma^{tr}} \{\nabla \Pi v\}\cdot [\![w]\!]\, ds &\leq \Big(\sum_{E\subset\Gamma\setminus\Gamma^{tr}} \|\sqrt{\mathbf{h}/\gamma_0}\nabla\Pi v\|_E^2\Big)^{\frac{1}{2}} \|\sqrt{\gamma_0/\mathbf{h}}[\![w]\!]\|_{\Gamma\setminus\Gamma^{tr}} \\ &\leq \Big(\sum_{K\in\mathcal{T}} \|\nabla v\|_K^2\Big)^{\frac{1}{2}} \|\sqrt{\gamma_0/\mathbf{h}}[\![w]\!]\|_{\Gamma\setminus\Gamma^{tr}},\end{aligned}$$

Combing these results, gives the bound.

□

Chapter 4

A posteriori and a priori error estimates for dG methods for elliptic interface problems

4.1 Introduction

We shall prove a reliable and efficient a posteriori error estimate for elliptic for the interior penalty discontinuous Galerkin (dG) method for the elliptic interface equation. The a posteriori error estimate is derived under the assumption that the triangulation is aligned with the interfaces although, crucially, extremely general curved element shapes are also allowed, as discussed above.

Let u be the exact solution of a PDE and u_h be some finite element approximation; an a posteriori error estimator Υ with Υ depending only on the the u_h and the PDE data is an approximation of the error $e := u - u_h$, in a certain norm $\|.\|$ such that $\|.\| \leq \Upsilon$. A posteriori estimates can be used to estimate the local error distribution, and can be incorporated in an adaptive algorithm. Such bounds are useful not only for adaptivity but also for the quality assessment of the approximate solution. An a posteriori estimator, Υ, is said to be reliable if there is C > 0, independent of the exact solution u and of u_h, such that

$$\|e\| \leq C\Upsilon, \tag{4.1}$$

while Υ is said to be efficient if there is $c > 0$, independent of the exact solution u and of u_h, such that

$$c\Upsilon \leq \|e\|. \tag{4.2}$$

The constants appearing in equations (4.1) and (4.2) are not always explicitly calculable. Related to this is the useful notion of the efectivity index, which defined as the ratio of the posteriori error indicator and the dG-norm of the actual error. We stress that the posteriori error bounds that derived for elliptic interface problem will be the key ingredient in the study of the error for non linear parabolic modelling in Chapter 5 .

4.2 A posteriori error bound

We begin by assessing the coercivity of the dG bilinear form D_h on $S_h^p \times S_h^p$, with respect to the dG-energy norm

$$|||v_h||| := \Big(\sum_{K\in\mathcal{T}} \|\nabla v_h\|_K^2 + \|\sqrt{\gamma_0/\mathbf{h}}[\![v_h]\!]\|_{\Gamma\setminus\Gamma^{tr}}^2 + C_{tr}\|[\![v_h]\!]\|_{\Gamma^{tr}}^2 \Big)^{\frac{1}{2}}, \tag{4.3}$$

for $\gamma_0 \equiv \gamma_0(p) > 0$ sufficiently large. We note carefully that the definition of the discontinuity-pernalization parameter γ_0 to be given below will only depend on the polynomial degree p and the shape-regularity of the mesh, through the respective dependence of the inverse estimates from Lemmata 3.11 and 3.12.

Letting $\Pi : L_2(\Omega) \to S_h^p$ denote the orthogonal L_2-projection operator onto the discontinuous finite element space, we begin by defining the a posteriori error indicator

$$\Upsilon := \Big(\sum_{K\in\mathcal{T}} \Upsilon_K^2 \Big)^{1/2}, \quad \text{with} \quad \Upsilon_K := \Big(\Upsilon_{R_K}^2 + \Upsilon_{E_K}^2 + \Upsilon_{J_K}^2 + \Upsilon_{Tr_K}^2 \Big)^{1/2}, \tag{4.4}$$

comprising of the interior, normal flux, jump and interface residuals

$$\Upsilon_{R_K} := \|\mathbf{h}(\Pi f + \Delta u_h)\|_K, \quad \Upsilon_{E_K} := \|\sqrt{\mathbf{h}}[\![\nabla u_h]\!]\|_{\partial K\cap\Gamma^{int}},$$
$$\Upsilon_{J_K} := \|\gamma_0\mathbf{h}^{-1/2}[\![u_h]\!]\|_{\partial K\cap\Gamma\setminus\Gamma^{tr}}, \ \Upsilon_{Tr_K} := \sum_{i=1}^{2} \|\sqrt{\mathbf{h}}(C_{tr}[\![u_h]\!] + \nabla u_h)\cdot\mathbf{n}^i\|_{\partial K\cap\Gamma^{tr}}.$$

We also define the data oscillation term

$$\Theta_1 := \|\mathbf{h}(f - \Pi f)\|,$$

along its restriction on each K, $\Theta_{1,K} := \|\mathbf{h}(f - \Pi f)\|_K$.

4.2.1 Upper bound

For the proof of an a posteriori bound, we use the conforming recovery operator. To this end, we decompose the error into conforming and non-conforming parts $u - u_h = e^c + u_h^d$, with $e^c := u - \mathcal{E}(u_h)$ and $u_h^d := \mathcal{E}(u_h) - u_h$, noting that $e^c \in \mathcal{H}_0^1$.

Then, from (3.19) we have immediately that $\hat{D}_h(w, v) = D_h(w, v)$ for all $w, v \in S_h^p$, and also $\hat{D}_h(w, v) = D(w, v)$ for all $w, v \in \mathcal{H}_0^1$. The error equation can be derived as follows

$$\begin{aligned}
|||e^c|||^2 &= D(e^c, e^c) = D(u, e^c) - \hat{D}_h(u_h, e^c) - \hat{D}_h(u_h^d, e^c) \\
&= \int_\Omega f e^c \, dx - \hat{D}_h(u_h, e^c) - \hat{D}_h(u_h^d, e^c) + D_h(u_h, \Pi_0 e^c) - \int_\Omega f \Pi_0 e^c \, dx \\
&= \Big(\int_\Omega f(e^c - \Pi_0 e^c) \, dx - \hat{D}_h(u_h, e^c - \Pi_0 e^c) \Big) - \hat{D}_h(u_h^d, e^c) =: I - II.
\end{aligned}$$

We estimate the terms I and II above in the following lemmata.

Lemma 4.1. *We have*

$$I \le C\big(\Upsilon^2 + \Theta_1^2\big)^{1/2} \|\nabla e^c\|,$$

for $\gamma_0 = \gamma \max\{\sqrt{\theta\eta}, 1\}$ *for some* $\gamma > 1$ *large enough.*

Proof. Integration by parts yields

$$\begin{aligned}
I = &\sum_{K \in \mathcal{T}} \int_K (f + \Delta u_h)(e^c - \Pi_0 e^c) \, dx - \int_{\Gamma^{int}} [\![\nabla u_h]\!] \cdot \{e^c - \Pi_0 e^c\} ds \\
&+ \int_{\Gamma \setminus \Gamma^{tr}} [\![u_h]\!] \cdot \{\nabla \Pi (e^c - \Pi_0 e^c)\} ds - \int_{\Gamma \setminus \Gamma^{tr}} \frac{\gamma_0}{\mathbf{h}} [\![u_h]\!] \cdot [\![e^c - \Pi_0 e^c]\!] ds \qquad (4.5) \\
&- \int_{\Gamma^{tr}} \Big(C_{tr} [\![u_h]\!] \cdot [\![e^c - \Pi_0 e^c]\!] + [\![\nabla u_h (e^c - \Pi_0 e^c)]\!] \Big) ds.
\end{aligned}$$

We focus on estimating the third term on the right-hand side of (4.5), which can be bounded as

$$\|\gamma_0^{-1} \sqrt{\mathbf{h}} \{\nabla \Pi (e^c - \Pi_0 e^c)\}\|_{\Gamma \setminus \Gamma^{tr}} \|\gamma_0 \mathbf{h}^{-1/2} [\![u_h]\!]\|_{\Gamma \setminus \Gamma^{tr}}. \qquad (4.6)$$

The term involving e^c can be further bounded by

$$\begin{aligned}
&\sum_{E\in\Gamma\setminus\Gamma^{tr}} \|\gamma_0^{-1}\sqrt{\mathbf{h}}\{\nabla\Pi(e^c-\Pi_0 e^c)\}\|_E^2 \le C\sum_{K\in\mathcal{T}} \|\gamma_0^{-1}\nabla\Pi(e^c-\Pi_0 e^c)\|_K^2\\
&\le C\sum_{K\in\mathcal{T}} \|\gamma_0^{-1}\sqrt{\theta}\nabla\Pi(e^c-\Pi_0 e^c)\|_{\tilde{K}}^2 \le C\sum_{K\in\mathcal{T}} \|(\gamma_0\mathbf{h})^{-1}\sqrt{\theta}\Pi(e^c-\Pi_0 e^c)\|_{\tilde{K}}^2\\
&\le C\sum_{K\in\mathcal{T}} \|\sqrt{\theta\eta}(\gamma_0\mathbf{h})^{-1}\Pi(e^c-\Pi_0 e^c)\|_K^2 \le C\sum_{K\in\mathcal{T}} \|\nabla e^c\|_K^2,
\end{aligned}$$

using Lemma 3.12, Lemma 3.6, a standard inverse estimate on $\tilde{K}$, and Lemma 3.7, respectively, upon selecting $\gamma_0=\gamma\max\{\sqrt{\theta\eta},1\}$ for some $\gamma>1$ large enough; hence, we get

$$\int_{\Gamma\setminus\Gamma^{tr}} [\![u_h]\!]\cdot\{\nabla\Pi(e^c-\Pi_0 e^c)\}ds \le C\|\gamma_0\mathbf{h}^{-1/2}[\![u_h]\!]\|_{\Gamma\setminus\Gamma^{tr}}\|\nabla e^c\|.$$

Working in a standard fashion for the remaining terms, we deduce

$$\begin{aligned}
I \le C\Big(\sum_{K\in\mathcal{T}} h_K^2\|f+\Delta u_h\|_K^2 + \|\sqrt{\mathbf{h}}[\![\nabla u_h]\!]\|_{\Gamma^{int}}^2 + \|\gamma_0\mathbf{h}^{-1/2}[\![u_h]\!]\|_{\Gamma\setminus\Gamma^{tr}}^2\Big)^{\frac{1}{2}}\|\nabla e^c\|\\
+ C\sum_{i=1}^{2}\sum_{K\in\mathcal{T}^{tr}} \|\sqrt{\mathbf{h}}(C_{tr}[\![u_h]\!]+\nabla u_h)\cdot\mathbf{n}^i\|_{\partial K\cap\Gamma^{tr}}\|\nabla e^c\|_K,
\end{aligned}$$

using the approximation bounds given in Lemma 3.4. The result already follows. □

To estimate II, we use (3.18) for $\hat{D}_h$, along with the following bound.

Lemma 4.2. *With the above mesh assumptions and with γ_0 as in the statement of Lemma 4.1, we have*

$$|||u_h^d|||^2 \le C\sum_{K\in\mathcal{T}} \big(\gamma^{-1}+\gamma^{-2}(1+h_K C_{tr})\big)\Upsilon_{J_K}^2, \tag{4.7}$$

for $C>0$ generic constant, independent of $\mathbf{h}$ and of u_h.

Proof. Using Lemma 3.14, we have

$$\begin{aligned}
\sum_{K\in\mathcal{T}} \|\nabla u_h^d\|_K^2 + \|\sqrt{\gamma_0/\mathbf{h}}[\![u_h^d]\!]\|_{\Gamma\setminus\Gamma^{tr}}^2 &\le \sum_{E\subset\Gamma\setminus\Gamma^{tr}} \|\sqrt{\theta\eta}\mathbf{h}^{-1/2}[\![u_h^d]\!]\|_E^2 + \|\gamma_0(\gamma\mathbf{h})^{-1/2}[\![u_h^d]\!]\|_{\Gamma\setminus\Gamma^{tr}}^2\\
&\le C\sum_{K\in\mathcal{T}} (C_1\gamma^{-2}+\gamma^{-1})\Upsilon_{J_K}^2,
\end{aligned}$$

For the third term on the right hand side of (4.3), we use (3.1) and Lemma 3.14 once more to deduce

$$C_{tr}\|[\![u_h^d]\!]\|_{\Gamma^{tr}}^2 \leq 2C_{tr}\sum_{j=1}^{2}\|u_h^d|_{\Omega_j}\|_{\Gamma^{tr}}^2 \leq 2CC_{tr}\sum_{K\in\mathcal{T}^{tr}}\left(h_K\|\nabla u_h^d\|_K^2 + h_K^{-1}\|u_h^d\|_K^2\right)$$
$$\leq 2CC_{tr}\Big(\big(C_1+C_0\big)\sum_{E\subset\Gamma^{int}}\|\sqrt{\theta\eta}[\![u_h]\!]\|_E^2\Big) \leq CC_{tr}\Big(\gamma^{-2}\sum_{K\in\mathcal{T}}h_K\Upsilon_{J_K}^2\Big).$$

Combining the last two bounds yields the result. □

Theorem 4.3 (Upper bound)**.** *Let u be the solution of (2.5) and let $u_h \in S_h^p$ be its dG approximation with γ_0 as in the statement of Lemma 4.1. Then, we have the following a posteriori error bound*

$$|||u-u_h|||^2 \leq C\left(\Upsilon^2+\Theta_1^2\right) + C\sum_{K\in\mathcal{T}}\left(\gamma^{-1}+\gamma^{-2}(1+h_KC_{tr})\right)\Upsilon_{J_K}^2. \tag{4.8}$$

Proof. The proof follows immediately from the error equation, the bounds on I and on II, along with the triangle inequality $|||u-u_h||| \leq |||e^c||| + |||u_h^d|||$. □

4.2.2 Lower bound

We employ standard bubble functions, [60], to show lower bounds for the above a posteriori estimator. A key challenge to overcome is the shape of interface elements $K \in \mathcal{T}^{tr}$, for which we do not posses any stability properties of respective elemental or face bubble functions. We shall overcome this by employing bubble functions on $\underline{K}$ and on $\underline{E}$ instead.

To this end, we denote by ω_E the union of the elements sharing an interior face $E \in \Gamma^{int}\backslash\Gamma_{tr}^{int}$, and by ψ_K and ψ_E the (standard) element and face bubble functions [60]. The functions $\psi_K \in H_0^1(K)$ and $\psi_E \in H_0^1(\omega_E)$ are such that $\|\psi_K\|_{L_\infty(K)} = 1$, and $\|\psi_E\|_{L_\infty(E)} = 1$. Moreover, for each $v \in S_h^p$, there exist positive constants c_1, c_2, independent of $\mathbf{h}$ and of v, such that

$$\|v\|_K^2 \leq c_1\|\sqrt{\psi_K}v\|_K^2, \quad \|v\|_E^2 \leq c_2\|\sqrt{\psi_E}v\|_E^2, \tag{4.9}$$

for all $K \in \mathcal{T}\backslash\mathcal{T}^{tr}$ and $E \subset \Gamma^{int}\backslash\Gamma_{tr}^{int}$. When $K \in \mathcal{T}^{tr}$ or when $E \in \Gamma_{tr}^{int}$, (4.9) holds for $\underline{K}$ or $\underline{E}$ instead, respectively, so that, by Lemma 3.6 and Lemma 3.7,

$$\|v\|_K^2 \leq \theta\eta(K)\|v\|_{\underline{K}}^2 \leq c_1\theta\eta(K)\|\sqrt{\psi_{\underline{K}}}v\|_{\underline{K}}^2, \tag{4.10}$$

where $\theta\eta(K) := \theta_{inv}(K)\eta_{inv}(K)$ and

$$\|v\|_E^2 \leq \theta\eta(E)\|v\|_{\underline{E}}^2 \leq c_2\theta\eta(E)\|\sqrt{\psi_{\underline{E}}}v\|_{\underline{E}}^2, \tag{4.11}$$

with $\theta\eta(E) := \theta_{inv}(E)\eta_{inv}(E)$. To treat both the cases $K \in \mathcal{T}\backslash\mathcal{T}^{tr}$ and $K \in \mathcal{T}^{tr}$ simultaneously, we shall carry over the θ and η terms (along with $\underline{K}$ and $\underline{E}$) for all $K \in \mathcal{T}$, recalling that $\theta_{inv}(K) = 1 = \eta_{inv}(K)$ (and $\underline{K} = K$, $\underline{E} = E$) when $K \in \mathcal{T}\backslash\mathcal{T}^{tr}$.

We can now show a lower bound for the a posteriori error estimator.

Theorem 4.4 (Lower bound)**.** *Let u be the solution of (2.5) and let $u_h \in S_h^p$ the dG solution given by* (2.21)*. Then, for all $K \in \mathcal{T}$, we have the following bound*

$$\Upsilon_{R_K}^2 + \Upsilon_{E_K}^2 \leq C \sum_{K' \in \omega_K} (\theta\eta(K'))^2\big(\|\nabla(u-u_h)\|_{K'}^2 + \Theta_{1,K'}^2\big), \tag{4.12}$$

where $\omega_K := \{K' \in \mathcal{T} : meas_{d-1}((\partial K \cap \partial K')\setminus\Gamma^{tr}) \neq 0\}$. Further, for two elements $K_i \in \mathcal{T}^{tr}$ sharing a face $E \subset \Gamma^{tr}$, we have the bound

$$\sum_{i=1}^{2} \|\sqrt{\mathbf{h}}(C_{tr}[\![u_h]\!]+\nabla u_h)\cdot\tilde{\mathbf{n}}^i\|_{\tilde{E}_i}^2 \leq\ C\sum_{i=1}^{2}\Big((\theta\eta(K_i))^2\big(\|\nabla(u-u_h)\|_{K_i}^2+\Theta_{1,K_i}^2\big)+\Theta_{2,K_i}^2\Big), \tag{4.13}$$

where $\tilde{E}_i := \tilde{E} \cap \partial\tilde{K}_i$, $i = 1, 2$, represent the related faces $\tilde{E}$, signifying that the values of a function on $\tilde{E}_i$ are taken from within $\tilde{K}_i$. Also, $\tilde{\mathbf{n}}^i$ denote the respective outward normal to $\tilde{E}_i$. Finally, $\Theta_{2,K_i} := |\tilde{K}_i \triangle K_i| h_{K_i}^{-d}\|C_{tr}[\![u_h]\!] + \nabla u_h\|_{\tilde{E}_i}$ is the interface oscillation term*, with $P \triangle Q := (P\backslash Q) \cup (Q\backslash P)$ denoting the symmetric difference between two sets P and Q.*

Proof. We first prove (4.12). For the interior residual, for $K \in \mathcal{T}$, we set $R|_K := (\Pi f + \Delta u_h)|_K$, and $M|_K := h_K^2 R\psi_{\underline{K}}$. Then, using (4.10), we have

$$\Upsilon_{R_K}^2 = h_K^2\|R\|_K^2 \leq c_1\theta\eta(K)h_K^2\|\sqrt{\psi_{\underline{K}}}R\|_{\underline{K}}^2 = c_1\theta\eta(K)\langle\Pi f + \Delta u_h, M\rangle_{\underline{K}}. \tag{4.14}$$

Using integration by parts along with (2.6) yields

$$\begin{aligned}\langle\Pi f + \Delta u_h, M\rangle_{\underline{K}} &= \langle\nabla(u-u_h), \nabla M\rangle_{\underline{K}} + \langle\Pi f - f, M\rangle_{\underline{K}} \\ &\leq \|\nabla(u-u_h)\|_K\|\nabla M\|_{\underline{K}} + h_K\|\Pi f - f\|_K h_K^{-1}\|M\|_{\underline{K}}.\end{aligned} \tag{4.15}$$

Further, as $h_K \sim h_{\underline{K}}$, we have $\|\nabla M\|^2_{\underline{K}} \leq Ch_K^{-2}\|M\|^2_{\underline{K}} \leq Ch_K^2\|R\|^2_K$, which, used on (4.15) and in view of (4.14), implies

$$\Upsilon^2_{R_K} \leq C\theta\eta(K)\big(\|\nabla(u-u_h)\|_K + \|\mathbf{h}(\Pi f - f)\|_K\big)\Upsilon_{R_K}, \tag{4.16}$$

which already gives the required bound.

For the normal flux residual, for $E \subset \Gamma^{int}$, we set $\omega_E := K_1 \cup K_2 \cup E$ with $K_1, K_2 \in \mathcal{T}$ such that $E = \partial K_1 \cap \partial K_2$ and, on ω_E, we define the function $\tau_E := h(E)[\![\nabla u_h]\!]\psi_{\underline{E}\cap\partial\underline{K}_1\cap\partial\underline{K}_2}$. Here, $[\![\nabla u_h]\!]$ in ω_E is understood as its constant extension in the normal direction to E. (Notice that $E \in \Gamma\backslash\Gamma^{tr}$ is *not* curved, so there is a unique normal direction to E.) Since $[\![\nabla u]\!] = 0$ on Γ^{int}, and $\tau_E|_{\partial\omega_E} = 0$, with $\omega_E = K_1 \cup K_2 \cup E$ we have, for $K \in \mathcal{T}$,

$$\Upsilon^2_{E_K} \leq c_2 \sum_{E\subset\partial K\cap\Gamma^{int}} \theta\eta(E)\langle[\![\nabla u_h]\!], \tau_E\rangle_E = c_2 \sum_{E\subset\partial K\cap\Gamma^{int}} \theta\eta(E)\langle[\![\nabla(u_h-u)]\!], \tau_E\rangle_E. \tag{4.17}$$

Integration by parts and (2.6) imply

$$\begin{aligned}\langle[\![\nabla(u_h-u)]\!], \tau_E\rangle_E &= \langle\Delta u_h + f, \tau_E\rangle_{\omega_E} + \langle\nabla(u_h-u), \nabla\tau_E\rangle_{\omega_E} \\ &= \langle\Pi f + \Delta u_h, \tau_E\rangle_{\omega_E} + \langle f - \Pi f, \tau_E\rangle_{\omega_E} + \langle\nabla(u_h-u), \nabla\tau_E\rangle_{\omega_E}.\end{aligned} \tag{4.18}$$

Observing that $\tau_E = 0$ on $(K_1\cup K_2\cup E)\backslash(\underline{K}_1\cup\underline{K}_2\cup(\underline{E}\cap\partial\underline{K}_1\cap\partial\underline{K}_2))$, a standard inverse estimate implies $\|\nabla\tau_E\|^2_{\underline{K}_i} \leq Ch_{K_i}^{-2}\|\tau_E\|^2_{\underline{K}_i} \leq Ch_{K_i}\|[\![\nabla u_h]\!]\|^2_{\underline{E}\cap\partial\underline{K}_i}$, which, used on (4.18) and in view of (4.17), implies

$$\Upsilon^2_{E_K} \leq Cc_2\bigg(\sum_{K'\in\omega_K}\big(\Upsilon^2_{R_{K'}} + \Theta^2_{K'}\big)^{\frac{1}{2}}\bigg)\Upsilon_{E_K}. \tag{4.19}$$

We now prove the bound on the interface residual (4.12). For $E \subset \partial K_1\cap\partial K_2\cap\Gamma^{tr}$, we consider the related face $\tilde{E}$ of $\tilde{K}_i$, $i = 1, 2$, and let also $\tilde{\mathbf{n}}$ signify the normal vector to $\tilde{E}$. We consider the face bubble $\psi^i_{\tilde{E}}$ supported in $\tilde{K}_i$, $i = 1, 2$, respectively. We shall also make use of the extension and/or restriction of $\psi^i_{\tilde{E}}$ onto K_i, $i = 1, 2$, denoted for simplicity also by $\psi^i_{\tilde{E}}$. Therefore, $\psi^i_{\tilde{E}} = 0$ on $\partial K_i\backslash E$ also, since $\psi^i_{\tilde{E}}$ is constructed to vanish on the $(d-1)$-dimensional hyperplanes containing the (straight) faces of K_i not belonging to the interface. We define

$$r^i_E := h(E)\big((C_{tr}[\![u_h]\!] + \nabla u_h)\cdot\tilde{\mathbf{n}}\,\psi^i_{\tilde{E}}\big)|_{K_i},$$

for $i = 1, 2$, where $(C_{tr}[\![u_h]\!] + \nabla u_h) \cdot \tilde{\mathbf{n}}$ in K_i is understood as its constant extension in the $\tilde{\mathbf{n}}$-direction. Setting $r_E|_{K_i} := r_E^i$, $i = 1, 2$, we have $r_E \in \mathcal{H}_0^1$ by construction. Using the interface conditions in 2.5 along with (2.6), we deduce

$$\begin{aligned} &\sum_{i=1}^{2} \langle (C_{tr}[\![u_h]\!] + \nabla u_h) \cdot \mathbf{n}^i, r_E \rangle_{E_i} \\ &= \langle C_{tr}[\![u_h - u]\!], [\![r_E]\!] \rangle_E + \langle \Delta u_h + f, r_E \rangle_{K_1 \cup K_2} + \langle \nabla (u_h - u), \nabla r_E \rangle_{K_1 \cup K_2}, \end{aligned} \tag{4.20}$$

with $E_i := E \cap \partial K_i$, and $\mathbf{n}^i := \mathbf{n}|_{\Omega_i}$. Setting $N := C_{tr}[\![u_h]\!] + \nabla u_h$ for brevity, and using (4.20), we get

$$\begin{aligned} c_2^{-1} \sum_{i=1}^{2} \|\sqrt{\mathbf{h}} N \cdot \tilde{\mathbf{n}}^i\|_{\tilde{E}_i}^2 &\leq \sum_{i=1}^{2} \langle N \cdot \tilde{\mathbf{n}}^i, r_E \rangle_{\tilde{E}_i} \\ &= \langle C_{tr}[\![u_h - u]\!], [\![r_E]\!] \rangle_E + \langle \Delta u_h + f, r_E \rangle_{K_1 \cup K_2} + \langle \nabla (u_h - u), \nabla r_E \rangle_{K_1 \cup K_2} \\ &\quad + \sum_{i=1}^{2} \Big(\langle N \cdot \tilde{\mathbf{n}}^i, r_E \rangle_{\tilde{E}_i} - \langle N \cdot \mathbf{n}^i, r_E \rangle_{E_i} \Big). \end{aligned} \tag{4.21}$$

Note that $\sqrt{\mathbf{h}} N \cdot \tilde{\mathbf{n}}^i$ is a polynomial and, therefore, the constant c_2 in the first inequality above is *independent* of E. Now, recalling that E and $\tilde{E}$ have the same endpoints, for the last two terms on the right-hand side of (4.21), we have

$$\langle N \cdot \tilde{\mathbf{n}}^i, r_E \rangle_{\tilde{E}_i} - \langle N \cdot \mathbf{n}^i, r_E \rangle_{E_i} = \oint_{\tilde{E}_i \cup E_i} (N r_E) \cdot \mathbf{n} \, ds = \int_{\tilde{K}_i \triangle K_i} \nabla \cdot (N r_E) \, dx, \tag{4.22}$$

from the divergence theorem.

Combining (4.21) and (4.22), along with the Cauchy-Schwarz inequality yields

$$\begin{aligned} &c_2^{-1} \sum_{i=1}^{2} \|\sqrt{\mathbf{h}} N \cdot \tilde{\mathbf{n}}^i\|_{\tilde{E}_i}^2 \\ &\leq \|C_{tr}[\![u_h - u]\!]\|_E \|[\![r_E]\!]\|_E + \sum_{i=1}^{2} \Big(\|\nabla (u_h - u)\|_{K_i} \|\nabla r_E^i\|_{K_i} \\ &\qquad + \|\mathbf{h}(\Delta u_h + f)\|_{K_i} \|\mathbf{h}^{-1} r_E^i\|_{K_i} + \|\nabla \cdot (N r_E)\|_{L^1(\tilde{K}_i \triangle K_i)} \Big). \end{aligned} \tag{4.23}$$

Now, Lemma 3.5, and a standard inverse estimate give, respectively,

$$\begin{aligned} \|\nabla r_E^i\|_{K_i}^2 &\leq C h_{K_i}^d \|\nabla r_E^i\|_{L^\infty(K_i)}^2 = C h_{K_i}^d \|\nabla r_E^i\|_{L^\infty((K_i)_\flat(\nabla r_E^i))}^2 \\ &\leq C h_{K_i}^{d-2} \|r_E^i\|_{L^\infty((K_i)_\flat(\nabla r_E^i))}^2 \leq C h_{K_i}^{d-2} \|r_E^i\|_{L^\infty(K_i)}^2 \\ &= C h_{K_i}^{d-2} \|r_E^i\|_{L^\infty(\tilde{E}_i)}^2 \leq C h_{K_i}^{-1} \|r_E^i\|_{\tilde{E}_i}^2 \leq C \|\sqrt{\mathbf{h}} N \cdot \tilde{\mathbf{n}}^i\|_{\tilde{E}_i}^2, \end{aligned}$$

since r_E^i is constant in the direction of $\tilde{\mathbf{n}}^i$. Also, from Lemma 3.11, we have

$$\|r_E^i\|_{E_i}^2 \leq Ch_{K_i}^{-1}\|r_E^i\|_{K_i}^2 \leq Ch_{K_i}^{d-1}\|r_E^i\|_{L^\infty(\tilde{E}_i)}^2 \leq Ch_{K_i}\|\sqrt{\mathbf{h}}N\cdot\tilde{\mathbf{n}}^i\|_{\tilde{E}_i}^2.$$

Finally, using Lemma 3.5, along with standard inverse estimates, we have

$$\begin{aligned}
\|\nabla\cdot(Nr_E)\|_{L^1(\tilde{K}_i\triangle K_i)} &\leq |\tilde{K}_i\triangle K_i|\|\nabla\cdot(Nr_E)\|_{L^\infty(\tilde{K}_i\triangle K_i)}\\
&\leq |\tilde{K}_i\triangle K_i|\|\nabla\cdot(Nr_E)\|_{L^\infty(\tilde{K}_i\cup K_i)}\\
&= |\tilde{K}_i\triangle K_i|\|\nabla\cdot(Nr_E)\|_{L^\infty((\tilde{K}_i\cup K_i)_\flat(Nr_E))}\\
&\leq C|\tilde{K}_i\triangle K_i|h_{K_i}^{-1}\|Nr_E\|_{L^\infty((\tilde{K}_i\cup K_i)_\flat(Nr_E))}\\
&\leq C|\tilde{K}_i\triangle K_i|h_{K_i}^{-1}\|Nr_E\|_{L^\infty(\tilde{E}_i)}\\
&\leq C|\tilde{K}_i\triangle K_i|h_{K_i}^{-d}\|Nr_E\|_{L^1(\tilde{E}_i)}\\
&\leq C|\tilde{K}_i\triangle K_i|h_{K_i}^{-d}\|N(\sqrt{\mathbf{h}}N\cdot\tilde{\mathbf{n}}^i)\|_{L^1(\tilde{E}_i)}\\
&\leq C|\tilde{K}_i\triangle K_i|h_{K_i}^{-d}\|N\|_{\tilde{E}_i}\|(\sqrt{\mathbf{h}}N\cdot\tilde{\mathbf{n}}^i)\|_{\tilde{E}_i}.
\end{aligned}$$

Combining the above bounds and using (4.16), we deduce from (4.23):

$$\begin{aligned}
\sum_{i=1}^{2}\|\sqrt{\mathbf{h}}N\cdot\tilde{\mathbf{n}}^i\|_{\tilde{E}_i}^2 \leq C\Big(\sum_{i=1}^{2}&\|\sqrt{\mathbf{h}}C_{tr}[\![u_h-u]\!]\|_{E_i}^2 + |\tilde{K}_i\triangle K_i|^2h_{K_i}^{-2d}\|N\|_{\tilde{E}_i}^2\\
&+(\theta\eta(K_i))^2\big(\|\nabla(u-u_h)\|_{K_i}^2+\|\mathbf{h}(\Pi f-f)\|_{K_i}^2\big)\Big),
\end{aligned}$$

which implies the result.

□

Remark 4.5. For the jump residual, we trivially have

$$\Upsilon_{J_K}^2 = \gamma_0\|\sqrt{\gamma_0/\mathbf{h}}[\![u-u_h]\!]\|_{\partial K\cap\Gamma\setminus\Gamma^{tr}}^2, \tag{4.24}$$

so it is omitted in the lower bound.

We observe that the interface oscillation term $\Theta_{2,K}$ is equal to zero when $K=\tilde{K}$, i.e., on non-curved elements. When $K\neq\tilde{K}$, the size of $\Theta_{2,K}$ depends on the ratio between the d-dimensional volume of the symmetric difference between K and $\tilde{K}$, divided by $h_K^d\sim|K|$.

4.3 A priori error bound

Since no a priori error bound is available for the (fitted) discontinuous Galerkin method proposed above for the elliptic interface problem, we use the above a posteriori bounds to show a basic a priori convergence result in the spirit of the celebrated work of Gudi [34]. Here, however, we need to account also for the oscillation term arising from the treatment of the interface.

Theorem 4.6. *Let $u \in \mathcal{H}_0^1$ and $u_h \in S_h^p$ be the solutions of (2.6) and (2.21) respectively. Then, the error bound*

$$|||u - u_h||| \leq C \inf_{v_h \in S_h^p} \Big(|||u - v_h||| + \Theta_1 + \Theta_2 \Big), \tag{4.25}$$

holds with $\Theta_2|_K := \Theta_{2,K}$, $K \in \mathcal{T}$.

Proof. Let $v_h \in S_h^p$ with $v_h \neq u_h$ and set $\psi := u_h - v_h \in S_h^p$. Coercivity, (2.6), (2.16), and continuity imply

$$\begin{aligned}
\frac{1}{2}|||u_h - v_h|||^2 &\leq \hat{D}_h(u_h - v_h, \psi) = \langle f, \psi \rangle - \hat{D}_h(v_h, \psi) \\
&= \hat{D}_h(u - v_h, \mathcal{E}(\psi)) + \langle f, \psi - \mathcal{E}(\psi) \rangle - \hat{D}_h(v_h, \psi - \mathcal{E}(\psi)) \\
&\leq C|||u - v_h|||\,|||\mathcal{E}(\psi)||| + \langle f, \psi - \mathcal{E}(\psi) \rangle - \hat{D}_h(v_h, \psi - \mathcal{E}(\psi)).
\end{aligned}$$

Noting that Lemma 3.14 implies $|||\mathcal{E}(\psi)||| \leq C|||\psi|||$, for some constant $C > 0$ depending on $\theta\eta$, after division by by $|||\psi|||$, we arrive at

$$|||u_h - v_h||| \leq C|||u - v_h||| + 2\frac{\langle f, \psi - \mathcal{E}(\psi) \rangle - \hat{D}_h(v_h, \psi - \mathcal{E}(\psi))}{|||\psi|||}. \tag{4.26}$$

Now, to estimate the second term on the right-hand side of (4.26), integration by parts gives

$$\begin{aligned}
\mathcal{R} &:= \int_\Omega f(\psi - \mathcal{E}(\psi))\,dx - \hat{D}_h(v_h, \psi - \mathcal{E}(\psi)) \\
&= \sum_{K \in \mathcal{T}} \int_K (f + \Delta v_h)(\psi - \mathcal{E}(\psi))\,dx - \int_{\Gamma^{int}} [\![\nabla v_h]\!] \cdot \{\psi - \mathcal{E}(\psi)\} ds \\
&\quad + \int_{\Gamma \setminus \Gamma^{tr}} [\![v_h]\!] \cdot \{\nabla \Pi(\psi - \mathcal{E}(\psi))\} ds - \int_{\Gamma \setminus \Gamma^{tr}} \frac{\gamma_0}{\mathbf{h}} [\![v_h]\!] \cdot [\![\psi]\!] ds \\
&\quad - \int_{\Gamma^{tr}} \Big(C_{tr} [\![v_h]\!] \cdot [\![\psi - \mathcal{E}(\psi)]\!] + [\![\nabla v_h (\psi - \mathcal{E}(\psi))]\!] \Big) ds.
\end{aligned} \tag{4.27}$$

Working in a standard fashion to estimate the terms on the right-hand side of (4.27), we have

$$\begin{aligned}\mathcal{R} \leq C\Big(\sum_{K\in\mathcal{T}} h_K^2\|f+\Delta v_h\|_K^2 + h_K\|[\![\nabla v_h]\!]\|^2_{\partial K\cap\Gamma^{int}} + h_K^{-1}\|[\![v_h]\!]\|^2_{\partial K\cap\Gamma\setminus\Gamma^{tr}}\Big)^{\frac{1}{2}} \\ \times \Big(\sum_{K\in\mathcal{T}} h_K^{-2}\|\psi-\mathcal{E}(\psi))\|_K^2\Big)^{\frac{1}{2}} \\ + \Big(\sum_{K\in\mathcal{T}^{tr}}\sum_{i=1}^{2} h_K\|(C_{tr}[\![v_h]\!]+\nabla v_h)\cdot\mathbf{n}^i\|^2_{\partial K\cap\Gamma^{tr}}\Big)^{\frac{1}{2}} \\ \times \Big(\sum_{j=1}^{2}\|\mathbf{h}^{-1/2}(\psi-\mathcal{E}(\psi))|_{\Omega_j}\|^2_{\Gamma_{tr}}\Big)^{\frac{1}{2}}.\end{aligned} \tag{4.28}$$

For the last term on the right-hand side of (4.28), we use Lemmata 3.11 and 3.14 to deduce

$$\sum_{j=1}^{2}\|\mathbf{h}^{-1/2}(\psi-\mathcal{E}(\psi))|_{\Omega_j}\|^2_{\Gamma_{tr}} \leq C\sum_{K\in\mathcal{T}^{tr}}\|\mathbf{h}^{-1}(\psi-\mathcal{E}(\psi))\|_K^2 \leq C\|\sqrt{\theta\eta}\mathbf{h}^{-1/2}[\![\psi]\!]\|^2_{\Gamma\setminus\Gamma^{tr}}.$$

Noting that the fact that u_h is the dG solution was not used in the proof of the lower bound (Theorem 4.4 above), it can be replaced by any $v_h \in S_h^p$. Therefore, Theorem 4.4 (with v_h replacing u_h) and the triangle inequality yield the result. □

The above result offers a basic convergence proof for the proposed (fitted) discontinuous Galerkin method for interface problems. Note that the regularity of solutions to such interface problems, which may involve *piecewise smooth* interface manifolds, is not well understood in the literature. Therefore, such basic convergence results, not requiring any regularity of the underlying solution, are desirable.

4.4 Higher order interface approximation

The saturation of the approximation of the geometry by the mesh, (3.5) and (3.6), is required to be satisfied for the above a posteriori error bounds to hold. One way of achieving this in practice is an initial refinement step in the vicinity of $\mathcal{T}^{tr}$. This approach is expected to deliver optimal convergence rates for the respective adaptive algorithm when $p = 1, 2$. Indeed, from the a priori error analysis of finite element methods with local basis of degree p and with boundary and/or

interface approximation, we can expect optimal convergence rates when the curved boundaries/interfaces are approximated locally by interpolants of degree $p-1$.

To ensure that the above interface approximation requirements (3.5), (3.6) do not result to potentially excessive and unnecessary refinement in the vicinity of Γ^{tr}, when higher order elements are used, we can employ a (non-standard) *fitted* approach based on parametric elemental mappings, which we shall now describe.

Each element $K \in \mathcal{T}^{tr}$ is assumed to be constructed via a parametric elemental mapping $F_K : \hat{K} \to K$ of polynomial degree $q \in \mathbb{N}$, from a *curved* reference element $\hat{K}$ with $|\hat{K}| \sim O(1)$.

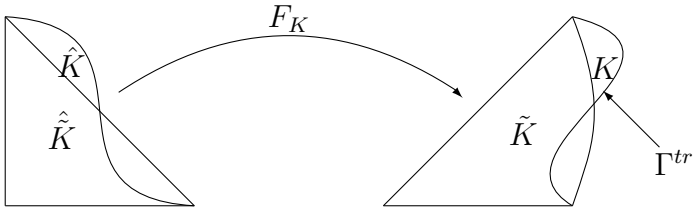

FIGURE 4.1: A curved element $K \in \mathcal{T}^{tr}$ and the related q-degree parametric element $\tilde{K}$ as the mapping of the respective reference elements $\hat{K}$ and $\hat{\tilde{K}}$.

More precisely, we begin by considering a parametric mesh of degree $q \in \mathbb{N}$, whose skeleton approximates the interface Γ^{tr} with a piecewise interpolant of degree q. Setting $\tilde{K}$ to be one such (unfitted) parametric element with non-trivial intersection with Γ^{tr}, we consider the q-degree parametric mapping $F_{\tilde{K}} : \hat{\tilde{K}} \to \tilde{K}$ with $\hat{\tilde{K}}$ being the (classical) reference element, i.e., it may be the d-simplex, the reference d-hypercube or the reference d-prism, the latter constructed as tensor-product of the reference $(d-1)$-simplex and the interval $[0,1]$. By considering the extension of $F_{\tilde{K}}$ on a larger domain $\hat{Y} \supset \hat{\tilde{K}}$ with the same (polynomial) formula, we can precisely define $\hat{Y}$ as the $F_{\tilde{K}}$-pre-image of $K \cup \tilde{K}$ where $K \in \mathcal{T}^{tr}$ is the *fitted* element related to $\tilde{K}$; we denote the extension of $F_{\tilde{K}}$ to $\hat{Y}$ by F_K. We refer to Figure 4.1 for an illustration. Hence, the reference element $\hat{K} := F_K^{-1}(K)$ will, in general, be curved.

We, now, define the *mapped* discontinuous finite element space $S_h^{p,q}$, subortinate to the mesh $\mathcal{T} = \{K\}$, by

$$S_h^{p,q} = \{v \in L^2(\Omega) : v \circ F_K^{-1}|_K \in \mathcal{R}_p(\hat{K})\}, \tag{4.29}$$

where $\mathcal{R}_p(\hat{K}) \in \{\mathcal{P}_p(\hat{K}), \mathcal{Q}_p(\hat{K})\}$, and $\mathcal{Q}_p(\hat{K})$ denotes space of tensor-product polynomials of degree p in each variable; when $\hat{\tilde{K}}$ is a d-simplex, we may select

$\mathcal{R}_p(\hat{K}) = \mathcal{P}_p(\hat{K})$, while we select $\mathcal{R}_p(\hat{K}) = \mathcal{Q}_p(\hat{K})$, in general, otherwise to ensure optimal approximation rates.

The key motivation for the above construction is that we can re-use the above developments in this fitted mapped setting also, by first applying the elemental mappings F_K and then use the results from Section 3.3 on the curved reference element $\hat{K}$ instead. An inspection of the proofs from Section 3.3 shows that *all* results hold true in this setting also, with the constants in the estimates now depending also on the nature of the mapping F_K, as is standard in parametric finite elements.

4.5 Numerical experiments

We shall now illustrate the performance of the a posteriori error estimator within a standard adaptive algorithm, through an implementation based on the `deal.II` finite element library [7]. This allows for the use of curved elements via high-order parametric mappings of tensor-product reference elements. We take advantage this capability and approximate curved interfaces via tensor-product elements defined through parametric mappings of degree *higher* than linear, as described in Section 4.4.

Although not discussed above merely for simplicity of the presentation, the extension of the proposed dG method to problems with non-homogeneous Dirichlet boundary conditions is straightforward; the a posteriori bound is then modified accordingly [42]. In all cases considered below the interface residual term $\Theta_{2,K}$ was omitted due to its insignificant magnitude (Example 1 below) or simply because it is equal to zero (Example 2 below). We set $\gamma = 10$ throughout.

4.5.1 Example 1

We consider the problem (2.6) with $\Omega = (-1, 1)^2$ and the interface Γ^{tr} being a circle of radius $r = 0.5$, centred at the origin. The Dirichlet boundary conditions and the source term f are determined by the exact solution

$$u = \begin{cases} r^3, & \text{in } \Omega_1 \\ r^3 + 1, & \text{in } \Omega_2 \end{cases}$$

DoFs	estimator	rate	$\|\|\|.\|\|\|$-error	rate	L^2-error	H^1-error
192	1.3381e+01	—	1.7550e+00	—	6.2516e-02	1.3886e+00
768	7.6174e+00	0.81	8.4388e-01	1.06	2.0201e-02	7.2406e-01
3072	3.9838e+00	0.94	3.9950e-01	1.08	5.7567e-03	3.6434e-01
12288	2.0259e+00	0.95	1.9147e-01	1.06	1.5192e-03	1.8187e-01
49152	1.0202e+00	0.99	9.3267e-02	1.04	3.8765e-04	9.0744e-02
196608	5.1826e-01	0.98	4.6010e-02	1.02	9.7624e-05	4.5323e-02

TABLE 4.1: Example 1. Convergence of estimator and errors; quadratic mapping with $p = 1$.

DoFs	estimator	rate	$\|\|\|.\|\|\|$-error	rate	L^2-error	H^1-error
432	1.8278e+00	—	4.5728e-01	—	7.6800e-03	1.9028e-01
1728	3.8913ee-01	2.2	8.4015e-02	2.44	6.2879e-04	3.3034e-02
6912	9.2506ee-02	2.07	1.8457e-02	2.19	5.9084e-05	6.8618e-03
27648	2.2127ee-02	2.06	4.2318e-03	2.12	5.7411e-06	1.5135e-03
110592	5.5103e-03	2.00	1.0017e-03	2.08	5.7413e-07	3.4841e-04

TABLE 4.2: Example 1. Convergence of estimator and errors; quadratic mapping with $p = 2$.

DoFs	estimator	rate	$\|\|\|.\|\|\|$-error	rate	L^2-error	H^1-error
768	6.5923e-02	–	4.3641e-02	—	8.5525e-05	3.0614e-02
3072	8.1666e-03	3.01	4.6166e-03	3.24	5.7611e-06	3.7515e-04
12288	1.0233e-03	2.99	5.289e-05	3.12	3.8178e-07	4.6925e-05
49152	1.2937e-04	2.98	6.3781e-06	3.05	2.4791e-08	5.9393e-06
196608	1.7042e-05	2.92	8.0091e-07	2.99	1.5886e-09	7.5685e-07

TABLE 4.3: Example 1. Convergence of estimator and errors; quadratic mapping with $p = 3$.

where $r = \sqrt{x^2 + y^2}$ and $C_{tr} = 0.75$.

Upon satisfactory approximation of the interface geometry, the above problem does not admit singular behaviour and we expect to observe optimal convergence rates. To simulate a fitted approach, presented above, we use parametric maps of degree higher than linear for the interface elements. We set $\gamma = 10$.

Dofs	Estimate	Rate	E.norm	Rate	L2-error	H1-error
192	1.3359e+01	–	1.7552e+00	—	6.2249e-02	1.3886e+00
768	7.6144e+00	0.81	8.439e-01	1.05	2.02e-02	7.2405e-01
3072	3.9829e+00	0.93	3.9949e-01	1.07	5.7576e-03	3.6433e-01
12288	2.0255e+00	0.97	1.9147e-01	1.06	1.5194e-03	1.8187e-01
49152	1.02e+00	0.98	9.3261e-02	1.03	3.8766e-04	9.0742e-02
196608	5.1507e-01	0.98	4.5982e-02	1.02	9.7628e-05	4.5315e-02

TABLE 4.4: Example 1.Convergence of estimator and errors; cubic mapping with $p = 1$.

Dofs	Estimate	Rate	E.norm	Rate	L2-error	H1-error
192	1.3383e+01	–	1.7546e+00	—	0.062308	1.3879
768	7.6178e+00	0.81	8.437e-01	1.05	0.020188	0.7239
3072	3.9836e+00	0.93	3.9946e-01	1.07	0.0057546	0.3643
12288	2.0257e+00	0.97	1.9146e-01	1.06	0.0015189	0.18186
49152	1.02e+00	0.98	9.3261e-02	1.03	0.00038766	0.090742
196608	5.1507e-01	0.98	4.5982e-02	1.02	9.7628e-05	0.045315

TABLE 4.5: Example 1. Convergence of estimator and errors; mapping =4 with $p = 1$.

4.5.2 Example 2

Let, now, $\Omega = (-1, 1) \times (0, 1)$, subdivided into $\Omega_1 = (-1, 0) \times (0, 1)$, $\Omega_2 = (0, 1)^2$, i.e., interfacing at $x = 0$. The Dirichlet boundary conditions and the source term f are determined by the exact solution

$$u = \begin{cases} (x^2 + y^2)^{3/4} + x & \text{in} \quad \Omega_1; \\ 1 + y^{3/2} + x & \text{in} \quad \Omega_2, \end{cases}$$

which has a point singularity at $(0, 0)$. This example studies the interaction of the interface discontinuity, with the point singularity at one interface endpoint. The convergence under uniform as well as adaptive refinement is given in Figure 4.6 for $p = 1, 2$, while the respective effectivity indices (i.e., the ratio between estimator and exact solution) and adapted meshes are given in Figure 4.7.

We begin by assessing the decay of the estimators under uniform refinement, using quadratic parametric mappings ($q = 2$) for the elements on Γ^{tr}: in Tables 4.1, 4.2, and 4.3, the convergence of the a posteriori estimator, of the energy norm, of the H^1-seminorm and of the L^2-norm of the error are reported, along with the respective convergence rates for the estimator and for the energy error, for $p = 1, 2$, and 3, respectively. The estimator and the dG-norm of the actual error are plotted in

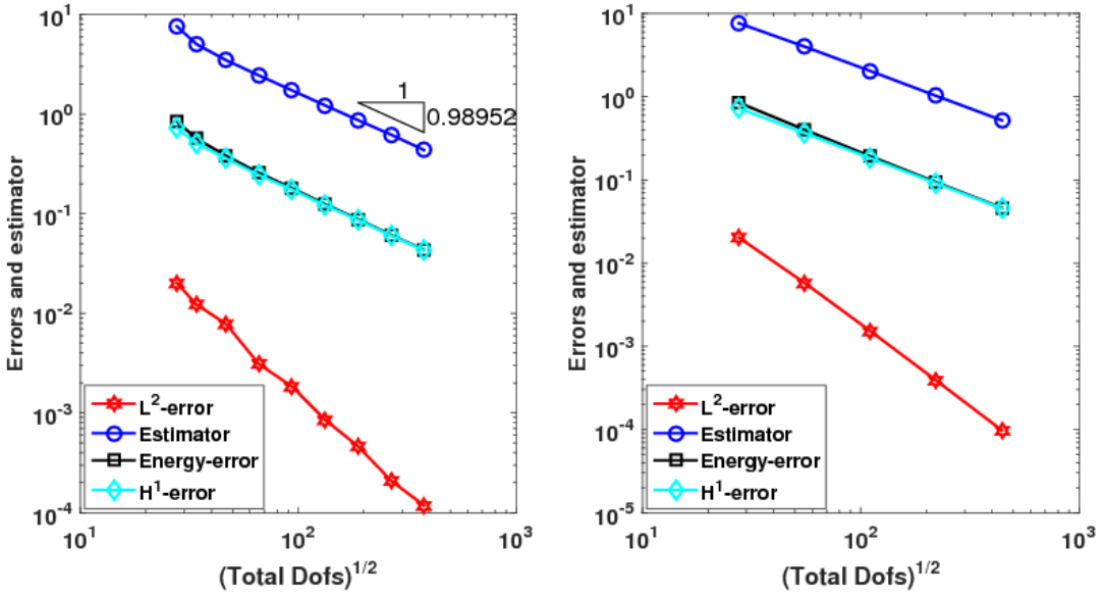

(a) Quadratic mapping with $p = 1$.

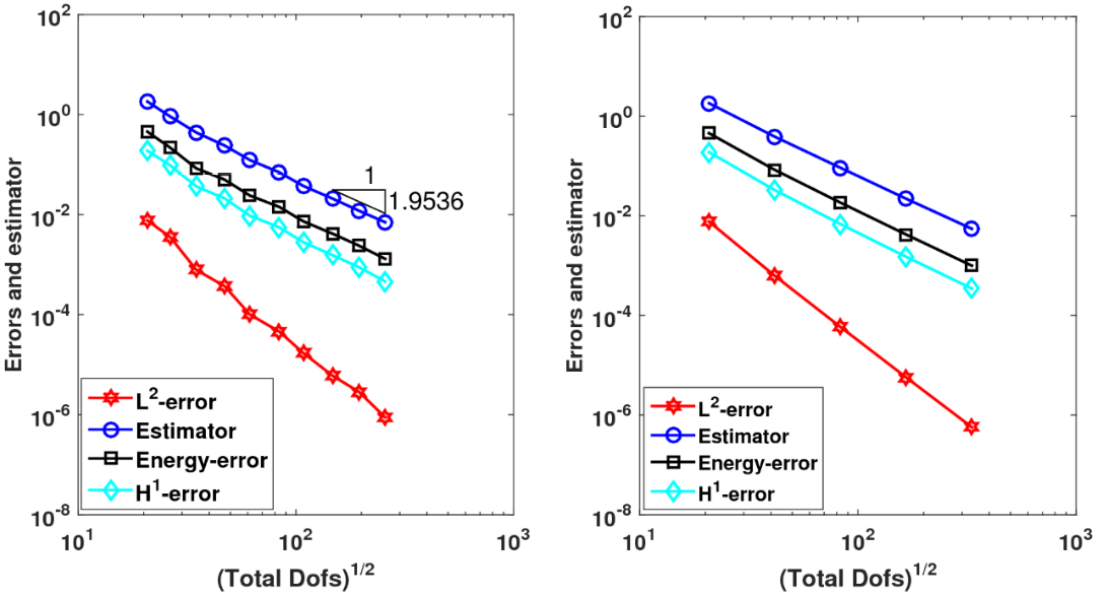

(b) Quadratic mapping with $p = 2$.

FIGURE 4.2: Example 1. Plot estimator and errors of convergence for adaptive mesh in the left and uniform mesh in the right.

Figure 4.2, for both adaptive and uniform refinement; for the adaptive refinement a standard bulk criterion is used. Optimal convergence rates are observed in all cases.

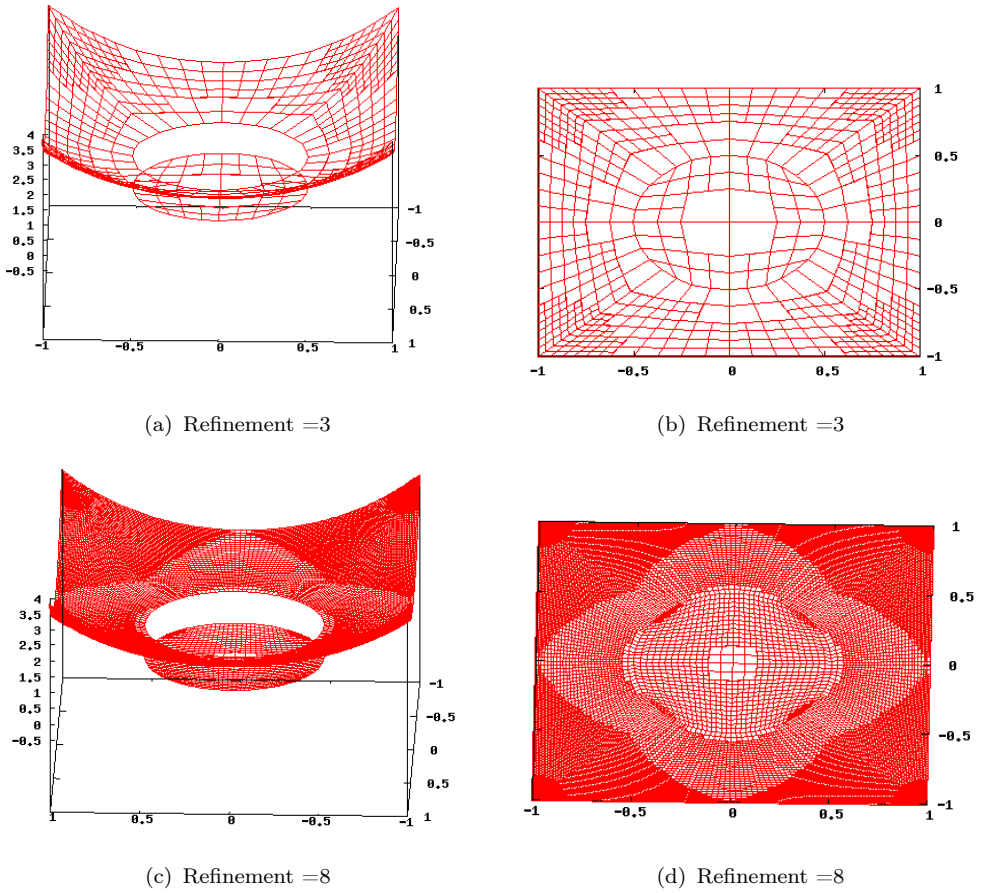

(a) Refinement =3

(b) Refinement =3

(c) Refinement =8

(d) Refinement =8

FIGURE 4.3: Example 1. Solution profiles for quadratic mapping; with $p = 1$, in the left and meshes produced for quadratic mapping; with $p = 1$, in the right.

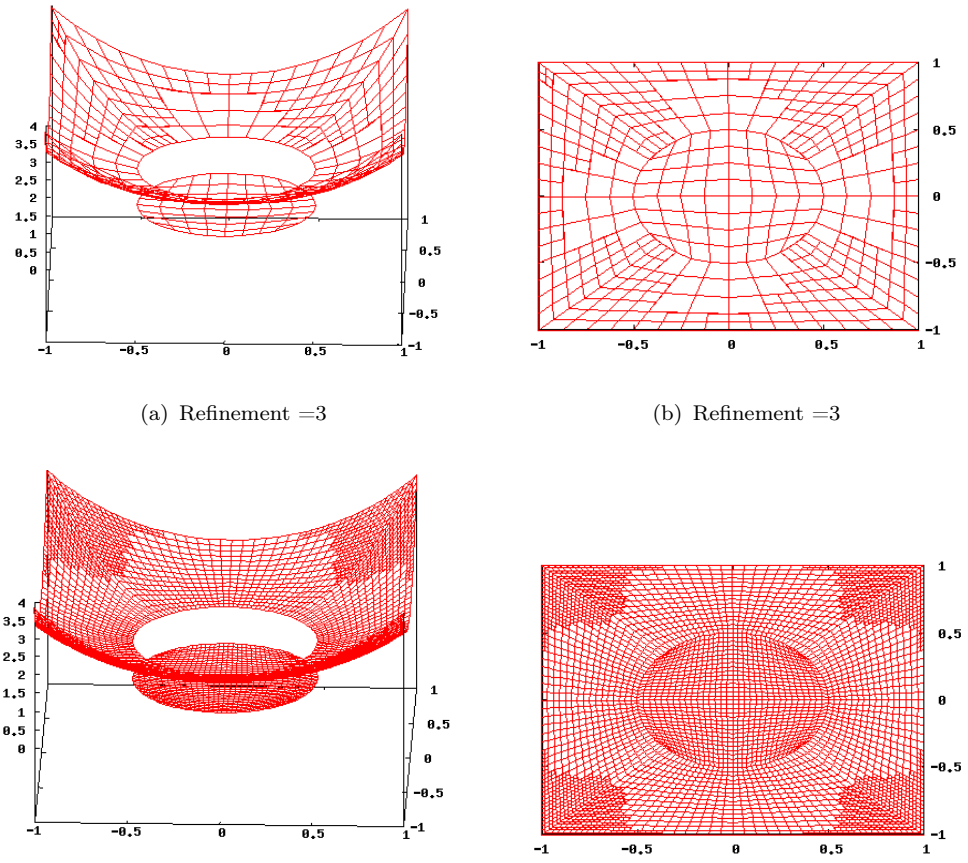

(a) Refinement =3

(b) Refinement =3

(c) Refinement =8

(d) Refinement =8

FIGURE 4.4: Example 1. Solution profiles for quadratic mapping; with $p = 2$, in the left and meshes produced for quadratic mapping; with $p = 2$, in the right.

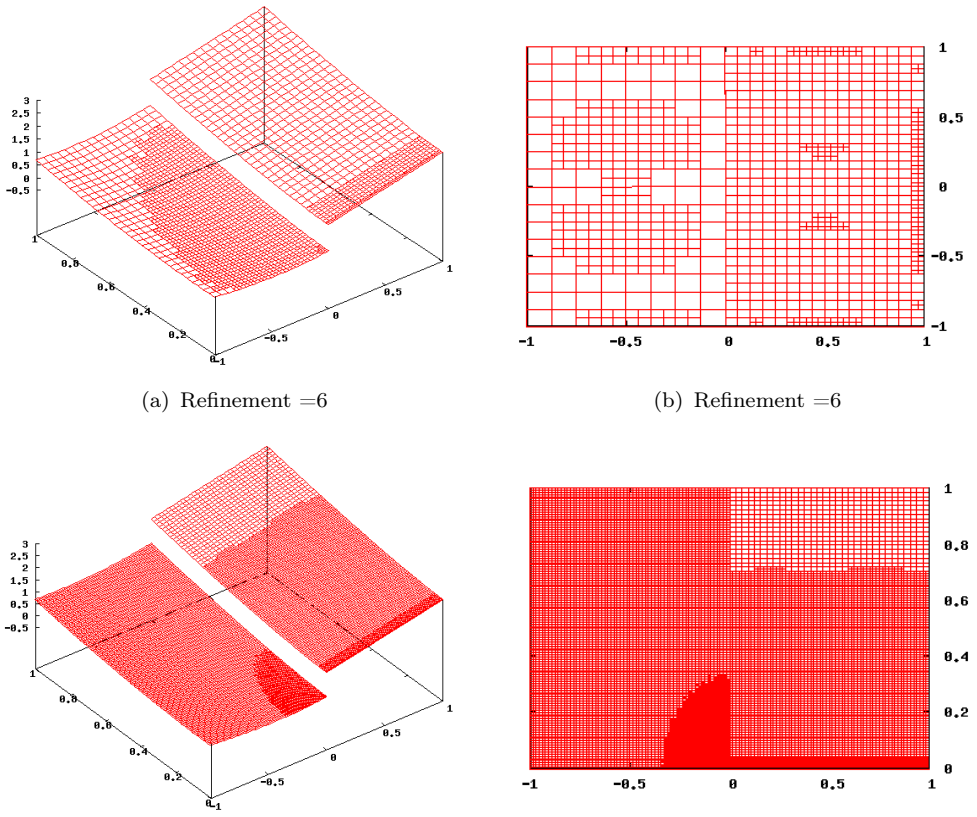

(a) Refinement =6

(b) Refinement =6

(c) Refinement =9

(d) Refinement =9

FIGURE 4.5: Example 2. Solution profiles for $p = 2$; in the left and meshes produced for $p = 2$, in the right

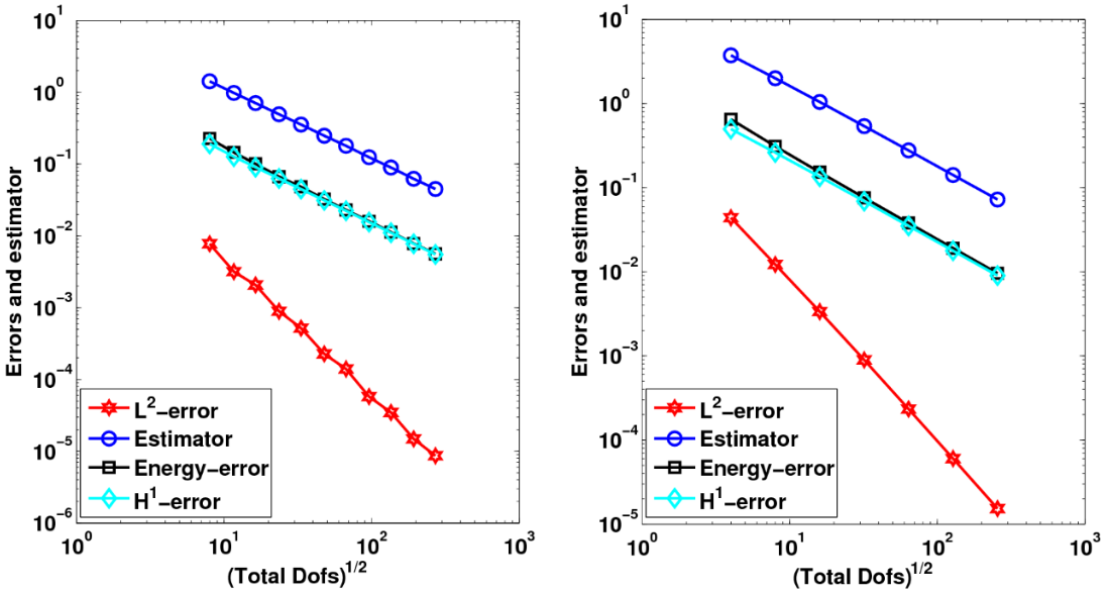

(a) $p = 1$.

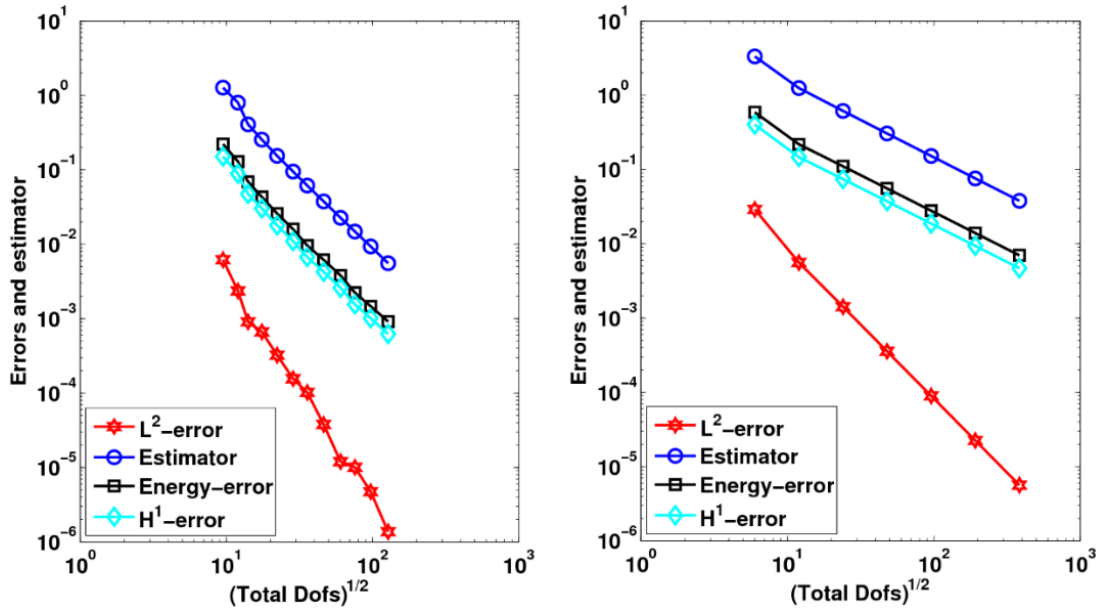

(b) $p = 2$.

FIGURE 4.6: Example 2. Plot estimator and errors of convergence for adaptive mesh in the left and uniform mesh in the right.

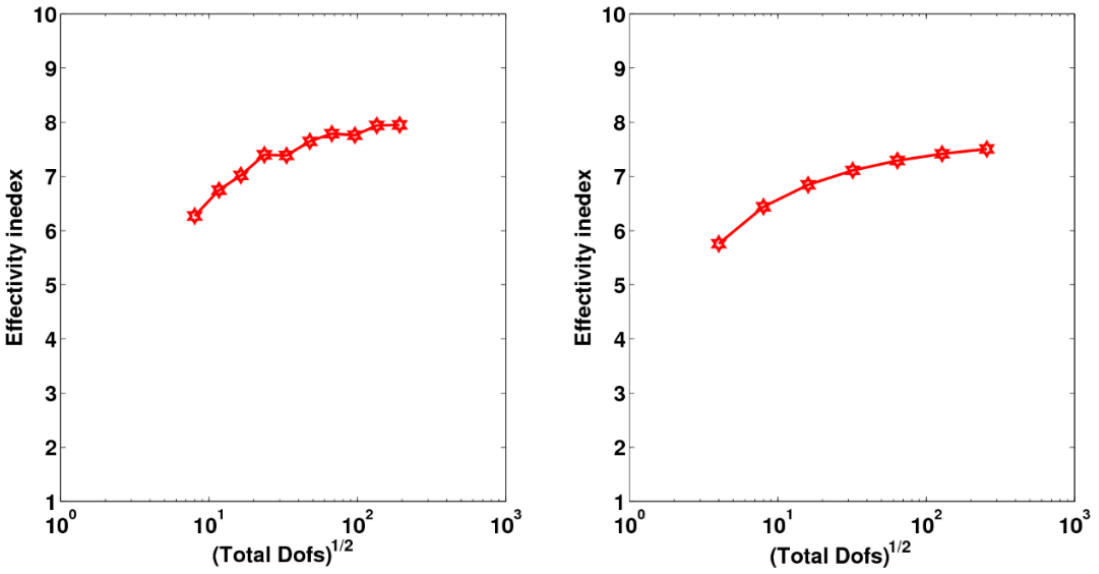

(a) $p = 1$.

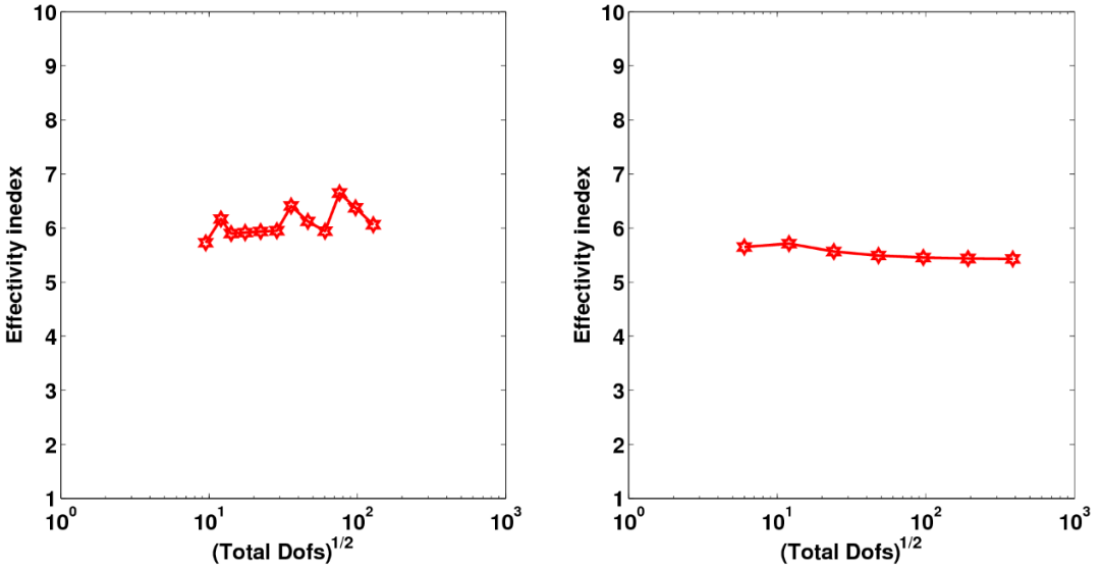

(b) $p = 2$.

FIGURE 4.7: Example 2. Plot effectivity index of convergence of adaptive mesh in the left and uniform mesh in the right.

Chapter 5

Convergence of the adaptive algorithm

5.1 Introduction

The aim of this chapter is to prove the convergence of a standard adaptive algorithm applied to the elliptic interface problems introduced in Chapter 2, based on the a posteriori error bounds derived in Chapter 4. The proof of convergence is based on the techniques developed in [11, 42]. However, the condition at the curved interface poses a series of difficulties, particularly in view of proving a contraction result. We will need to assume that angle remain uniform bounded when refining curved elements at the vicinity of the interface boundary by newest vertex bisection. It should be possible to generalise such property through a set of mild mesh assumption, although we leave this issue to future work.

5.2 Convergence analysis

We begin by defining

$$\begin{aligned}\Upsilon^2_{\mathcal{T}}(u_h) := &\sum_{K\in\mathcal{T}} h_K^2 \|f + \Delta u_h\|_K^2 + \sum_{E\in\Gamma^{int}} h_E \|[\![\nabla u_h]\!]\|_E^2 \\ &+ \sum_{j=1}^{2} \|\mathbf{h}^{1/2}\left(C_{tr}[\![u_h]\!] + \nabla u_h\right)\cdot \mathbf{n}^i\|^2_{\Gamma^{tr}}.\end{aligned} \tag{5.1}$$

The following Lemma generalises to the present setting the result in Karakashian and Pascal [42].

Lemma 5.1. *Let $\mathcal{E}(u_h) \in \mathcal{H}_0^1$ be the continuity recovery of u_h given in Lemma 3.14 and assume that*

$$\max_{\Omega}\{\sqrt{\theta\eta}\} \leq 2. \tag{5.2}$$

Then, there exists a constant $\gamma > 0$, depending only on the shape regularity of the triangulations, such that

$$\|\gamma_0 \mathbf{h}^{-1/2}[\![u_h]\!]\|^2_{\Gamma\setminus\Gamma^{tr}} \leq C\Upsilon^2_{\mathcal{T}}(u_h), \tag{5.3}$$

for $\gamma_0 = \gamma \max\{\sqrt{\theta\eta}, 1\}$.

Proof. The coercivity of the dG bilinear form D_h implies

$$\|\sqrt{\gamma_0/\mathbf{h}}[\![u_h]\!]\|^2_{\Gamma\setminus\Gamma^{tr}} \leq |||u_h - \mathcal{E}(u_h)|||^2 \leq 2D_h(u_h - \mathcal{E}(u_h), u_h - \mathcal{E}(u_h)).$$

The dG method gives

$$\mathcal{A} := D_h\left(u_h - \mathcal{E}(u_h), u_h - \mathcal{E}(u_h)\right) = \int_\Omega f\left(u_h - \mathcal{E}(u_h)\right) dx - D_h\left(\mathcal{E}(u_h), u_h - \mathcal{E}(u_h)\right).$$

Using the continuity of $\mathcal{E}(u_h)$, the above implies

$$\begin{aligned}
\mathcal{A} = &\int_\Omega f\left(u_h - \mathcal{E}(u_h)\right) dx - \sum_{K\in\mathcal{T}} \int_K \nabla u_h \cdot \nabla\left(u_h - \mathcal{E}(u_h)\right) dx \\
&+ \sum_{K\in\mathcal{T}} \int_K \nabla\left(u_h - \mathcal{E}(u_h)\right) \cdot \nabla\left(u_h - \mathcal{E}(u_h)\right) dx \\
&+ \int_{\Gamma\setminus\Gamma^{tr}} \{\nabla\mathcal{E}(u_h)\} \cdot [\![u_h - \mathcal{E}(u_h)]\!] ds \\
&+ \int_{\Gamma^{tr}} C_{tr}[\![u_h - \mathcal{E}(u_h)]\!] \cdot [\![u_h - \mathcal{E}(u_h)]\!] ds \\
&- \int_{\Gamma^{tr}} C_{tr}[\![u_h]\!] \cdot [\![u_h - \mathcal{E}(u_h)]\!] ds.
\end{aligned} \tag{5.4}$$

Integration by parts on the second term on the right-hand side of (5.4) yields

$$
\begin{aligned}
-\sum_{K\in\mathcal{T}}\int_K \nabla u_h\cdot\nabla\left(u_h-\mathcal{E}(u_h)\right)dx &= \sum_{K\in\mathcal{T}}\int_K \Delta u_h\left(u_h-\mathcal{E}(u_h)\right)dx \\
&\quad-\int_{\Gamma\setminus\Gamma^{tr}}\{\nabla u_h\}\cdot[\![u_h-\mathcal{E}(u_h)]\!]ds-\int_{\Gamma\setminus\Gamma^{tr}}\{u_h-\mathcal{E}(u_h)\}\cdot[\![\nabla u_h]\!]ds \\
&\quad-\sum_{i=1}^{2}\int_{\Gamma^{tr}} n^i\cdot\nabla u_{h,i}\left(u_{h,i}-\mathcal{E}(u_{h,i})\right)ds,
\end{aligned}
\tag{5.5}
$$

using the notation $v_i := v|_{\Omega_i}$, $i=1,2$ for a function $v\in\mathcal{H}_0^1$. Combing (5.4) and (5.5) gives

$$
\begin{aligned}
|\mathcal{A}| &\le C\Upsilon_{\mathcal{T}}(u_h)\Big(\|\mathbf{h}^{-1}(u_h-\mathcal{E}(u_h))\|+\|\mathbf{h}^{-1/2}(u_h-\mathcal{E}(u_h))\|_{\Gamma\setminus\Gamma^{tr}}\Big)\\
&\quad+C\Upsilon_{\mathcal{T}}(u_h)\Big(\sum_{j=1}^{2}\|\mathbf{h}^{-1/2}\big(u_h-\mathcal{E}(u_h)|_{\Omega_j}\big)\|^2_{\Gamma_{tr}}\Big)^{1/2}+\sum_{K\in\mathcal{T}}\|\nabla\left(u_h-\mathcal{E}(u_h)\right)\|^2_K\\
&\quad+\|(\theta\eta/\mathbf{h})^{1/2}[\![u_h]\!]\|_{\Gamma\setminus\Gamma^{tr}}\|(\mathbf{h}/\theta\eta)^{1/2}\{\nabla\mathcal{E}(u_h)-\nabla u_h\}\|_{\Gamma\setminus\Gamma^{tr}}\\
&\quad+\sum_{E\in\Gamma^{tr}}C_{tr}\|[\![u_h-\mathcal{E}(u_h)]\!]\|^2.
\end{aligned}
$$

Now, applying Lemmas 3.11 and 3.12, along with Lemma 3.14, we arrive at the bound

$$
\begin{aligned}
|\mathcal{A}| &\le C\Upsilon_{\mathcal{T}}(u_h)\big\|\sqrt{\theta\eta}\mathbf{h}^{-1/2}[\![u_h]\!]\big\|_{\Gamma\setminus\Gamma^{tr}}\\
&\quad+C(1+C_{tr}\sqrt{h}_{\max})\big\|\sqrt{\theta\eta}\mathbf{h}^{-1/2}[\![u_h]\!]\big\|^2_{\Gamma\setminus\Gamma^{tr}}.
\end{aligned}
\tag{5.6}
$$

Selecting now $\gamma>0$ large enough such that, for the coefficient of the second term on the right-hand side of (5.6), it holds $\gamma\ge 8C(1+C_{tr}\sqrt{h}_{\max})$, we have

$$
\begin{aligned}
\|\sqrt{\gamma_0/\mathbf{h}}[\![u_h]\!]\|^2_{\Gamma\setminus\Gamma^{tr}} &\le \frac{C}{\gamma}\Upsilon_{\mathcal{T}}(u_h)\big\|\gamma_0\mathbf{h}^{-1/2}[\![u_h]\!]\big\|_{\Gamma\setminus\Gamma^{tr}}+\frac{1}{8\gamma}\big\|\gamma_0\mathbf{h}^{-1/2}[\![u_h]\!]\big\|^2_{\Gamma\setminus\Gamma^{tr}}\\
&\le \frac{C}{\gamma}\Upsilon^2_{\mathcal{T}}(u_h)+\frac{1}{4\gamma}\big\|\gamma_0\mathbf{h}^{-1/2}[\![u_h]\!]\big\|^2_{\Gamma\setminus\Gamma^{tr}},
\end{aligned}
\tag{5.7}
$$

and, thus,

$$
\Big(1-\frac{1}{4}\max\{\max_{\Omega}\sqrt{\theta\eta},1\}\Big)\|\gamma_0\mathbf{h}^{-1/2}[\![u_h]\!]\|^2_{\Gamma\setminus\Gamma^{tr}}\le C\max\{\max_{\Omega}\sqrt{\theta\eta},1\}\Upsilon^2_{\mathcal{T}}(u_h),
\tag{5.8}
$$

which already implies the result. □

Therefore, under the assumptions of Lemma 5.1, the a posteriori bound from Theorem 4.3 can be reduced to

$$|||u - u_h|||^2 \leq C\Upsilon^2_{\mathcal{T}}(u_h), \tag{5.9}$$

i.e., the penalty term disappears from the estimator. This is crucial, since the penalty term involves the mesh-size h with a negative power.

5.2.1 Adaptive procedure

We consider a sequence $\{S_m\}_{m\in\mathbb{N}_0}$ of *fitted* dG spaces $S_m := (S^p_h)_m$ subordinate to a mesh $\mathcal{T}_m$, constructed following the above assumptions. We shall describe and analyze an adaptive discontinuous Galerkin method admitting an iteration of the form `SOLVE` $\rightarrow$ `ESTIMATE` $\rightarrow$ `MARK` $\rightarrow$ `REFINE`, which will determine $\{S_m\}_m$ automatically.

`SOLVE`: In this step, on a mesh $\mathcal{T}_m$, the dG approximation $u_m \in S_m$ is computed by solving

$$D_m(u_m, v_m) = \langle f, v_m\rangle \quad \forall v_m \in S_m, \tag{5.10}$$

with D_m denoting the discrete bilinear form with respect to the mesh $\mathcal{T}_m$, (2.16).

`ESTIMATE`: In this step, for each element $K \in \mathcal{T}_m$, we evaluate the local a posteriori error estimators $\Upsilon_{\mathcal{T}_m}(u_m, K)$, given by

$$\begin{aligned}\Upsilon^2_{\mathcal{T}_m}(u_m, K) = &\sum_{K\in\mathcal{T}_m} h^2_K\|f + \Delta u_m\|^2_K + \sum_{E\in\partial K\cap\Gamma^{int}_m} h_E\|[\![\nabla u_m]\!]\|^2_E \\ &+ \sum_{j=1}^{2}\|\mathbf{h}^{1/2}\left(C_{tr}[\![u_m]\!] + \nabla u_m\right)\cdot\mathbf{n}^i\|^2_{\partial K\cap\Gamma^{tr}_m};\end{aligned} \tag{5.11}$$

note that, with this notation, we have

$$\Upsilon^2_{\mathcal{T}_m}(u_m) = \sum_{K\in\mathcal{T}_m}\Upsilon^2_{\mathcal{T}_m}(u_m, K).$$

`MARK`: The third step is based on the, so-called, *Dörfler* or bulk marking strategy [28], whereby, given $0 < \mu < 1$, we find a collection of elements $\mathcal{M}_m \subset \mathcal{T}_m$ such that

$$\mu\Upsilon^2_{\mathcal{T}_m}(u_m) \leq \Upsilon^2_{\mathcal{T}_m}(u_m, \mathcal{M}_m) := \sum_{K\in\mathcal{M}_m}\Upsilon^2_{\mathcal{T}_m}(u_m, K); \tag{5.12}$$

the collection $\mathcal{M}_m$ is called the set of *marked elements.*

`REFINE:` Finally, the elements and faces that have been marked are subdivided by bisection into children see below (cf., [28]). This process gives $\mathcal{T}_{m+1}$.

A crucial challenge for the interface problem compared to the, now standard, proof of convergence of the above adaptive procedure applied to single domain problem is that the steps `MARK` and `REFINE` require to be compatible with the interface approximation saturation assumption (5.2).

In what follows, we shall use a subscript m to denote quantities related to mesh $\mathcal{T}_m$. Now, let β_1 and β_2 be two constants depending only on the initial triangulation and such that $0 < \beta_1 < \beta_2 < 1$. If $\mathcal{T}_m$ is constructed from $\mathcal{T}_{m-1}$ by adding a new vertex or edges using a bisection technique, then for $K \in \mathcal{T}_{m-1}$ and $\hat{K} \in \mathcal{T}_m$, we have

$$\kappa_1 h_{\hat{K}} \leq h_K \leq k_2 h_{\hat{K}}, \tag{5.13}$$

where $\kappa_1 := 2^{1/2}\beta_1/\beta_2$ and $\kappa_2 := 2^{1/2}\beta_2/\beta_1$, for all elements not having a face on the interface. For the elements on Γ^{tr}, we make (5.13) an assumption

Next, we show an estimator reduction property (cf., [25], Corollary 4.4).

Lemma 5.2. *Let $\delta = 1 - 2^{-1/2}$ and $0 < \mu < 1$. Then, we have*

$$\begin{aligned}\Upsilon^2_{\mathcal{T}_m}(u_m) \leq\ & (1 - \frac{\delta\mu}{2})\Upsilon^2_{\mathcal{T}_{m-1}}(u_{m-1}) + (1 + \frac{2}{\delta\mu})\max\{1, C_{tr}\} \\ & \times \Big(\sum_{K\in\mathcal{T}_m} \|\nabla(u_m - u_{m-1})\|^2_K + \|\sqrt{\theta\eta/\mathbf{h}_m}[\![u_m - u_{m-1}]\!]\|^2_{\Gamma_m\setminus\Gamma^{tr}_m}\Big)\end{aligned} \tag{5.14}$$

Proof. Set $v_m := u_m - u_{m-1}$, $m \in \mathbb{N}$, for brevity. Using a standard Poincaré-Friedrichs inequality along with Lemma 3.14, we have

$$\begin{aligned}\|v_m\|^2 &\leq 2\|\mathcal{E}(v_m)\|^2 + 2\|v_m - \mathcal{E}(v_m)\|^2 \\ &\leq C\sum_{j=1,2}\|\nabla\mathcal{E}(v_m)\|^2_{\Omega_j} + C\|\sqrt{\theta\eta\mathbf{h}_m}[\![v_m]\!]\|^2_{\Gamma_m\setminus\Gamma^{tr}_m} \\ &\leq C\sum_{K\in\mathcal{T}_m}\big(\|\nabla v_m\|^2_K + \|\nabla(v_m - \mathcal{E}(v_m))\|^2_K\big) \\ &\quad + C\|\sqrt{\theta\eta\mathbf{h}_m}[\![v_m]\!]\|^2_{\Gamma_m\setminus\Gamma^{tr}_m} \\ &\leq C\sum_{K\in\mathcal{T}_m}\|\nabla v_m\|^2_K + C\|\sqrt{\theta\eta/\mathbf{h}_m}[\![v_m]\!]\|^2_{\Gamma_m\setminus\Gamma^{tr}_m}.\end{aligned} \tag{5.15}$$

Therefore, using Lemma 3.11 and (5.15), we have

$$\begin{aligned}\sum_{K\in\mathcal{T}_m}\|\mathbf{h}_m\Delta v_m\|_K^2+\|\mathbf{h}_m^{1/2}[\![\nabla v_m]\!]\|_{\Gamma_m^{int}}^2+\sum_{j=1,2}C_{tr}\|\mathbf{h}_m^{1/2}\left([\![v_m]\!]+\nabla v_m\right)\cdot\mathbf{n}^i\|_{\Gamma_m^{tr}}^2\\ \leq C\sum_{K\in\mathcal{T}_m}\|\nabla v_m\|_K^2+CC_{tr}\|v_m\|^2\\ \leq C\max\{1,C_{tr}\}\sum_{K\in\mathcal{T}_m}\|\nabla v_m\|_K^2+CC_{tr}\|\sqrt{\theta\eta/\mathbf{h}_m}[\![v_m]\!]\|_{\Gamma_m\setminus\Gamma_m^{tr}}^2,\end{aligned}\tag{5.16}$$

for $C>0$, constant depending only on the local geometry of the triangulation.

Using the elementary identity $(a+b)^2\leq(1+\lambda)a^2+(1+\lambda^{-1})b^2$, for $a,b,\lambda\in\mathbb{R}$, $\lambda>0$, we have

$$\begin{aligned}\sum_{K\in\mathcal{T}_m}\|\mathbf{h}_m(f+\Delta u_m)\|_K^2\leq(1+\lambda)\sum_{K\in\mathcal{T}_m}\|\mathbf{h}_m(f+\Delta u_{m-1})\|_K^2\\ +(1+\lambda^{-1})\sum_{K\in\mathcal{T}_m}\|\mathbf{h}_m\Delta v_m\|_K^2,\end{aligned}\tag{5.17}$$

$$\|\mathbf{h}_m^{1/2}[\![\nabla u_m]\!]\|_{\Gamma_m^{int}}^2\leq(1+\lambda)\|\mathbf{h}_m^{1/2}[\![\nabla u_{m-1}]\!]\|_{\Gamma_m^{int}}^2+(1+\lambda^{-1})\|\mathbf{h}_m^{1/2}[\![\nabla v_m]\!]\|_{\Gamma_m^{int}}^2,\tag{5.18}$$

and

$$\begin{aligned}\sum_{j=1,2}\|\mathbf{h}_m^{1/2}([\![u_m]\!]+\nabla u_m)\cdot\mathbf{n}^i\|_{\Gamma_m^{tr}}^2\\ \leq(1+\lambda)\sum_{j=1,2}\|\mathbf{h}_m^{1/2}([\![u_{m-1}]\!]+\nabla u_{m-1})\cdot\mathbf{n}^i\|_{\Gamma_m^{tr}}^2\\ +(1+\lambda^{-1})\sum_{j=1,2}\|\mathbf{h}_m^{1/2}([\![v_m]\!]+\nabla v_m)\cdot\mathbf{n}^i\|_{\Gamma_m^{tr}}^2.\end{aligned}\tag{5.19}$$

Combing (5.17), (5.18) and (5.19), with (5.16), we deduce

$$\begin{aligned}\Upsilon_{\mathcal{T}_m}^2(u_m)\leq(1+\lambda)\Upsilon_{\mathcal{T}_{m-1}}^2(u_{m-1})+(1+\lambda^{-1})C\max\{1,C_{tr}\}\\ \times\Big(\sum_{K\in\mathcal{T}_m}\|\nabla v_m\|_K^2+\|\sqrt{\theta\eta/\mathbf{h}_m}[\![v_m]\!]\|_{\Gamma_m\setminus\Gamma_m^{tr}}^2\Big).\end{aligned}\tag{5.20}$$

Now, for each element $K\in\mathcal{M}_{m-1}$, i.e., elements refined at the $(m-1)$-st iteration, let $\mathcal{R}_m:=\{K'\in\mathcal{T}_m:K'\subset K\}$. Then, for all $K'\in\mathcal{R}_m$,

we have $h_{K'} \leq \left(\frac{\beta_2}{\beta_1}\right) 2^{-1/2} h_K \leq 2^{-1/2} h_K$ and

$$\begin{aligned}\Upsilon^2_{\mathcal{T}_{m-1}}(u_{m-1}) &= \Upsilon^2_{\mathcal{T}_{m-1}}(u_{m-1}, \mathcal{T}_{m-1}\backslash\mathcal{M}_{m-1}) + \Upsilon^2_{\mathcal{T}_m}(u_{m-1}, \{\mathcal{R}_m : K \in \mathcal{M}_{m-1}\}) \\ &\leq \Upsilon^2_{\mathcal{T}_{m-1}}(u_{m-1}, \mathcal{T}_{m-1}\backslash\mathcal{M}_{m-1}) + 2^{-1/2}\Upsilon^2_{\mathcal{T}_{m-1}}(u_{m-1}, \mathcal{M}_{m-1}) \\ &\leq \Upsilon^2_{\mathcal{T}_{m-1}}(u_{m-1}, \mathcal{T}_{m-1}) - (1 - 2^{-1/2})\Upsilon^2_{\mathcal{T}_{m-1}}(u_{m-1}, \mathcal{M}_{m-1}) \\ &\leq (1 - \delta\mu)\Upsilon^2_{\mathcal{T}_{m-1}}(u_{m-1}, \mathcal{T}_{m-1}),\end{aligned} \tag{5.21}$$

making use of the a Dörfler-type marking strategy property (5.12) in the last step. Substituting (5.21) into (5.20), and selecting $\lambda = \delta\mu/2$, the result already follows by noting that

$$\left(1 + \frac{\delta\mu}{2}\right)(1 - \delta\mu) \leq 1 - \frac{\delta\mu}{2}.$$

□

5.2.2 Quasi-orthogonality

We now prove a mesh perturbation result, which we shall use to establish the quasi-orthogonality in Lemma 5.4 below.

Lemma 5.3. *For $\gamma_0 > 0$ sufficiently large, and $C_G = \frac{3C2^{-r/2}-1}{2}$, then we have*

$$\hat{D}_m(z, z) \leq 2\hat{D}_{m-1}(z, z) + \frac{C_G}{\gamma}\|\gamma_0 \mathbf{h}^{-1/2}[\![z]\!]\|^2_{\Gamma_{m-1}\backslash\Gamma^{tr}_{m-1}} \tag{5.22}$$

for all $z \in S_{m-1} + \mathcal{H}^1_0$, with $r \in \mathbb{N}$ denoting the minimum number of refinements on the elements on Γ^{tr}, required to satisfy $\max_\Omega\{\sqrt{\theta\eta}\} \leq 2$ in the transition from $\mathcal{T}_{m-1}$ to $\mathcal{T}_m$. Here $\hat{D}_m$ denoted the inconsistent bilinear form introduced in section 4.2.1.

Proof. Since $\mathcal{T}_m$ is a refinement of $\mathcal{T}_{m-1}$, we have $z \in S_m + \mathcal{H}^1_0$ also. Hence, associated to Z_m.

$$\begin{aligned}\hat{D}_m(z, z) = \hat{D}_{m-1}(z, z) &+ 2\int_{\Gamma_m\backslash\Gamma^{tr}_m} \{\Pi\nabla z\} \cdot [\![z]\!] ds - 2\int_{\Gamma_{m-1}\backslash\Gamma^{tr}_{m-1}} \{\Pi\nabla z\} \cdot [\![z]\!] ds \\ &+ \|\sqrt{\gamma_0/\mathbf{h}_m}[\![z]\!]\|^2_{\Gamma_m\backslash\Gamma^{tr}_m} - \|\sqrt{\gamma_0/\mathbf{h}_{m-1}}[\![z]\!]\|^2_{\Gamma_{m-1}\backslash\Gamma^{tr}_{m-1}},\end{aligned}$$

since

$$\|[\![z]\!]\|^2_{\Gamma^{tr}_m} = \|[\![z]\!]\|^2_{\Gamma^{tr}_{m-1}}, \quad \sum_{K\in\mathcal{T}_m} \|\nabla z\|^2 = \sum_{K\in\mathcal{T}_{m-1}} \|\nabla z\|^2.$$

Using (5.13), we have

$$\|\mathbf{h_m}^{-1/2}[\![z]\!]\|^2_{\Gamma_m\setminus\Gamma_m^{tr}} \leq C2^{-r/2}\|\mathbf{h_{m-1}}^{-1/2}[\![z]\!]\|^2_{\Gamma_{m-1}\setminus\Gamma_{m-1}^{tr}}. \tag{5.23}$$

Using similar arguments as in Lemma 3.17, gives

$$\begin{aligned} 2\int_{\Gamma_m\setminus\Gamma_m^{tr}}\{\Pi\nabla z\}\cdot[\![z]\!]ds &\leq C\Big(\sum_{K\in\mathcal{T}_m}\|\gamma_0^{-1/2}\nabla z\|_K^2\Big)^{1/2}\|\sqrt{\gamma_0/\mathbf{h}_m}[\![z]\!]\|_{\Gamma_m\setminus\Gamma_m^{tr}} \\ &\leq \frac{1}{2}\hat{D}_m(z,z)+\frac{1}{2}\|\sqrt{\gamma_0/\mathbf{h}_m}[\![z]\!]\|^2_{\Gamma_m\setminus\Gamma_m^{tr}}, \end{aligned} \tag{5.24}$$

for γ_0 sufficiently large, and, as in the proof of Lemma 4.2, we immediately have

$$\|\sqrt{\gamma_0/\mathbf{h}_m}[\![z]\!]\|^2_{\Gamma_m\setminus\Gamma_m^{tr}} \leq \frac{1}{\gamma}\|\gamma_0\mathbf{h}_m^{-1/2}[\![z]\!]\|^2_{\Gamma_m\setminus\Gamma_m^{tr}}. \tag{5.25}$$

and

$$\begin{aligned} 2\int_{\Gamma_{m-1}\setminus\Gamma_{m-1}^{tr}}\{\Pi\nabla z\}\cdot[\![z]\!]ds &\leq C\Big(\sum_{K\in\mathcal{T}_{m-1}}\|\gamma_0^{-1/2}\nabla z\|_K^2\Big)^{1/2}\|\sqrt{\gamma_0/\mathbf{h}_{m-1}}[\![z]\!]\|_{\Gamma_{m-1}\setminus\Gamma_{m-1}^{tr}} \\ &\leq \frac{1}{2}\hat{D}_{m-1}(z,z)+\frac{1}{2}\|\sqrt{\gamma_0/\mathbf{h}_{m-1}}[\![z]\!]\|^2_{\Gamma_{m-1}\setminus\Gamma_{m-1}^{tr}}. \end{aligned}$$

Combining the above bounds the assertion already follows. □

Lemma 5.4. *Let $e_m := u - u_m$ and $C_R = \frac{3}{2}C + 2C(4+C_F)\gamma + C_G$. Then, we have*

$$\begin{aligned} \hat{D}_m(e_m,e_m) &= (2+\gamma^{-1})\hat{D}_{m-1}(e_{m-1},e_{m-1}) - \frac{1}{4}|||u_m-u_{m-1}|||^2 \\ &\quad + \frac{C_R}{\gamma}\Big(\Upsilon^2_{\mathcal{T}_m}(u_m)+\Upsilon^2_{\mathcal{T}_{m-1}}(u_{m-1})\Big), \end{aligned} \tag{5.26}$$

for $\gamma_0 = \gamma\max\{\sqrt{\theta\eta},1\}$, and $\gamma > 0$ sufficiently large.

Proof. For brevity, we set $v_m := u_m - u_{m-1}$ and $w_m := v_m - \mathcal{E}(v_m)$, $m \in \mathbb{N}$.

Using the PDE problem along with straightforward manipulations reveals the identity

$$\begin{aligned} \hat{D}_m(e_m,e_m) &= \hat{D}_m(e_{m-1},e_{m-1}) - \hat{D}_m(v_m,v_m) + 2\hat{D}_m(e_m,w_m) \\ &\quad - 2\Big(\hat{D}_m(u_m,w_m) - \langle f,w_m\rangle\Big). \end{aligned} \tag{5.27}$$

We now consider bound each term in turns. Applying Lemma 5.3, gives

$$\hat{D}_m(e_{m-1}, e_{m-1}) \leq 2\hat{D}_{m-1}(e_{m-1}, e_{m-1}) + \frac{C_G}{\gamma}\|\gamma_0 \mathbf{h}^{-1/2}[\![e_{m-1}]\!]\|^2_{\Gamma_{m-1}\setminus\Gamma^{tr}_{m-1}}.$$

The coercivity of the bilinear form $\hat{D}_m$ gives

$$\hat{D}_m\left(v_m, v_m\right) \geq \frac{1}{2}|||v_m|||^2. \tag{5.28}$$

To bound the third term on the right-hand side of (5.27), we start by observing that

$$2\hat{D}_m\left(e_m, w_m\right) = 2\hat{D}_m\left(e_{m-1}, w_m\right) + 2\hat{D}_m\left(v_m, w_m\right). \tag{5.29}$$

The first term on the right-hand side of the above equation can be bounded by (5.13) as follows:

$$\begin{aligned}
&\hat{D}_m\left(e_{m-1}, w_m\right)\\
&\leq \|\nabla e_{m-1}\|\|\nabla w_m\| + \|\nabla e_{m-1}\|\|\sqrt{\gamma_0/\mathbf{h}_m}[\![w_m]\!]\|_{\Gamma_m\setminus\Gamma^{tr}_m}\\
&+ \|\nabla w_m\|\|\sqrt{\gamma_0/\mathbf{h}_m}[\![e_{m-1}]\!]\|_{\Gamma_m\setminus\Gamma^{tr}_m} + C_{tr}\|[\![e_{m-1}]\!]\|_{\Gamma^{tr}_m}\|[\![w_m]\!]\|_{\Gamma^{tr}_m}\\
&+ \|\sqrt{\gamma_0/\mathbf{h}_{m-1}}[\![e_{m-1}]\!]\|_{\Gamma_m\setminus\Gamma^{tr}_m}\|\sqrt{\gamma_0/\mathbf{h}_m}[\![w_m]\!]\|_{\Gamma_m\setminus\Gamma^{tr}_m}\\
&\leq \Big(\|\nabla w_m\|^2 + \|\sqrt{\gamma_0/\mathbf{h}_m}[\![w_m]\!]\|^2_{\Gamma_m\setminus\Gamma^{tr}_m} + C_{tr}\|[\![w_m]\!]\|^2_{\Gamma^{tr}_m}\Big)^{1/2}\\
&\quad\times\Big(\|\nabla e_{m-1}\|^2 + C2^{-r/2}\|\sqrt{\gamma_0/\mathbf{h}_{m-1}}[\![e_{m-1}]\!]\|^2_{\Gamma_{m-1}\setminus\Gamma^{tr}_{m-1}} + C_{tr}\|[\![e_{m-1}]\!]\|^2_{\Gamma^{tr}_{m-1}}\Big)^{1/2}\\
&\leq C_F|||e_{m-1}|||\,|||w_m|||.
\end{aligned} \tag{5.30}$$

where $C_F = \left(\max\{1, C2^{-r/2}\}\right)^{1/2}$. Using Lemma 3.17, gives

$$\hat{D}_m\left(e_{m-1}, w_m\right) \leq \frac{1}{2\gamma}|||e_{m-1}|||^2 + \frac{\gamma C_F}{2}|||w_m|||^2. \tag{5.31}$$

The second term on the right hand side of (5.31) can be bound by using (4.7), we have

$$\begin{aligned}
\hat{D}_m\left(e_{m-1}, w_m\right) &\leq \frac{1}{2\gamma}|||e_{m-1}|||^2 + \frac{\gamma C_F}{2}\Big(C\sum_{K\in\mathcal{T}_m}(\gamma^{-1} + \gamma^{-2}(1 + C_{tr}\sqrt{h}_{\max})\Big)\\
&\quad\times\|\gamma_0\mathbf{h}_m^{-1/2}[\![v_m]\!]\|^2_{\Gamma_m\setminus\Gamma^{tr}_m},\\
&\leq \gamma^{-1}\hat{D}_{m-1}\left(e_{m-1}, e_{m-1}\right) + CC_F\|\gamma_0\mathbf{h}_m^{-1/2}[\![v_m]\!]\|^2_{\Gamma_m\setminus\Gamma^{tr}_m}.
\end{aligned} \tag{5.32}$$

Next, for the second term on right-hand side of (5.29), we also have

$$\begin{aligned} 2\hat{D}_m\left(v_m, w_m\right) &\leq \frac{1}{4}|||v_m|||^2 + 4C|||w_m|||^2 \\ &\leq \frac{1}{4}|||v_m|||^2 + 4C\|\gamma_0 \mathbf{h}_m^{-1/2}[\![v_m]\!]\|^2_{\Gamma_m \setminus \Gamma_m^{tr}}. \end{aligned} \tag{5.33}$$

Collecting all of these results, we obtain

$$2\hat{D}_m\left(e_m, w_m\right) \leq \gamma^{-1}\hat{D}_{m-1}\left(e_{m-1}, e_{m-1}\right) + \frac{1}{4}|||v_m|||^2 + C(4+C_F)\|\gamma_0 \mathbf{h}_m^{-1/2}[\![v_m]\!]\|^2_{\Gamma_m \setminus \Gamma_m^{tr}}.$$

To bound the final term in equation (5.27), we begin with setting

$$\mathcal{B} := \langle f, w_m\rangle - \hat{D}_m\left(u_m, w_m\right) = \int_\Omega f w_m dx - \hat{D}_m\left(u_m, w_m\right).$$

Integration by parts on the above implies

$$\begin{aligned} |\mathcal{B}| \leq\ & C\Upsilon_{\mathcal{T}}(u_m)\Big(\|\mathbf{h}_m^{-1} w_m\| + \|\mathbf{h}_m^{-1/2} w_m\|_{\Gamma_m \setminus \Gamma_m^{tr}}\Big) \\ & + C\Upsilon_{\mathcal{T}}(u_m)\Big(\sum_{j=1}^{2} \|\mathbf{h}_m^{1/2} w_m|_{\Omega_j}\|^2_{\Gamma_m^{tr}}\Big)^{1/2} \\ & + \|(\theta\eta/\mathbf{h}_m)^{1/2}[\![u_m]\!]\|_{\Gamma_m \setminus \Gamma_m^{tr}} \|(\mathbf{h}_m/\theta\eta)^{1/2}\{\nabla w_m\}\|_{\Gamma_m \setminus \Gamma_m^{tr}}. \end{aligned}$$

Now, applying Lemmas 3.11 and 3.12, along with Lemma 3.14, we arrive at the bound

$$|\mathcal{B}| \leq C\Upsilon^2_{\mathcal{T}_m}(u_m)\big\|\sqrt{\theta\eta}\mathbf{h}_m^{-1/2}[\![v_m]\!]\big\|_{\Gamma_m \setminus \Gamma_m^{tr}} + C\big\|\sqrt{\theta\eta}\mathbf{h}_m^{-1/2}[\![v_m]\!]\big\|^2_{\Gamma_m \setminus \Gamma_m^{tr}}. \tag{5.34}$$

Selecting now $\gamma > 0$ large enough so that, for the coefficient of the second term on the right-hand side of (5.34), we have $\gamma \geq 8C$, we obtain

$$\begin{aligned} |\mathcal{B}| &\leq \frac{C}{\gamma}\Upsilon_{\mathcal{T}_m}(u_m)\big\|\gamma_0 \mathbf{h}_m^{-1/2}[\![v_m]\!]\big\|_{\Gamma_m \setminus \Gamma_m^{tr}} + \frac{1}{8\gamma}\big\|\gamma_0 \mathbf{h}_m^{-1/2}[\![v_m]\!]\big\|^2_{\Gamma_m \setminus \Gamma_m^{tr}} \\ &\leq \frac{C}{\gamma}\Upsilon^2_{\mathcal{T}_m}(u_m) + \frac{1}{4\gamma}\big\|\gamma_0 \mathbf{h}_m^{-1/2}[\![v_m]\!]\big\|^2_{\Gamma_m \setminus \Gamma_m^{tr}}. \end{aligned} \tag{5.35}$$

Finally, applying the triangle inequality and Lemma 5.1, gives

$$\begin{aligned} \|\gamma_0 \mathbf{h}_m^{-1/2}[\![u_m - u_{m-1}]\!]\|^2_{\Gamma_m \setminus \Gamma_m^{tr}} &\leq \|\gamma_0 \mathbf{h}_m^{-1/2}[\![u_m]\!]\|^2_{\Gamma_m \setminus \Gamma_m^{tr}} + \|\gamma_0 \mathbf{h}_{m-1}^{-1/2}[\![u_{m-1}]\!]\|^2_{\Gamma_{m-1} \setminus \Gamma_{m-1}^{tr}} \\ &\leq C\Upsilon^2_{\mathcal{T}_m}(u_m) + C\Upsilon^2_{\mathcal{T}_{m-1}}(u_{m-1}). \end{aligned}$$

Recalling that $\gamma_0 = \gamma \max\{\sqrt{\theta\eta}, 1\}, \gamma > 1$ and combining the above bounds the results already follows. □

5.2.3 Contraction property

We are now ready to prove the main theorem of this Chapter.

Theorem 5.5. *Let $u \in \mathcal{H}_0^1$. Then, there exist constants $\beta > 0$ and $0 < \rho < 1$ depending only on the shape regularity of the triangulations and on the marking parameter μ, such that*

$$\hat{D}_m\left(e_m, e_m\right) + \beta \Upsilon^2_{\mathcal{T}_m}\left(u_m\right) \leq \rho \left(\hat{D}_{m-1}\left(e_{m-1}, e_{m-1}\right) + \beta \Upsilon^2_{\mathcal{T}_{m-1}}\left(u_{m-1}\right)\right) \tag{5.36}$$

Proof. Using Lemma 5.2 and Lemma 5.4, we have

$$\begin{aligned}
&\hat{D}_m\left(e_m, e_m\right) + \beta \Upsilon^2_{\mathcal{T}_m}\left(u_m\right) \\
\leq\ & \left(2 + \gamma^{-1}\right) \hat{D}_{m-1}\left(e_{m-1}, e_{m-1}\right) - \frac{1}{4} |\!|\!| u_m - u_{m-1} |\!|\!|^2 \\
&+ \frac{C_R}{\gamma} \Upsilon^2_{\mathcal{T}_{m-1}}\left(u_{m-1}\right) + (\frac{C_R}{\gamma} + \beta) \Upsilon^2_{\mathcal{T}_m}\left(u_m\right)) \\
\leq\ & \left(2 + \gamma^{-1}\right) \hat{D}_{m-1}\left(e_{m-1}, e_{m-1}\right) - \frac{1}{4} |\!|\!| u_{m+1} - u_m |\!|\!|^2 \\
&+ \left(\frac{C_R}{\gamma} + (\frac{C_R}{\gamma} + \beta)(1 - \frac{\delta\mu}{2}) \right) \Upsilon^2_{\mathcal{T}_{m-1}}\left(u_{m-1}, \mathcal{T}_{m-1}\right) \\
&+ (1 + \frac{2}{\delta\mu}) \max\{1, C_{tr}\} (\frac{C_R}{\gamma} + \beta) \\
&\times \Big(\sum_{K \in \mathcal{T}_m} \|\nabla(u_m - u_{m-1})\|^2_K + \| \sqrt{\theta\eta / \mathbf{h}_m} [\![u_m - u_{m-1}]\!] \|^2_{\Gamma_m \setminus \Gamma^{tr}_m} \Big).
\end{aligned} \tag{5.37}$$

If we choose $\beta = \left(4(1 + \frac{2}{\delta\mu}) \max\{1, C_{tr}\} \right)^{-1} - \frac{C_R}{\gamma}$, this leads to cancellation of the term $|\!|\!| u_{m+1} - u_m |\!|\!|$ on the right hand side of (5.37) with the last component of the fourth term on the right hand side of(5.37). Setting $\gamma = \frac{C_R}{\epsilon\beta}$ we obtain

$$\begin{aligned}
\hat{D}_m\left(e_m, e_m\right) + \beta \Upsilon^2_{\mathcal{T}_m}\left(u_m\right) \leq\ & (2 + \epsilon\beta)\, \hat{D}_{m-1}\left(e_{m-1}, e_{m-1}\right) \\
&+ (2\epsilon + 1 - \frac{\mu\delta}{2}) \beta \Upsilon^2_{\mathcal{T}_{m-1}}\left(u_{m-1}\right).
\end{aligned} \tag{5.38}$$

Due to (5.9), we deduce

$$\begin{aligned}
\hat{D}_m\left(e_m, e_m\right) + \beta \Upsilon^2_{\mathcal{T}_m}\left(u_m\right) \leq\ & (2 - \epsilon\beta)\, \hat{D}_{m-1}\left(e_{m-1}, e_{m-1}\right) \\
&+ (2\epsilon(C + 1) + 1 - \frac{\delta\mu}{2}) \beta \Upsilon^2_{\mathcal{T}_{m-1}}\left(u_{m-1}\right).
\end{aligned} \tag{5.39}$$

Choosing $\epsilon = \frac{\delta\mu}{8(C+1)}$ and γ_0 large enough to make $\beta > 0$, we have

$$\begin{aligned}\hat{D}_m\left(e_m, e_m\right) + \beta\Upsilon^2_{\mathcal{T}_m}\left(u_m\right) \leq & \left(2 - \frac{\delta\beta\mu}{8(C+1)}\right)\hat{D}_m\left(e_{m-1}, e_{m-1}\right) \\ & + \left(1 - \frac{\delta\mu}{4}\right)\beta\Upsilon^2_{\mathcal{T}_{m-1}}\left(u_{m-1}\right).\end{aligned} \tag{5.40}$$

The proof follows by choosing

$$\rho = \max\left\{2 - \frac{\delta\beta\mu}{8(C+1)}, 1 - \frac{\delta\mu}{4}\right\}. \tag{5.41}$$

□

The contraction of $\hat{D}_m\left(e_m, e_m\right) + \beta\Upsilon^2_{\mathcal{T}_m}\left(u_m\right)$ as $m \to \infty$ implies that $\hat{D}_m\left(e_m, e_m\right) \to 0$ as $m \to \infty$, which, in true, implies $|||e_m||| \to 0$ as $m \to \infty$.

5.3 Numerical experiments

The main objective of this section is to illustrate the practical performance of the adaptive algorithm. All results shown are obtained with an implementation based on the `deal.II` finite element library [7]. Here, we present the result of three numerical examples, with $\gamma = 10$ and polynomials of degree one and two in all the examples. In all the cases, the starting mesh is the uniform square mesh node of 16×16 elements. Although not discussed above merely for simplicity of the presentation, it is straightforward to extend the proposed dG method to problems with non-homogeneous Dirichlet boundary conditions.

5.3.1 Example 1

Let $\Omega = (-1, 1)^2$ and subdivide it into two subdomains interfacing at $x = 0$; thus $\Omega_1 = (-1, 0) \times (-1, 1)$, $\Omega_2 = (0, 1) \times (-1, 1)$. Dirichlet boundary conditions and source term f are determined by the exact solution

$$u(x) = \begin{cases} \left(4x + 4x^2\right) e^{\left(y^2-1\right)^2} & \text{in} \quad \Omega_1; \\ \left(-5x^3 + 4x + 1\right) e^{\left(y^2-1\right)^2} & \text{in} \quad \Omega_2. \end{cases}$$

Both components obey non-homogeneous Dirichlet boundary condition. Further, the solution u is compatible with the transmission condition (defined in (2.5)) with respect to the permeability $C_{tr} \equiv 4$.

The numerical solution obtained after few iterations of the adaptive algorithm presented above is plotted in Figure 5.1 together with the respective meshes.

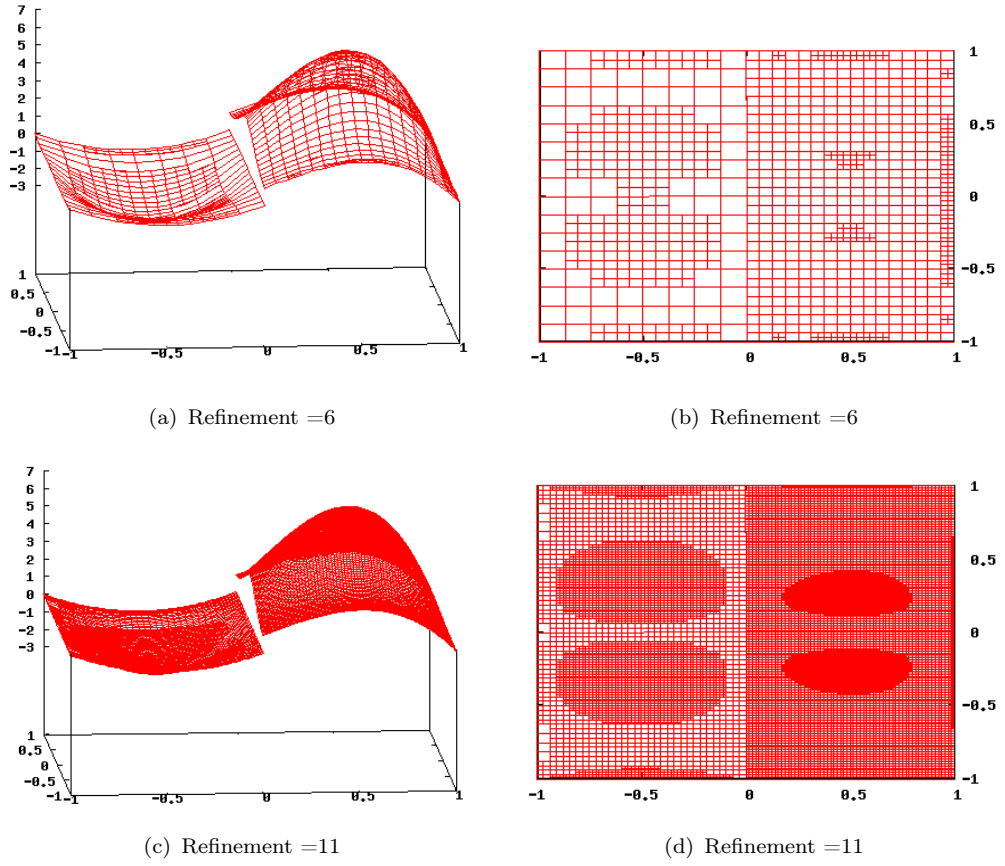

(a) Refinement =6 (b) Refinement =6

(c) Refinement =11 (d) Refinement =11

FIGURE 5.1: Example 1. Solution profiles ; with $p = 1$, in the left and meshes produced ; with $p = 1$, in the right.

We begin by assessing the decay of the estimators on uniform meshes. Numerical results are reported in Table 5.1 and Table 5.2 in the case of linear and quadratic elements, respectively. In both cases, the a posteriori estimator appears to be of optimal rate under uniform refinement. The estimator and the dG-norm of the error are plotted in Figure 5.2 under both uniform and adaptive mesh refinement; in Figure 5.3, we plot the respective effectivity indices, defined as the ratio of the posteriori error indicator and the dG-norm error. Optimal rates of convergence are observed with respect to the degrees of freedom for both the estimator and

DoFs	estimator	rate	$\|\|\|.\|\|\|$-error	rate	L^2-error	H^1-error
16	8.86664e+01	–	2.26145e+01	—	1.49369+01	1.5493e+01
64	4.50136e+01	0.97	1.08152e+01	1.06	5.40166e-01	0.810062e+01
256	2.37694e+01	0.92	0.495936e+01	1.12	1.75040e-01	0.40658e+01
1024	1.23039e+01	0.95	0.226606e+01	1.13	5.07852e-02	0.200753e+01
4096	0.626679e+01	0.97	0.106339e+01	1.09	1.37406e-02	9.93241e-01
16384	0.316349e+01	0.98	5.11661e-01	1.05	3.57951e-03	4.93316e-01
65536	0.158947e+01	0.99	2.50428e-01	1.03	9.13994e-04	2.4573e-01

TABLE 5.1: Example 1. Decay of the a posteriori error estimator and errors for $p = 1$.

DoFs	estimator	rate	$\|\|\|.\|\|\|$-error	rate	L^2-error	H^1-error
36	5.89003e+01	–	1.72413e+01	–	0.16731e+01	1.17844e+01
144	1.43043e+01	2.04	0.342048e+01	2.33	1.71202e-01	0.23397e+01
576	0.345626e+01	2.04	8.33096e-01	2.03	1.93163e-02	5.55376e-01
2304	7.92704e-01	2.12	0.178967e-01	2.21	1.91641e-03	1.17387e-01
9216	1.83402e-01	2.11	3.83275e-02	2.22	1.80756e-04	2.46368e-02
36864	4.34877e-02	2.07	8.47322e-03	2.17	1.66339e-05	5.32887e-03
147456	1.05398e-02	2.04	1.95167e-03	2.11	1.52498e-06	1.20475e-03

TABLE 5.2: Example 1.Decay of the a posteriori error estimator and errors for $p = 2$.

the error. Furthermore, the effectivity indices appear to be bounded asymptotically and remain between 4 and 6, and between 3 and 6 for linear and quadratic elements, respectively.

5.3.2 Example 2

Let $\Omega = (-1,1)^2 \backslash (0,1) \times (-1,0)$ and subdivide it into two subdomains interfacing at $x = 0.125$. We consider the classical problem with $f = 0$ and non-homogeneous Dirichlet boundary conditions compatible to the exact solution

$$u = r^{2/3} sin(2\theta/3),$$

with $r = \sqrt{x^2 + y^2}$, $\theta = tan^{-1}(y/x)$, and $C_{tr} \equiv 1$.

The purpose of this example is to observe the behaviour of the adaptive procedure based on the presented a posteriori error estimator, in presence of both a singularity (at the reentrant corner) and the jump discontinuity at the interface. Numerical solutions obtained after few iterations of the adaptive algorithm presented above is plotted in Figure 5.4. The refinement near the origin by adaptive

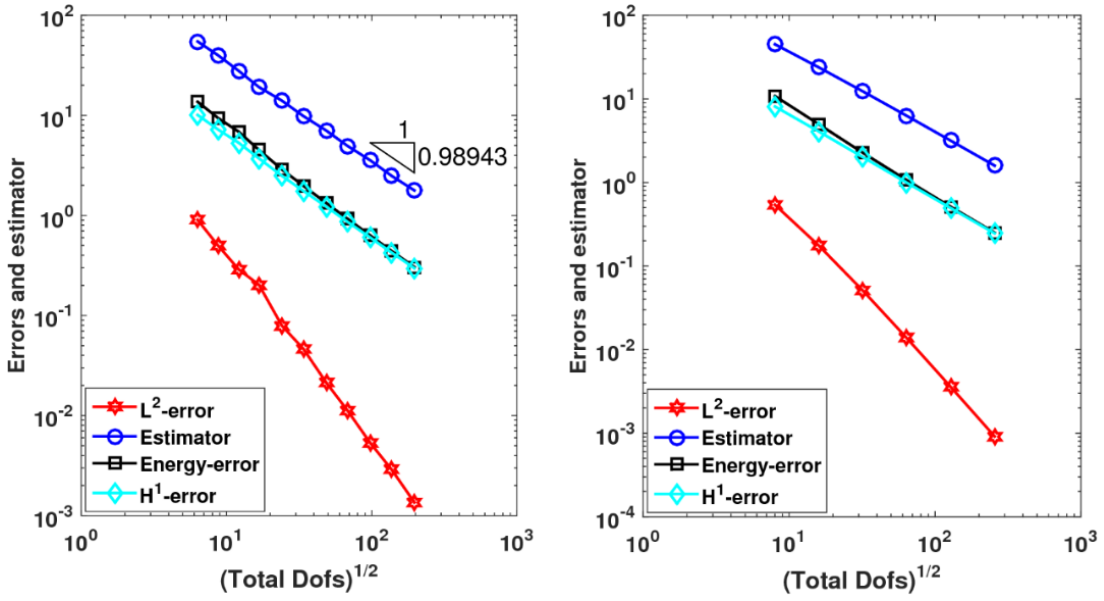

(a) $p = 1$.

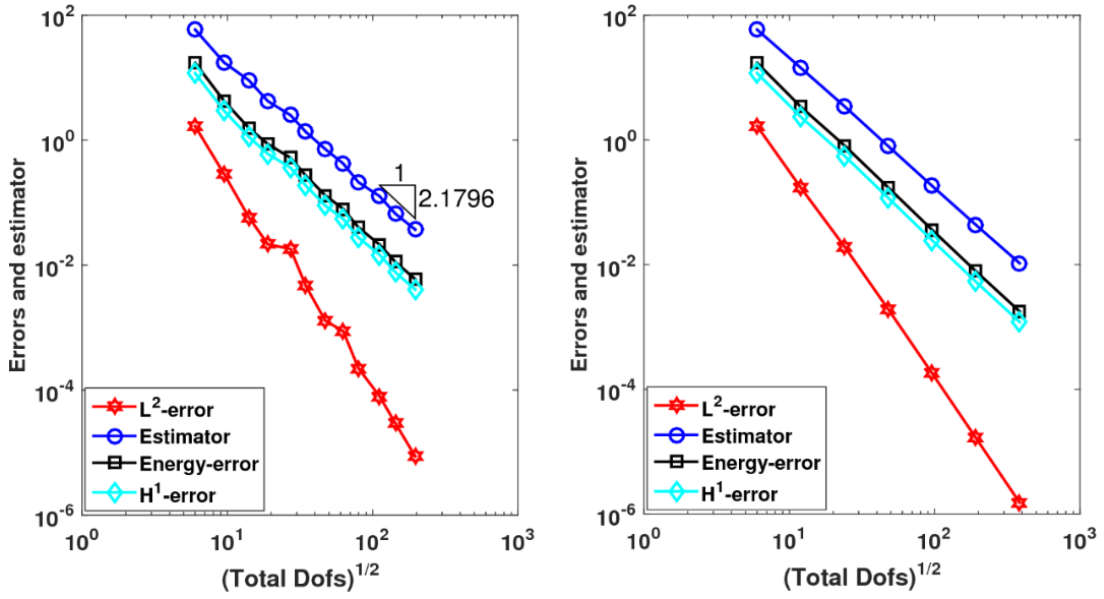

(b) $p = 2$.

FIGURE 5.2: Example 1. Estimator and errors for adaptive mesh in the left and uniform mesh in the right ($p = 1, 2$).

algorithm clearly indicates that the error estimator is practical and captures the interface and singularity. The convergence plots reported in Figure 5.5 confirm that the estimator tends to zero at the expected rate.

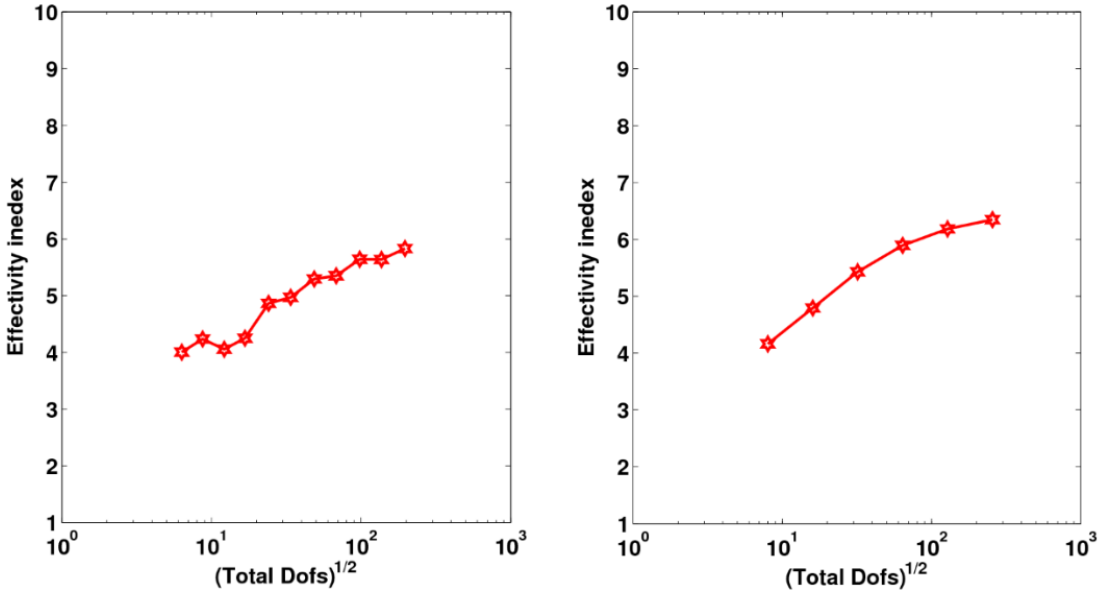

(a) $p = 1$.

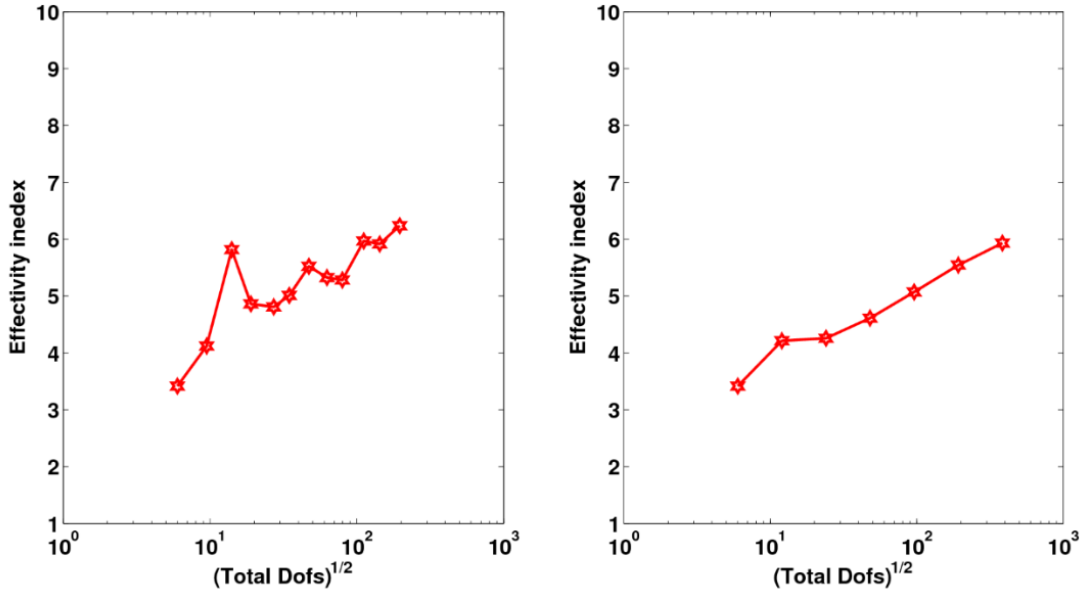

(b) $p = 2$.

FIGURE 5.3: Example 1. Effectivity index for adaptive (left) and uniform mesh (right).

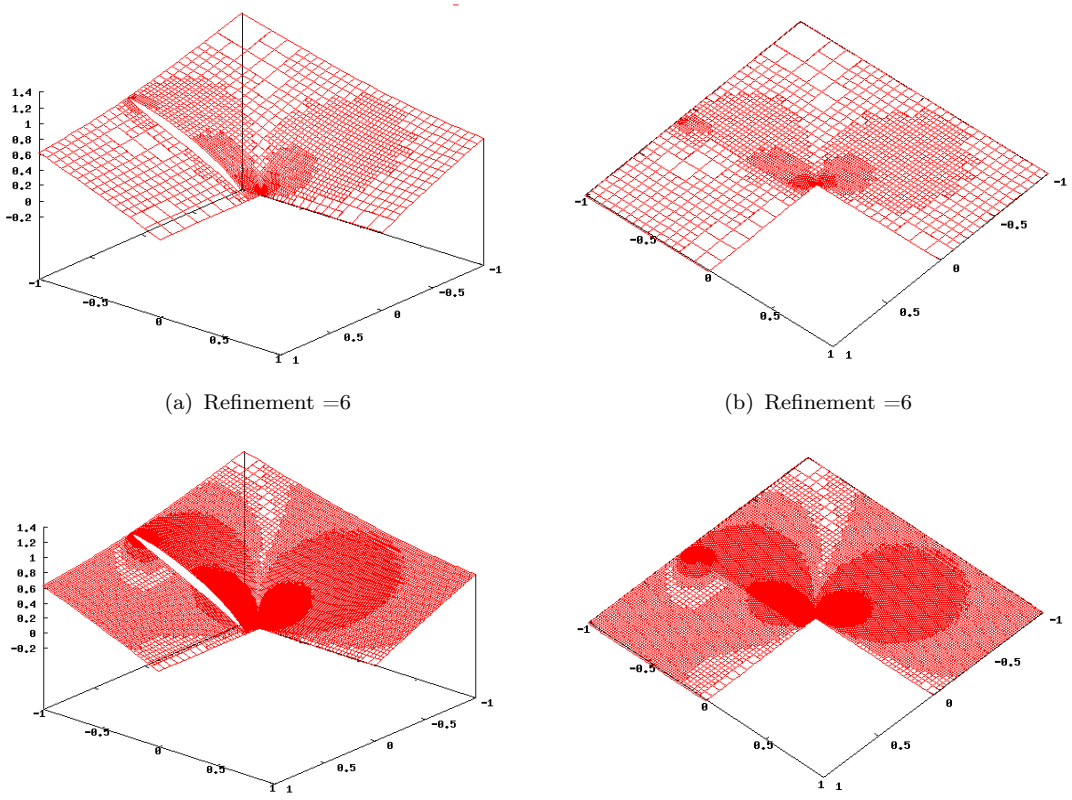

(a) Refinement =6

(b) Refinement =6

(c) Refinement =10

(d) Refinement =10

FIGURE 5.4: Example 2. Solution profiles; with $p = 1$, in the left and meshes produced; with $p = 1$, in the right.

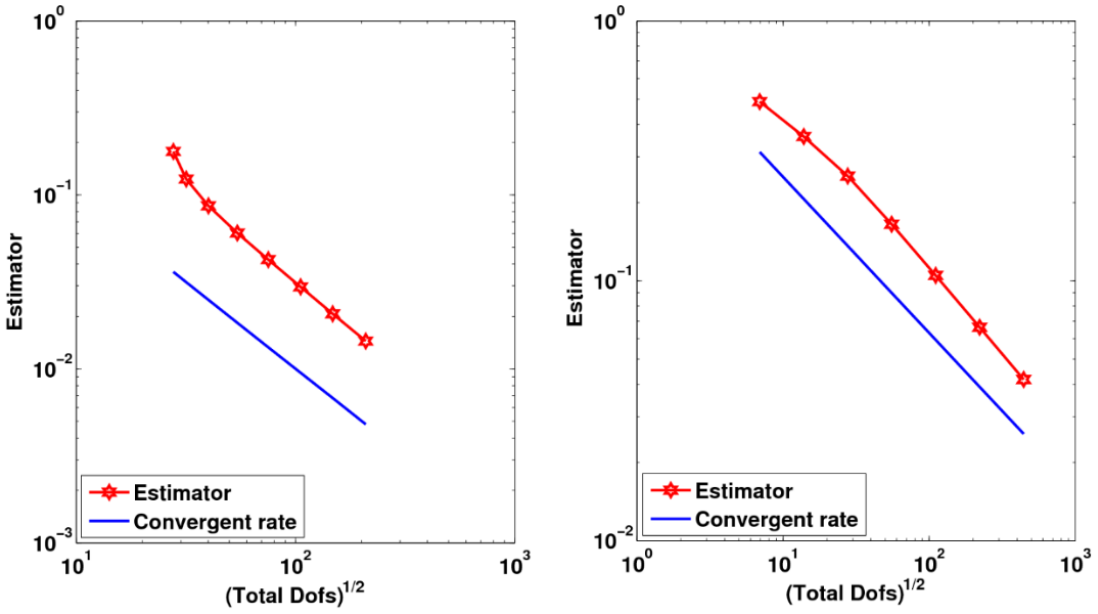

(a) $p = 1$.

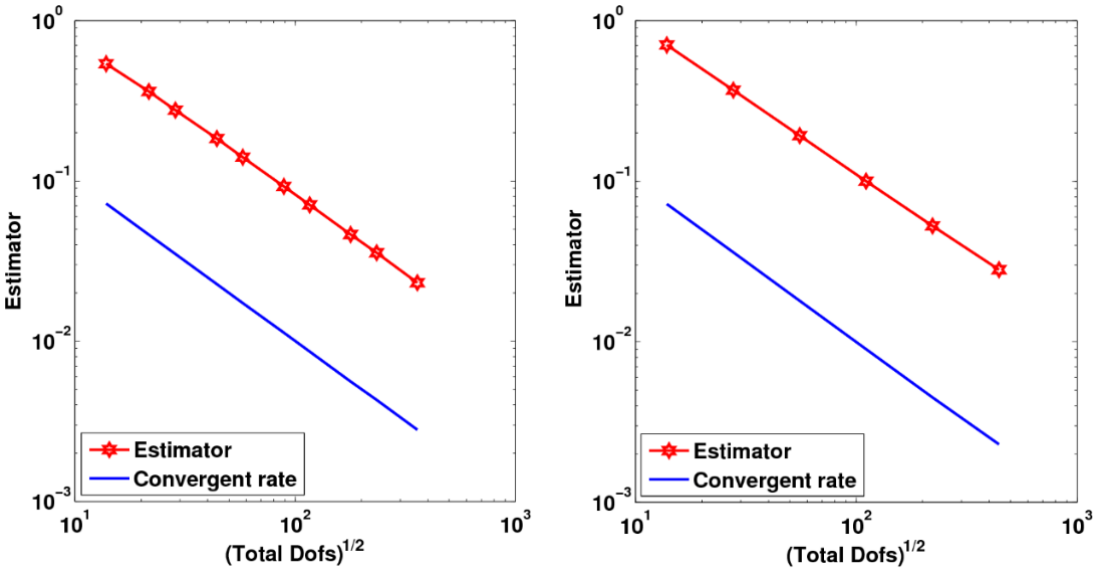

(b) $p = 2$.

FIGURE 5.5: Example 2. Estimator and convergence rate for adaptive (left) and uniform (right) mesh for $p = 1$ (above) and $p = 2$ (below).

Chapter 6

A posteriori error estimates for dG methods for parabolic interface problems

6.1 Introduction

We will now derive a posteriori error bounds for both the spatially-discrete dG method and a fully-discrete backward-Euler-dG scheme for the solution of parabolic interface problems. The key technique used in the proofs is the elliptic reconstruction idea, introduced by Makridakis and Nochetto for spatially discrete conforming FEM [48] and extended to fully discrete conforming FEM by Lakkis and Makridakis [44]. These ideas have been carried forward also to fully discrete schemes involving spatially non-conforming/dG methods in [33]. The choice of this technique for deriving a posteriori error for parabolic problem is motivated by the following factors. First, elliptic reconstruction allows us to utilise the readily available elliptic interface a posteriori estimates derived in Chapter 4 to bound the main part of the spatial error. Second, this technique combines the energy approach and appropriate pointwise representation of the error in order to arrive to optimal order a posteriori estimators in the $L_\infty(L_2)$-norm. As a result, this approach will lead to optimal order in both $L_2(H^1)$ and $L_\infty(L_2)$-type norms, while the results obtained by the standard energy methods are only optimal order in $L_2(H^1)$-type norms. To the best of our knowledge, no results in the context of non-linear parabolic interface problems exist for the $L_\infty(L_2)$-norm. The main contribution in this chapter is to prove such an a posteriori error estimator. For an a

posteriori error analysis in the $L_\infty(L_2) + L_2(H^1)$-type norm using backward Euler in time and a *fitted* interior-penalty discontinuous Galerkin method in space for *straight* interfaces we refer to [50].

6.2 Elliptic reconstruction and revisiting a posteriori error bounds for elliptic interface problems

In this section, we will define the suitable elliptic reconstruction of spatially discrete dG functions. A key observation we will make is that the elliptic reconstruction is the *exact* solution to an elliptic problem, whose dG approximation is the dG approximation to the parabolic problem at a particular time. Therefore, we will be able to utilise a posteriori error bounds for elliptic problems to estimate the difference between the elliptic reconstruction and the a dG approximation. To do so, we return to the a posteriori error estimation for the fitted discontinuous Galerkin method for interface elliptic problems from Section 2.2.4. In particular, we will extend the energy-norm a posteriori error bounds from Chapter 4 to *nonlinear* elliptic interface problems including also a reaction term, and we prove a posteriori error bounds in the L_2-norm, too. The a posteriori analysis follows using technical developments from the a priori analysis presented in [20]. The latter was inspired by a, non-standard, elliptic projection construction of Douglas and Dupont [29] for the treatment of non linear boundary conditions in a classical a priori error analysis setting, cf., also [20].

To this end, for the a posteriori error analysis, we define the elliptic reconstruction $w \in \mathcal{H}_0^1$ to be the solution of the problem: for $t \in [0,T]$, find $w \equiv w(t, Z_h) \in \mathcal{H}_0^1$, related to a dG function $Z_h \in S_h^p$, such that

$$D(t; w, v) + \lambda\langle w, v\rangle + \mathcal{M}(w, v) = \langle g, v\rangle \quad \forall v \in \mathcal{H}_0^1, \tag{6.1}$$

for some fixed $\lambda > 0$ at our disposal, where $g \equiv g(t) \in L_2(\Omega)$ denotes the Riesz representer of the linear functional given by the right-hand side of (6.1), with respect to the L^2-inner product, with

$$\langle g, v_h\rangle = \tilde{D}_h(t; Z_h, v_h) + \lambda\langle Z_h, v_h\rangle + \mathcal{M}(Z_h, v_h), \tag{6.2}$$

for all $v_h \in S_h^p$, where

$$\tilde{D}_h(t; Z_h, v_h) = \sum_{K\in\mathcal{T}} \int_K \nabla Z_h \cdot \nabla v_h dx - \int_{\Gamma\setminus\Gamma^{tr}} (\{\nabla \Pi Z_h\} \cdot [\![v_h]\!] + \{\nabla \Pi v_h\} \cdot [\![Z_h]\!]) ds + \int_{\Gamma\setminus\Gamma^{tr}} \frac{\gamma_0}{\mathbf{h}} [\![Z_h]\!] \cdot [\![v_h]\!] ds;$$

we emphasise that $\tilde{D}_h$ differs from D_h defined in Chapter 2 in that it does *not* include the interface term. We remark on the technical point that g is first defined for $v \in S_h^p$ by (6.2) and then we consider an (arbitrary) extension of g into $\mathcal{H}_0^1 + S_h^p$ by Hahn-Banach theorem.

To ensure the well-posedness of the reconstruction w, the constant λ has to be chosen large enough, as we shall see below.

Lemma 6.1. *Problem* (6.1) *is well-posed and* $w \in \mathcal{H}_0^1$ *is unique when* $\lambda > 0$ *is chosen sufficiently large.*

Proof. To show the well-posedness for (6.1), we shall prove the associated mapping is coercivity on $\mathcal{H}_0^1$. We begin by recalling a standard trace estimate (2.2). We note carefully the crucial fact that ψ can be a strict subset of $\partial\omega$.

Using the assumption that $\tilde{p}(z) = \mathcal{P}(z)\,(z_1 - z_2) \in C^{0,1}(\mathbb{R}^{2n})$, we have

$$\begin{aligned} |\mathcal{M}(w,v)| &\le \int_{\Gamma^{tr}} C_{\tilde{p}} |[\![w]\!]| |[\![v]\!]| \, ds \le C_{\tilde{p}} \sum_{j=1}^{2} \|w|_{\Omega_j}\|_{\Gamma^{tr}} \sum_{j=1}^{2} \|v|_{\Omega_j}\|_{\Gamma^{tr}} \\ &\le C_{trace} C_{\tilde{p}} \sum_{j=1}^{2} \left(\delta^{-1}\|w\|_{\Omega_j}^2 + \delta\|\nabla w\|_{\Omega_j}^2\right)^{\frac{1}{2}} \sum_{j=1}^{2} \left(\delta^{-1}\|v\|_{\Omega_j}^2 + \delta\|\nabla v\|_{\Omega_j}^2\right)^{\frac{1}{2}}, \end{aligned} \tag{6.3}$$

where $C_{\tilde{p}}$ is the Lipschitz constant of $\tilde{p}$; here we have made use of (2.2) with $\psi = \Gamma^{tr}$ and $\omega = \Omega_j$. Choosing, therefore, $\delta = (4C_{trace}C_{\tilde{p}})^{-1}$, and $\lambda > 16C_{trace}^2 C_{\tilde{p}}^2$, which implies that $\lambda > 4\delta^{-1}C_{trace}C_{\tilde{p}}$, we arrive at

$$|\mathcal{M}(w,v)| \le \frac{1}{4} \sum_{j=1}^{2} \left(\lambda\|w\|_{\Omega_j}^2 + \|\nabla w\|_{\Omega_j}^2\right)^{\frac{1}{2}} \sum_{j=1}^{2} \left(\lambda\|v\|_{\Omega_j}^2 + \|\nabla v\|_{\Omega_j}^2\right)^{\frac{1}{2}}. \tag{6.4}$$

Setting $v = w$ in the last bound, we deduce

$$|\mathcal{M}(w,w)| \le \frac{1}{4}\Big(\sum_{j=1}^{2} \left(\lambda\|w\|_{\Omega_j}^2 + \|\nabla w\|_{\Omega_j}^2\right)^{\frac{1}{2}}\Big)^2 \le \frac{1}{2} \sum_{j=1}^{2} \left(\lambda\|w\|_{\Omega_j}^2 + \|\nabla w\|_{\Omega_j}^2\right). \tag{6.5}$$

Therefore, (6.2) implies

$$\begin{aligned} D(t;w,w)+\lambda\|w\|^2+\mathcal{M}(w,w) &\geq \sum_{j=1}^{2}\|\nabla w\|^2_{\Omega_j}+\lambda\|w\|^2-|\mathcal{M}(w,w)| \\ &\geq \frac{1}{2}\Big(\sum_{j=1}^{2}\|\nabla w\|^2_{\Omega_j}+\lambda\|w\|^2\Big), \end{aligned}$$

which yields the strong monotonicity of the differential operator in weak form with respect to the quantity $\sum_{j=1}^{2}\|\nabla w\|^2_{\Omega_j}+\lambda\|w\|^2$ which is a norm in $\mathcal{H}^1_0$. The continuity follows from (6.1). Therefore, the problem is well-posed upon choosing $\lambda > 16C^2_{trace}C^2_{\tilde{p}}$. □

Now that the well-posedness of the reconstruction is settled, we make the following crucial observation: $Z_h \in S^p_h$ is the dG solution to the PDE problem (6.1) which has exact solution $w \in \mathcal{H}^1_0$. Indeed, letting $Y_h \in S^p_h$ to be the dG solution to (6.1), i.e., we have for all $V_h \in S^p_h$ that

$$\tilde{D}_h(t;Y_h,V_h)+\lambda\langle Y_h,V_h\rangle+\mathcal{M}(Y_h,V_h)=\langle g,V_h\rangle. \tag{6.6}$$

From the definition of g this implies

$$\tilde{D}_h(t;Y_h-Z_h,V_h)+\lambda\langle Y_h-Z_h,V_h\rangle+\mathcal{M}(Y_h,V_h)-\mathcal{M}(Z_h,V_h)=0, \tag{6.7}$$

noting carefully that g is defined against all of $L^2(\Omega)$ so testing with functions in S^p_h is permitted. Set $V_h = Y_h - Z_h$. Focusing on the last two terms on the left-hand side of the previous equation, Lipschitz continuity and lemma 3.16 imply

$$\begin{aligned} &|\mathcal{M}(Y_h,Y_h-Z_h)-\mathcal{M}(Z_h,Y_h-Z_h)| \leq C_{\tilde{p}}\|Y_h-Z_h\|^2_{\Gamma^{tr}} \\ &\leq C_{trace}C_{\tilde{p}}\Big(\varepsilon^{-1}\|Y_h-Z_h\|^2_K \\ &\qquad +\varepsilon\Big(\sum_{K\in\mathcal{T}}\|\nabla(Y_h-Z_h)\|^2_K+\|\sqrt{\theta\eta/\mathbf{h}}[\![Y_h-Z_h]\!]\|^2_{\Gamma^{int}}\Big)\Big), \end{aligned} \tag{6.8}$$

for $\varepsilon > h_{\max}$. Note that this is not really an essential restriction as ε will be of modest size as we shall now see. Indeed, choosing $\varepsilon = (4C_{trace}C_{\tilde{p}})^{-1}$ and $\lambda > 16C^2_{trace}C^2_{\tilde{p}}$, as in Lemma 6.1 above, (6.7) and (6.8), along with the coercivity of

D_h, (3.17), imply

$$\sum_{K\in\mathcal{T}} \|\nabla(Y_h - Z_h)\|_K^2 + \|Y_h - Z_h\|_K^2 + \|\sqrt{\gamma_0\mathbf{h}}[\![Y_h - Z_h]\!]\|_{\Gamma^{int}}^2 = 0,$$

noting that $\gamma > \frac{1}{2}\theta\eta$. The left-hand side is a norm (as it includes the L_2 norm) and, therefore, we conclude $Y_h = Z_h$.

Upon redefining the dG-norm as

$$|||v||| := \Big(\sum_{K\in\mathcal{T}} \|\nabla v\|_K^2 + \|\sqrt{\gamma_0/\mathbf{h}}[\![v]\!]\|_{\Gamma\setminus\Gamma^{tr}}\Big)^{1/2},$$

we now show the following result.

Lemma 6.2 (Energy-norm a posteriori error bound)**.** *Let $w \in \mathcal{H}_0^1$ be defined by (6.1). Then, the following bound holds:*

$$|||w - Z_h|||^2 + \lambda\|w - Z_h\|^2 \le C\big(\Upsilon_{S_1^c}^2(Z_h) + \Upsilon_{S_1^d}^2(Z_h)\big), \tag{6.9}$$

and, if $\frac{\partial w}{\partial t} \in \mathcal{H}^1$, then

$$\Big|\Big|\Big|\frac{\partial}{\partial t}(w - Z_h)\Big|\Big|\Big|^2 + \lambda\|\frac{\partial}{\partial t}(w - Z_h)\|^2 \le C\big(\Upsilon_{S_2^c}^2(Z_h) + \Upsilon_{S_2^d}^2(Z_h)\big), \tag{6.10}$$

where

$$\begin{aligned}
\Upsilon_{S_1^c}(Z_h) &:= \Big(\sum_{K\in\mathcal{T}} \|\mathbf{h}(g - \lambda Z_h + \Delta Z_h)\|_K^2 + \|\sqrt{\mathbf{h}}[\![\nabla Z_h]\!]\|_{\partial K\cap\Gamma^{int}}^2 \\
&\quad + \sum_{i=1}^{2} \|\sqrt{\mathbf{h}}\mathcal{P}(Z_h)[\![Z_h]\!] + \nabla Z_h)\cdot\mathbf{n}^i\|_{\partial K\cap\Gamma^{tr}}^2\Big)^{\frac{1}{2}}, \\
\Upsilon_{S_1^d}(Z_h) &:= \Big(6(C_1\gamma^{-2} + \gamma^{-1})\|\gamma_0\mathbf{h}^{-1/2}[\![Z_h]\!]\|_{\Gamma\setminus\Gamma^{tr}}^2 + 6C_0\gamma^{-2}\lambda\|\gamma_0\mathbf{h}^{-1/2}[\![Z_h]\!]\|_{\Gamma\setminus\Gamma^{tr}}^2\Big)^{\frac{1}{2}}, \\
\Upsilon_{S_2^c}(Z_h) &:= \Big(\sum_{K\in\mathcal{T}} \|\mathbf{h}\frac{\partial}{\partial t}(g - \lambda Z_h + \Delta Z_h)\|_K^2 + \|\sqrt{\mathbf{h}}[\![\nabla(\frac{\partial Z_h}{\partial t})]\!]\|_{\partial K\cap\Gamma^{int}}^2 \\
&\quad + \sum_{i=1}^{2} \|\sqrt{\mathbf{h}}\mathcal{P}(\frac{\partial Z_h}{\partial t})[\![\frac{\partial Z_h}{\partial t}]\!] + \nabla(\frac{\partial Z_h}{\partial t}))\cdot\mathbf{n}^i\|_{\partial K\cap\Gamma^{tr}}^2 + \Upsilon_{S_\infty}^2(Z_h)\Upsilon_{S_1^c}^2(Z_h)\Big)^{\frac{1}{2}},
\end{aligned} \tag{6.11}$$

$$\begin{aligned}
\Upsilon_{S_2^d}(Z_h) &:= \Big(\frac{5}{2}(C_1\gamma^{-2} + \gamma^{-1})\|\gamma_0\mathbf{h}^{-1/2}[\![\frac{\partial Z_h}{\partial t}]\!]\|_{\Gamma\setminus\Gamma^{tr}}^2 + \frac{5}{2}C_0\lambda\gamma^{-2}\|\gamma_0\mathbf{h}^{-1/2}[\![\frac{\partial Z_h}{\partial t}]\!]\|_{\Gamma\setminus\Gamma^{tr}}^2 \\
&\quad + \Upsilon_{S_\infty}^2(Z_h)\Upsilon_{S_1^d}^2(Z_h)\Big)^{\frac{1}{2}},
\end{aligned} \tag{6.12}$$

with $\Upsilon_{S_\infty}(Z_h) := \sum_{j=1}^{2} \|\frac{\partial Z_h}{\partial t}|_{\Omega_j}\|_{\infty,\Gamma^{tr}}$.

Proof. Using Lemma 3.14, we split the error $\epsilon := w - Z_h = \epsilon^c + Z_h^d$ into conforming and non-conforming parts, respectively, with $\epsilon^c := w - Z_h^c \in \mathcal{H}_0^1$ and $Z_h^d := Z_h^c - Z_h$. Noting that $\tilde{D}_h(Z_h^c, \epsilon^c) = D(Z_h^c, \epsilon^c)$ since both arguments are in $\mathcal{H}_0^1$, we have

$$\begin{aligned} |||\epsilon^c|||^2 + \lambda\|\epsilon^c\|^2 &= D(t; w, \epsilon^c) - \tilde{D}_h(Z_h^c, \epsilon^c) + \lambda\langle w, \epsilon^c\rangle - \lambda\langle Z_h^c, \epsilon^c\rangle \\ &= \langle g, \epsilon^c\rangle - \mathcal{M}(w, \epsilon^c) - \tilde{D}_h(Z_h^c, \epsilon^c) - \lambda\langle Z_h^c, \epsilon^c\rangle, \end{aligned} \tag{6.13}$$

where in the last step we used (6.1). From (6.6), we have

$$\tilde{D}_h(t; Z_h, \Pi_0\epsilon^c) + \lambda\langle Z_h, \Pi_0\epsilon^c\rangle + \mathcal{M}(Z_h, \Pi_0\epsilon^c) - \langle g, \Pi_0\epsilon^c\rangle = 0. \tag{6.14}$$

Adding the last two identities, we arrive at

$$\begin{aligned} &|||\epsilon^c|||^2 + \lambda\|\epsilon^c\|^2 \\ &= \Big(\langle g, \epsilon^c - \Pi_0\epsilon^c\rangle - \tilde{D}_h(Z_h, \epsilon^c - \Pi_0\epsilon^c) - \lambda\langle Z_h, \epsilon^c - \Pi_0\epsilon^c\rangle\Big) \\ &\quad + \Big(\mathcal{M}(Z_h, \Pi_0\epsilon^c) - \mathcal{M}(w, \epsilon^c)\Big) + \Big(\tilde{D}_h(Z_h^d, \epsilon^c) + \lambda\langle Z_h^d, \epsilon^c\rangle\Big) \\ &= \Big(\langle g, \epsilon^c - \Pi_0\epsilon^c\rangle - \tilde{D}_h(Z_h, \epsilon^c - \Pi_0\epsilon^c) - \lambda\langle Z_h, \epsilon^c - \Pi_0\epsilon^c\rangle - \mathcal{M}(Z_h, \epsilon^c - \Pi_0\epsilon^c)\Big) \\ &\quad + \Big(\mathcal{M}(Z_h, \epsilon^c) - \mathcal{M}(w, \epsilon^c)\Big) + \Big(\tilde{D}_h(Z_h^d, \epsilon^c) + \lambda\langle Z_h^d, \epsilon^c\rangle\Big) \\ &\quad =: (I) + (II) + (III). \end{aligned} \tag{6.15}$$

Term I can be estimated in completely analogous fashion to the corresponding term without reaction in Lemma 4.1.

For term II, the assumption $\tilde{p} = \mathcal{P}(z)\,(z_1 - z_2) \in C^{0,1}(\mathbb{R}^{2n})$ and Lemma 3.16 imply

$$\begin{aligned} |II| &\le \int_{\Gamma^{tr}} \Big(\big|\tilde{p}(Z_h) - \tilde{p}(w)\big|\Big)\big|[\![\epsilon^c]\!]\big| \\ &\le \int_{\Gamma^{tr}} C_{\tilde{p}}\big|w - Z_h\big|\,|[\![\epsilon^c]\!]| \\ &\le \int_{\Gamma^{tr}} C_{\tilde{p}}\big(\big|w - Z_h^c\big| + \big|Z_h^c - Z_h\big|\big)|[\![\epsilon^c]\!]| \\ &\le 2C_{\tilde{p}} \sum_{j=1}^{2} \big(\|\epsilon^c|_{\Omega_j}\|_{\Gamma^{tr}}^2 + \|Z_h^d|_{\Omega_j}\|_{\Gamma^{tr}}^2\big) \\ &\le \frac{1}{2}|||\epsilon^c|||^2 + \frac{\lambda}{2}\|\epsilon^c\|^2 + \frac{1}{2}|||Z_h^d|||^2 + \frac{\lambda}{2}\|Z_h^d\|^2, \end{aligned} \tag{6.16}$$

working completely analogously to (6.8), using the assumption that $h_{\max}$ is small enough.

Finally, for term III, we work completely analogously to the proof of Lemma 4.2 (noting that the estimator Υ_{J_K} in Lemma 4.2 includes the constant γ_0, as opposed to the current discussion). Putting these bounds together, the result already follows.

We now prove of (6.10). Similarly as before, we have

$$\begin{aligned}\Big|\Big|\Big|\frac{\partial \epsilon^c}{\partial t}\Big|\Big|\Big|^2 + \lambda\|\frac{\partial \epsilon^c}{\partial t}\|^2 &= D(t;\frac{\partial w}{\partial t},\epsilon^c) - \tilde{D}_h(\frac{\partial Z_h^c}{\partial t},\epsilon^c) + \lambda\langle\frac{\partial w_h^c}{\partial t},\epsilon^c\rangle - \lambda\langle\frac{\partial Z_h^c}{\partial t},\epsilon^c\rangle \\ &= \langle\frac{\partial g}{\partial t},\epsilon^c\rangle - \frac{d}{dt}\mathcal{M}(w,\epsilon^c) - \tilde{D}_h(\frac{\partial Z_h^c}{\partial t},\epsilon^c) - \lambda\langle\frac{\partial Z_h^c}{\partial t},\epsilon^c\rangle,\end{aligned} \tag{6.17}$$

where in the last step we inserted (6.1) differentiated with respect to t. Similarly inserting (6.14) differentiated with respect to time, yields

$$\begin{aligned}\Big|\Big|\Big|\frac{\partial \epsilon^c}{\partial t}\Big|\Big|\Big|^2 + \lambda\|\frac{\partial \epsilon^c}{\partial t}\|^2 &= \Big(\langle\frac{\partial g}{\partial t},\epsilon^c - \Pi_0\epsilon^c\rangle - \tilde{D}_h(\frac{\partial Z_h}{\partial t},\epsilon^c - \Pi_0\epsilon^c) - \lambda\langle\frac{\partial Z_h}{\partial t},\epsilon^c - \Pi_0\epsilon^c\rangle \\ &\quad - \frac{d}{dt}\mathcal{M}(Z_h,\epsilon^c - \Pi_0\epsilon^c)\Big) \\ &\quad + \frac{d}{dt}\Big(\mathcal{M}(Z_h,\epsilon^c) - \mathcal{M}(w,\epsilon^c)\Big) + \Big(\tilde{D}_h(\frac{\partial Z_h^d}{\partial t},\epsilon^c) + \lambda\langle\frac{\partial Z_h^d}{\partial t},\epsilon^c\rangle\Big) \\ &=: (I) + (II) + (III).\end{aligned} \tag{6.18}$$

as before, term I can be estimated in completely analogous fashion as in the proof of Lemma 4.1.

Concerning term II, the assumption $\tilde{p}' \in C^{0,1}(\mathbb{R}^{2n})$ and Lemma 3.16 imply

$$\begin{aligned}|II| &\leq \int_{\Gamma^{tr}} \frac{d}{dt}\Big(\big|\tilde{p}(Z_h) - \tilde{p}(w)\big|\Big)\big|[\![\epsilon^c]\!]\big| \\ &\leq \int_{\Gamma^{tr}} \Big(\big|(\tilde{p}'(Z_h) - \tilde{p}'(w))[\frac{\partial Z_h}{\partial t}]\big| + \big|\tilde{p}'(w)[\frac{\partial \epsilon}{\partial t}]\big|\Big)\big|[\![\epsilon^c]\!]\big| \\ &\leq \left(C_{\tilde{p}}\,(\Upsilon_{S_\infty}(Z_h))\sum_{j=1}^2 \|\epsilon|_{\Omega_j}\|_{\Gamma^{tr}} + \sum_{j=1}^2 C_{\tilde{p}'}\|\frac{\partial \epsilon}{\partial t}|_{\Omega_j}\|_{\Gamma^{tr}}\right)\sum_{j=1}^2 \|\epsilon^c|_{\Omega_j}\|_{\Gamma^{tr}} \\ &\leq \big(1 + C_{\tilde{p}}^2\Upsilon_{S_\infty}^2(Z_h)\big)\sum_{j=1}^2 \|\epsilon|_{\Omega_j}\|_{\Gamma^{tr}}^2 + \sum_{j=1}^2\left(C_{\tilde{p}'}^2\|\frac{\partial \epsilon}{\partial t}|_{\Omega_j}\|_{\Gamma^{tr}}^2 + 2\|Z_h^d|_{\Omega_j}\|_{\Gamma^{tr}}^2\right) \\ &\leq \frac{1}{4}\Big(\big(1 + \Upsilon_{S_\infty}^2(Z_h)\big)\left(|||\epsilon|||^2 + \lambda\|\epsilon\|^2\right) + \Big|\Big|\Big|\frac{\partial \epsilon^c}{\partial t}\Big|\Big|\Big|^2 + \lambda\|\frac{\partial \epsilon^c}{\partial t}\|^2 \\ &\qquad + \Big|\Big|\Big|\frac{\partial Z^d}{\partial t}\Big|\Big|\Big|^2 + \lambda\|\frac{\partial Z^d}{\partial t}\|^2 + |||Z_h^d|||^2 + \lambda\|Z_h^d\|^2\Big),\end{aligned} \tag{6.19}$$

where, as before $C_{\tilde{p}}$ is the Lipschitz constant of $\tilde{p}$, and $C_{\tilde{p}'}$ is a bound for its Jacobian. Furthermore, we assumed that $\lambda > 16C_{trace}^2 \max\{2, C_{\tilde{p}}^2, C_{\tilde{p}'}^2\}$.

working completely analogously to (6.8), using the assumption that $h_{\max}$ is small enough.

Finally, for (III), we work completely analogously to the proof of Lemma 4.2 (noting that the estimator Υ_{J_K} in Lemma 4.2 includes the constant γ_0, as opposed to the current discussion). Putting these bounds together, the result already follows. □

We will now also prove an a posteriori error bound for the elliptic problem in the $L_2(\Omega)$ norm for the above nonlinear elliptic interface problem via an Aubin-Nitsche duality-type argument, To do so, we follow some ideas from [20, 29] in order to treat the nonlinear interface condition.

Denoting by $\mathcal{S}^*$ the dual space of $\mathcal{S} := \mathcal{H}_0^1 + S_h^p$, we consider the linear operator $\mathcal{M}(w, \cdot) : \mathcal{S} \to \mathbb{R}$, which can be viewed as an operator

$$\mathcal{M} : \mathcal{S} \to \mathcal{S}^*, \quad \text{by } w \mapsto \mathcal{M}(w, \cdot). \tag{6.20}$$

Then, we define the derivative $\mathcal{M}'$ is a mapping $\mathcal{S} \to \mathcal{L}(\mathcal{S}, \mathcal{S}^*)$, where $\mathcal{L}(\mathcal{S}, \mathcal{S}^*)$ is the space of linear mappings from $\mathcal{S}$ to $\mathcal{S}^*$. Using this, for $\epsilon_r := rw + (1-r)Z_h$, we define

$$\mathcal{G}(t, v) := \int_0^1 \mathcal{M}'\left(\epsilon_r(t, \cdot)\right)(v) dr. \tag{6.21}$$

Now, setting $v = w - Z_h$, we have

$$\begin{aligned} \mathcal{G}(t, w - Z_h) &= \int_0^1 \mathcal{M}'(\epsilon_r)(w - Z_h) dr = \int_0^1 \frac{\partial}{\partial r}\big(\mathcal{M}(\epsilon_r)\big) dr \\ &= \mathcal{M}(w(t, \cdot)) - \mathcal{M}(Z_h(t, \cdot)), \end{aligned} \tag{6.22}$$

using the fact that the mapping $[0, 1] \to \mathcal{S}^*$, given by $r \mapsto \mathcal{M}(\epsilon_r)$ is continuously differentiable as $\tilde{p} \in C^{1,1}(\mathbb{R}^{2n})$. For brevity, we will denote $\mathcal{G}(t, z(t, .))$ by $\mathcal{G}z$.

We will use $\mathcal{G}$ define above to assume the existence of a regular dual problem, as follows.

Assumption 6.3. We assume that the domains Ω_1 and Ω_2 are such that for $s \in (\frac{3}{2}, 2]$, there exist a solution $\psi \in \mathcal{H}_0^s$ (defined in the obvious fashion) of the *linear*

dual equation

$$D_h^{L_2}(v,\psi) + \lambda\langle v,\psi\rangle + \langle \mathcal{G}v,\psi\rangle = \langle v,\alpha_1\rangle + \langle v|_{\Gamma^{tr}},\alpha_2\rangle_{\Gamma^{tr}} \quad \forall v \in \mathcal{H}_0^s + S_h^p, \quad (6.23)$$

where for the (non-projected) dG bilinear form

$$D_h^{L_2}(t;v,\phi) = \sum_{K\in\mathcal{T}}\int_K \nabla v\cdot\nabla\phi dx - \int_{\Gamma\setminus\Gamma^{tr}}(\{\nabla v\}\cdot[\![\phi]\!] + \{\nabla\phi\}\cdot[\![v]\!])ds + \int_{\Gamma\setminus\Gamma^{tr}}\frac{\gamma_0}{\mathbf{h}}[\![v]\!]\cdot[\![\phi]\!]ds,$$

for all data $\alpha_1 \in L_2(\Omega)$ and $\alpha_2 \in (H^{1/2}(\Gamma^{tr}))^2$, so that ψ satisfies the elliptic regularity estimate

$$\sum_{j=1}^{2}\|\psi\|_{\mathcal{H}_0^s(\Omega_j)} \le C_{ell}\big(\|\alpha_1\| + \|\alpha_2\|_{H^{1/2}(\Gamma^{tr})}\big), \quad (6.24)$$

for $C_{ell} > 0$, independent of ψ, α_1 and α_2. Note also that here, as well as in subsequent instances, $v|_{\Gamma^{tr}}$ should be interpreted as the vector function whose component are the traces of v from the two subdomains.

Remark 6.4. We note that the above construction in Assumption 6.3 is well posed. Indeed, the higher regularity required in allows for the (non-projected) dG bilinear form $D_h^{L_2}(t;v,\phi)$ for $\phi, v \in \mathcal{H}_0^s + S_h^p$ to make sense. Therefore, noting that, for $\phi \in \mathcal{H}_0^s$, we have

$$D_h^{L_2}(t;v,\phi) = \sum_{K\in\mathcal{T}}\int_K \nabla v\cdot\nabla\phi dx - \int_{\Gamma\setminus\Gamma^{tr}}\{\nabla\phi\}\cdot[\![v]\!]ds;$$

a simple integration by parts shows the consistency of this bilinear form with the weak Laplacian.

We are now ready to prove the following $L_2(\Omega)$-norm a posteriori error bounds for the dG method for the elliptic interface problem.

Lemma 6.5. *Assume that* (6.24) *holds for some* $s \in (\frac{3}{2}, 2]$. *Then, we have the bound*

$$\|w - Z_h\|^2 \le C\Upsilon^2_{S_1,L_2}(s,Z_h). \quad (6.25)$$

and, if in addition $\tilde{p}$ is twice differentiable with bounded second partial derivatives,

$$\begin{aligned}\|\frac{\partial}{\partial t}(w-Z_h)\|^2 \leq\ & \Upsilon^2_{S_2,L_2}(s,Z_h)+C\Upsilon^2_{S_1,L_2}(s,Z_h)\\ &\times\Big(C_{\tilde{p}}^{-1/2}\big(\Upsilon^2_{S_2^c}(Z_h)+\Upsilon^2_{S_2^d}(Z_h)\big)+\Upsilon_{S_\infty^{1/2}}(Z_h)\Big),\end{aligned}\tag{6.26}$$

for some constants $C>0$, independent of the mesh and the functions involved in the bounds, where

$$\begin{aligned}\Upsilon_{S_1,L_2}(s,Z_h) :=& \Big(\sum_{K\in\mathcal{T}} C(\partial K\cap\Gamma^{tr})\big(\|\mathbf{h}^s(g-\lambda Z_h+\Delta Z_h)\|_K^2\\ &+\|\mathbf{h}^{s-1/2}[\![\nabla Z_h]\!]\|^2_{\partial K\cap\Gamma^{int}}+\|\gamma_0\mathbf{h}^{s-3/2}[\![Z_h]\!]\|^2_{\partial K\cap\Gamma\setminus\Gamma^{tr}}\\ &+\sum_{i=1}^{2}\|\mathbf{h}^{s-1/2}(\mathcal{P}(Z_h)[\![Z_h]\!]+\nabla Z_h)\cdot\mathbf{n}^i\|^2_{\partial K\cap\Gamma^{tr}}\big)\Big)^{\frac{1}{2}}.\\ \Upsilon_{S_2,L_2}(s,Z_h) :=& \Big(\sum_{K\in\mathcal{T}} C(\partial K\cap\Gamma^{tr})\big(\|\mathbf{h}^s\frac{\partial}{\partial t}(g-\lambda Z_h+\Delta Z_h)\|_K^2\\ &+\|\mathbf{h}^{s-1/2}[\![\nabla(\frac{\partial Z_h}{\partial t})]\!]\|^2_{\partial K\cap\Gamma^{int}}+\|\gamma_0\mathbf{h}^{s-3/2}[\![\frac{\partial Z_h}{\partial t}]\!]\|^2_{\partial K\cap\Gamma\setminus\Gamma^{tr}}\\ &+\sum_{i=1}^{2}\|\mathbf{h}^{s-1/2}(\mathcal{P}(\frac{\partial Z_h}{\partial t})[\![\frac{\partial Z_h}{\partial t}]\!]+\nabla(\frac{\partial Z_h}{\partial t}))\cdot\mathbf{n}^i\|^2_{\partial K\cap\Gamma^{tr}}\big)\Big)^{\frac{1}{2}}.\end{aligned}$$

with $\Upsilon_{S_\infty^{1/2}}(Z_h):=\sum_{j=1}^{2}\|\frac{\partial Z_h}{\partial t}|_{\Omega_j}\|_{H^{1/2}(\Gamma^{tr})}$. $\Upsilon^2_{S_2^c}(Z_h)$ and $\Upsilon^2_{S_2^d}(Z_h)$ defined as in Lemma 6.2.

Proof. Let ψ solve (6.23) with $\alpha_1=\epsilon$ and $\alpha_2=0$. Testing with $v=\epsilon$, where $\epsilon=w-Z_h$ and applying (6.1), we deduce that

$$\begin{aligned}\|\epsilon\|^2 &= D_h^{L_2}(\epsilon,\psi)+\lambda\langle\epsilon,\psi\rangle+\langle\mathcal{G}\epsilon,\psi\rangle\\ &= D(w,\psi)-D_h^{L_2}(Z_h,\psi)+\lambda\langle w,\psi\rangle-\lambda\langle Z_h,\psi\rangle\\ &\quad+\mathcal{M}(w,\psi)-\mathcal{M}(Z_h,\psi)\\ &= \langle g,\psi\rangle-D_h^{L_2}(Z_h,\psi)-\lambda\langle Z_h,\psi\rangle-\mathcal{M}(Z_h,\psi).\end{aligned}\tag{6.27}$$

Also from (6.6), we have

$$0=-\langle g,\Pi\psi\rangle+\tilde{D}_h(t;Z_h,\Pi\psi)+\lambda\langle Z_h,\Pi\psi\rangle+\mathcal{M}(Z_h,\Pi\psi).\tag{6.28}$$

Noting that $\tilde{D}_h(t; Z_h, \Pi\psi) = D_h^{L_2}(Z_h, \Pi\psi)$ and adding (6.28) and (6.27), we arrive at

$$\begin{aligned}\|\epsilon\|^2 = \langle g, \psi - \Pi\psi\rangle - D_h^{L_2}(t; Z_h, \psi - \Pi\psi) - \lambda\langle Z_h, \psi - \Pi\psi\rangle \\ - \mathcal{M}(Z_h, \psi - \Pi\psi).\end{aligned} \tag{6.29}$$

Integration by parts yields

$$\begin{aligned}D_h^{L_2}(t; Z_h, \psi - \Pi\psi) = & -\sum_{K\in\mathcal{T}}\int_K \Delta Z_h(\psi - \Pi\psi)dx + \int_{\Gamma^{int}} [\![\nabla Z_h]\!]\{\psi - \Pi\psi\}ds \\ & - \int_{\Gamma\setminus\Gamma^{tr}} [\![Z_h]\!]\{\nabla(\psi - \Pi\psi)\}ds \\ & + \int_{\Gamma^{tr}} [\![\nabla Z_h(\psi - \Pi\psi)]\!]ds - \mathcal{M}(Z_h, \psi - \Pi\psi).\end{aligned}$$

Using this, along with the approximation estimates

$$\begin{aligned}\|\psi - \Pi\psi\|_K &\le C(\partial K \cap \Gamma^{tr}) h_K^s |\psi|_{H^s(K)} \\ \|\psi - \Pi\psi\|_{\partial K} &\le C(\partial K \cap \Gamma^{tr}) h_K^{s-1/2} |\psi|_{H^s(K)} \\ \|\nabla(\psi - \Pi\psi)\|_{\partial K} &\le C(\partial K \cap \Gamma^{tr}) h_K^{s-3/2} |\psi|_{H^s(K)},\end{aligned} \tag{6.30}$$

and working as in the case of the energy-norm a posteriori bound in Chapter 4, we deduce the first bound.

Next, we prove the second bound. Following [20], we use the linearity of $\mathcal{G}$ in the second argument, to have

$$\frac{d}{dt}\mathcal{G}(t, \epsilon(t)) = (\frac{\partial \mathcal{G}}{\partial \epsilon})|_{(t,\epsilon(t))}\frac{\partial \epsilon}{\partial t} + (\frac{\partial \mathcal{G}}{\partial t})|_{(t,\epsilon(t))} = \mathcal{G}|_{(t,\epsilon(t))}\frac{\partial \epsilon}{\partial t} + (\frac{\partial \mathcal{G}}{\partial t})|_{(t,\epsilon(t))}.$$

Setting $v = \frac{\partial \epsilon}{\partial t}$, $\alpha_1 = \frac{\partial \epsilon}{\partial t}$ and $\alpha_2 = 0$ in (6.23), having exact solution $\Psi \in \mathcal{H}_0^s$, now, along with the last identity, yields for each t:

$$\begin{aligned}\left\|\frac{\partial \epsilon}{\partial t}\right\|^2 &= D_h^{L_2}\big(\frac{\partial \epsilon}{\partial t}, \Psi\big) + \lambda\langle\frac{\partial \epsilon}{\partial t}, \Psi\rangle + \langle\mathcal{G}\frac{\partial \epsilon}{\partial t}, \Psi\rangle \\ &= D_h^{L_2}\big(\frac{\partial w}{\partial t}, \Psi\big) - D_h^{L_2}\big(\frac{\partial Z_h}{\partial t}, \Psi\big) + \lambda\langle\frac{\partial w}{\partial t}, \Psi\rangle - \lambda\langle\frac{\partial Z_h}{\partial t}, \Psi\rangle \\ &\quad + \frac{d}{dt}\big(\mathcal{M}(w, \Psi) - \mathcal{M}(Z_h, \Psi)\big) - \langle\frac{\partial \mathcal{G}}{\partial t}, \Psi\rangle. \\ &= \langle\frac{\partial g}{\partial t}, \Psi\rangle - D_h^{L_2}\big(\frac{\partial Z_h}{\partial t}, \Psi\big) - \lambda\langle\frac{\partial Z_h}{\partial t}, \Psi\rangle - \frac{d}{dt}\big(\mathcal{M}(Z_h, \Psi)\big) - \langle\frac{\partial \mathcal{G}}{\partial t}, \Psi\rangle\end{aligned} \tag{6.31}$$

where, in the last step, we have inserted (6.1) differentiated with respect to time

and tested with Ψ. Similarly inserting (6.28) differentiated in time and tested with $\Pi_0\Psi$, implies

$$\begin{aligned}\Big\|\frac{\partial\epsilon}{\partial t}\Big\|^2 &= \Big(\langle\frac{\partial g}{\partial t},\Psi-\Pi\Psi\rangle - D_h^{L_2}\big(\frac{\partial Z_h}{\partial t},\Psi-\Pi\Psi\big) - \lambda\langle\frac{\partial Z_h}{\partial t},\Psi-\Pi\Psi\rangle \\ &\quad - \frac{d}{dt}\mathcal{M}\big(Z_h,\Psi-\Pi\Psi\big)\Big) - \Big(\langle\frac{\partial\mathcal{G}}{\partial t},\Psi\rangle\Big) \\ &\leq (I)+(II).\end{aligned} \tag{6.32}$$

Integration by parts to bound the first term on the right hand side of (6.32), gives

$$\begin{aligned}D_h^{L_2}(t;\frac{\partial Z_h}{\partial t},\Psi-\Pi\Psi) &= -\sum_{K\in\mathcal{T}}\int_K\Delta\big(\frac{\partial Z_h}{\partial t}\big)(\Psi-\Pi\Psi)dx \\ &\quad+\int_{\Gamma^{int}}[\![\nabla\big(\frac{\partial Z_h}{\partial t}\big)]\!]\{\Psi-\Pi\Psi\}ds - \int_{\Gamma\setminus\Gamma^{tr}}[\![\frac{\partial Z_h}{\partial t}]\!]\{\nabla(\Psi-\Pi\Psi)\}ds \\ &\quad+\int_{\Gamma^{tr}}[\![\nabla\big(\frac{\partial Z_h}{\partial t}\big)(\Psi-\Pi\Psi)]\!]ds - \frac{d}{dt}\mathcal{M}\left(Z_h,\Psi-\Pi\Psi\right).\end{aligned}$$

The term I can be bounded using (6.30) and working as in the case of the energy-norm a posteriori bound in Chapter 4.

Next, we move the second term II. To do this, using (6.33), we have

$$\begin{aligned}\langle\mathcal{G}|_{(t,\epsilon(t))},\Psi\rangle &= \Big\langle\int_0^1\mathcal{M}'(\epsilon_r)\epsilon(t)|_{\Gamma^{tr}}dr,\Psi|_{\Gamma^{tr}}\Big\rangle \\ &= \int_0^1\left\langle\left(\tilde{p}\left(\epsilon_r\right)\right)'\left[\epsilon(t)|_{\Gamma^{tr}}\right],[\![\Psi]\!]\right\rangle dr \\ &= \int_0^1\left(\int_{\Gamma^{tr}}\left(\tilde{p}\left(\epsilon_r\right)\right)'\left[\epsilon(t)|_{\Gamma^{tr}}\right]\cdot[\![\Psi]\!]\right)dr.\end{aligned} \tag{6.33}$$

Using the boundedness of the second derivatives of $\tilde{p}$, the elliptic regularity of Ψ (6.24), yields

$$\begin{aligned}
\langle \frac{\partial \mathcal{G}}{\partial t}|_{(t,\epsilon(t))}, \Psi\rangle &= \Big| \int_0^1 \left(\int_{\Gamma^{tr}} \left(\tilde{p}''(\epsilon_r)\Big[\frac{\partial \epsilon_r}{\partial t}, \epsilon(t)\Big]|_{\Gamma^{tr}} \cdot [\![\Psi]\!] \right) dr \right) \Big| \\
&\leq \int_0^1 \left(\int_{\Gamma^{tr}} |\tilde{p}''(\epsilon_r)| \Big| \frac{\partial \epsilon_r}{\partial t}|_{\Gamma^{tr}} \Big| |\epsilon(t)|_{\Gamma^{tr}}| |[\![\Psi]\!]| \right) dr \\
&\leq C_{\tilde{p}''} \left(\sum_{j=1}^{2} \|\Psi\|_{\infty,\Omega_j} \right) \int_{\Gamma^{tr}} \left(\Big| \frac{\partial \epsilon(t)}{\partial t}|_{\Gamma^{tr}} \Big| + \Big| \frac{\partial Z_h}{\partial t}|_{\Gamma^{tr}} \Big| \right) |\epsilon(t)|_{\Gamma^{tr}}| \\
&\leq C_{\tilde{p}''} C_{ell} \| \frac{\partial \epsilon(t)}{\partial t} \| \\
&\quad \sum_{j=1}^{2} \left(\sum_{E \in \Gamma^{tr}} \| \frac{\partial \epsilon(t)}{\partial t}|_{\Omega_j} \|_{H^{1/2}(E)} + \| \frac{\partial Z_h}{\partial t}|_{\Omega_j} \|_{H^{1/2}(\Gamma^{tr})} \right) \|\epsilon(t)|_{\Gamma^{tr}} \|_{H^{1/2}(\Gamma^{tr})^*},
\end{aligned} \tag{6.34}$$

where $H^{1/2}(\Gamma^{tr})^*$ indicates the dual space of $H^{1/2}(\Gamma^{tr})$. Applying trace theorem, on both terms on the right hand side of the above equation along with Lemma 6.2, gives

$$\begin{aligned}
\sum_{j=1}^{2} \sum_{E \in \Gamma^{tr}} \| \frac{\partial \epsilon(t)}{\partial t}|_{\Omega_j} \|_{H^{1/2}(E)} &= \sum_{j=1}^{2} \sum_{E \in \Gamma^{tr}} \left(\| \frac{\partial \epsilon(t)}{\partial t}|_{\Omega_j} \|_E^2 + | \frac{\partial \epsilon(t)}{\partial t}|_{\Omega_j} |_{H^{1/2}(E)}^2 \right)^{1/2} \\
&\leq \left(\sum_{j=1}^{2} \| \frac{\partial \epsilon(t)}{\partial t}|_{\Omega_j} \|_{\Gamma^{tr}}^2 \right)^{1/2} + C \left(\sum_{K \in \mathcal{T}^{tr}} | \frac{\partial \epsilon(t)}{\partial t}|_{H^1(K)}^2 \right)^{1/2} \\
&\leq (\frac{1}{\sqrt{C_{\tilde{p}}}} + C) \left(\frac{1}{4} \Big| \Big| \Big| \frac{\partial \epsilon}{\partial t} \Big| \Big| \Big|^2 + \frac{\lambda}{4} \| \frac{\partial \epsilon}{\partial t} \|^2 \right)^{1/2} \\
&\leq 2C(\frac{1}{\sqrt{C_{\tilde{p}}}} + C) \big(\Upsilon_{S_2^c}^2(Z_h) + \Upsilon_{S_2^d}^2(Z_h) \big)^{1/2},
\end{aligned} \tag{6.35}$$

where, in the last step, we have used Lemma 3.16.

To estimate $\|\epsilon(t)|_{\Gamma^{tr}}\|_{H^{1/2}(\Gamma^{tr})^*}$ we use a duality argument. Let $\tilde{\psi}$ be the solution of (6.23) with $\beta = \delta(\epsilon)$. Hence, δ is the duality between $\|\epsilon(t)|_{\Gamma^{tr}}\|_{H^{1/2}(\Gamma^{tr})}$ and $\|\epsilon(t)|_{\Gamma^{tr}}\|_{H^{1/2}(\Gamma^{tr})^*}$, such that $\|\delta(\epsilon)\|_{H^{1/2}(\Gamma^{tr})} = \|\epsilon(t)|_{\Gamma^{tr}}\|_{H^{1/2}(\Gamma^{tr})^*}$ and $\langle \epsilon(t), \delta(\epsilon)\rangle_{\Gamma^{tr}} =$

$\|\epsilon(t)|_{\Gamma^{tr}}\|_{H^{1/2}(\Gamma^{tr})^*}$, we obtain

$$\begin{aligned}\|\epsilon(t)|_{\Gamma^{tr}}\|^2_{H^{1/2}(\Gamma^{tr})^*} &= \langle \epsilon, \delta(\epsilon)\rangle_{\Gamma^{tr}} \\ &= \tilde{D}_h\big(w,\tilde{\psi}\big) - \hat{D}_h\big(Z_h,\tilde{\psi}\big) + \lambda\langle\epsilon,\tilde{\psi}\rangle + \mathcal{M}\big(w,\tilde{\psi}\big) - \mathcal{M}\big(Z_h,\tilde{\psi}\big) \\ &= \langle g, \tilde{\psi}-\Pi\tilde{\psi}\rangle - \tilde{D}_h\big(Z_h,\tilde{\psi}-\Pi\tilde{\psi}\big) - \lambda\langle Z_h,\tilde{\psi}-\Pi\tilde{\psi}\rangle \\ &\quad - \mathcal{M}\big(Z_h,\tilde{\psi}-\Pi\tilde{\psi}\big)\end{aligned}$$

From here, the same steps used to derived (6.25) can be followed, yielding,

$$\|\epsilon(t)|_{\Gamma^{tr}}\|_{H^{1/2}(\Gamma^{tr})^*} \leq C\Upsilon_{S_1,L_2}(s,Z_h). \tag{6.36}$$

Combining (6.36) and (6.35) with (6.34) we can bound the last term on the right hand of (6.32) and this concludes the proof. □

6.3 A posteriori bounds for the semi-discrete case

We can now proceed to the derivation of a posteriori error bounds for the spatially discrete problem in various norms.

6.3.1 $(L_\infty(L_2)+L_2(H^1))$-norm a posteriori error bounds

We derive a posteriori error bounds for the $(L_\infty(L_2)+L_2(H^1))$-equivalent norm, which defined as

$$\|e\|_* \equiv \|e\|_*(t) := \Big(\|e\|^2_{L_\infty(0,t;L_2(\Omega))} + \int_0^t |||e|||^2\,ds\Big)^{1/2}. \tag{6.37}$$

The key idea in our analysis is to utilise the elliptic reconstruction framework discussed above. In particular, we begin by defining for each $t\in[0,T]$ the elliptic reconstruction $w\equiv w(t,u_h)\in\mathcal{H}^1_0$, to be the unique solution of the problem

$$D(t;w,v)+\mathcal{M}(w,v)+\lambda\langle w,v\rangle = \langle f-\frac{\partial u_h}{\partial t}+\lambda u_h, v\rangle, \qquad v\in\mathcal{H}^1_0, \tag{6.38}$$

i.e., we set $g=f-\frac{\partial u_h}{\partial t}+\lambda u_h$ to (6.1); the idea to define the elliptic reconstruction via the temporal derivative can be also found in [50]. Notice that from (2.21), we

have

$$\langle\frac{\partial u_h}{\partial t}, v_h\rangle + \tilde{D}_h(t; u_h, v_h) + \mathcal{M}(u_h, v_h) = \langle f, v_h\rangle, \qquad \text{for all } v_h \in S_h^p,$$

which immediately implies

$$\tilde{D}_h(t; u_h, v_h) + \mathcal{M}(u_h, v_h) + \lambda\langle u_h, v_h\rangle = \langle f - \frac{\partial u_h}{\partial t} + \lambda u_h, v_h\rangle, \tag{6.39}$$

i.e., (6.2) with $Z_h = u_h$!

Lemma 6.6. *(error relation) Let u and u_h be the solutions of (2.19) and (2.21), respectively, and let w be given by* (6.38)*. Setting*

$$e := \rho + \epsilon, \qquad \rho := u - w, \qquad \epsilon := w - u_h,$$

we have the identity

$$\langle\frac{\partial e}{\partial t}, v\rangle + D(\rho, v) + \mathcal{M}(u, v) - \mathcal{M}(w, v) = \lambda\langle\epsilon, v\rangle. \tag{6.40}$$

Proof. For each $v \in \mathcal{H}_0^1$, from (2.19), we have

$$\begin{aligned} &\langle\frac{\partial e}{\partial t}, v\rangle + D(\rho, v) + \mathcal{M}(u, v) - \mathcal{M}(w, v) + \lambda\langle\rho, v\rangle \\ &= \langle f, v\rangle - \langle\frac{\partial u_h}{\partial t}, v\rangle - D(w, v) - \mathcal{M}(w, v) + \lambda\langle\rho, v\rangle \\ &= \lambda\langle e, v\rangle, \end{aligned} \tag{6.41}$$

using (6.38) for the last equality. The result follows by noting that $e = \rho + \epsilon$. □

Theorem 6.7 ($(L_\infty(L_2) + L_2(H^1))$-norm estimate)**.** *For each $t \in [0, T]$, and λ as defined above, we have*

$$\begin{aligned} \|e\|_*^2 \le 4\mathrm{e}^{2\lambda T}\Bigg(&\Big(\|u_0 - u_h(0)\| + C_0\|\sqrt{\theta\eta\mathbf{h}}[\![u_h(0)]\!]\|_{\Gamma\setminus\Gamma^{tr}}\Big)^2 \\ &+ C\int_0^T \big(\Upsilon_{S_1^c}^2(u_h) + \Upsilon_{S_1^d}^2(u_h)\big)dt + \frac{2}{\lambda}\|\sqrt{\theta\eta\mathbf{h}}[\![\frac{\partial u_h}{\partial t}]\!]\|_{\Gamma\setminus\Gamma^{tr}}^2\Bigg) \\ &+ 2\|\sqrt{\theta\eta\mathbf{h}}[\![u_h]\!]\|_{L_\infty(0,T;L_2(\Omega))}^2. \end{aligned} \tag{6.42}$$

Proof. We begin by decomposing u_h into conforming $u_h^c := \mathcal{E}(u_h)$ and non-conforming parts $u_h^d := u_h - \mathcal{E}(u_h)$ with the help of Lemma 3.14. We also (re)set $e^c := u - u_h^c$, and $\epsilon^c := w - u_h^c$, thereby, we have $e = e^c - u_h^d$, $\epsilon = \epsilon^c - u_h^d$ and $e^c = \rho + \epsilon^c$.

Setting $v = e^c$ in (6.54), therefore, we have

$$\begin{aligned} &\frac{1}{2}\frac{d}{dt}\|e^c\|^2 + D(t; e^c, e^c) = \langle \frac{\partial e^c}{\partial t}, e^c\rangle + D(t; e^c, e^c) \\ &= \langle \frac{\partial u_h^d}{\partial t}, e^c\rangle + D(t; \epsilon^c, e^c) - \mathcal{M}(u, e^c) + \mathcal{M}(w, e^c) + \lambda\langle \epsilon, e^c\rangle. \end{aligned} \tag{6.43}$$

Working completely analogously to (6.19), for λ large enough, we have

$$\begin{aligned} |\mathcal{M}(u, e^c) - \mathcal{M}(w, e^c)| &\leq C_{\tilde{p}} \sum_{j=1}^{2} \left(\|\rho|_{\Omega_j}\|^2_{\Gamma^{tr}} + \|e^c|_{\Omega_j}\|^2_{\Gamma^{tr}} \right) \\ &\leq 2C_{\tilde{p}} \sum_{j=1}^{2} \left(\|e^c|_{\Omega_j}\|^2_{\Gamma^{tr}} + \|\epsilon^c|_{\Omega_j}\|^2_{\Gamma^{tr}} \right) \\ &\leq \frac{1}{2}|||e^c|||^2 + \frac{\lambda}{2}\|e^c\|^2 + \frac{1}{2}|||\epsilon^c|||^2 + \frac{\lambda}{2}\|\epsilon^c\|^2. \end{aligned} \tag{6.44}$$

Using the Cauchy-Schwarz inequality and Lemma 3.17, we also have

$$\begin{aligned} |\lambda\langle \epsilon, e^c\rangle| &\leq \lambda\|\epsilon\|^2 + \frac{\lambda}{4}\|e^c\|^2, \\ |\langle \frac{\partial u_h^d}{\partial t}, e^c\rangle| &\leq \lambda^{-1}\|\frac{\partial u_h^d}{\partial t}\|^2 + \frac{\lambda}{4}\|e^c\|^2, \\ |D(t; \epsilon^c, e^c)| &\leq C|||\epsilon^c|||^2 + \frac{1}{4}|||e^c|||^2 \leq C|||\epsilon|||^2 + C|||u_h^d|||^2 + \frac{1}{4}|||e^c|||^2. \end{aligned} \tag{6.45}$$

Combing all of these bounds together, yields

$$\begin{aligned} \frac{d}{dt}\|e^c\|^2 + \frac{1}{2}|||e^c|||^2 \leq\ & 2\lambda\|e^c\|^2 + C|||\epsilon|||^2 + 3\lambda\|\epsilon\|^2 \\ & + C|||u_h^d|||^2 + \lambda\|u_h^d\|^2 + \frac{2}{\lambda}\|\frac{\partial u_h^d}{\partial t}\|^2. \end{aligned} \tag{6.46}$$

Integrating the time variable for $s \in (0, t)$, we have

$$\|e^c(t)\|^2 + \frac{1}{2}\int_0^t |||e^c|||^2 ds \leq 2\lambda \int_0^t \|e^c\|^2 ds + \mathcal{R}(t), \tag{6.47}$$

where

$$\mathcal{R}(t) := \|e^c(0)\|^2 + \int_0^t \left(C|||\epsilon|||^2 + 3\lambda\|\epsilon\|^2 + C|||u_h^d|||^2 + \lambda\|u_h^d\|^2 + \frac{2}{\lambda}\|\frac{\partial u_h^d}{\partial t}\|^2 \right) ds.$$

and using Gronwall inequality (2.4), we deduce

$$\|e^c(t)\|^2 + \frac{1}{2}\int_0^t |||e^c|||^2 ds \leq \mathrm{e}^{2\lambda t}\mathcal{R}(t), \tag{6.48}$$

noting the trivial bound $\|e^c\|^2 \leq \|e^c\|^2 + \int_0^s |||e^c|||^2 d\tilde{s}$. Since $\|e^c(t)\|$ is assumed to be continuous with respect to t, we can select $t = t_*$ such that $\|e^c(t_*)\| = \|e^c\|_{L_\infty(0,T;L_2(\Omega))}$. Therefore, (6.48) for $t = t_*$ implies

$$\|e^c\|^2_{L_\infty(0,T;L_2(\Omega))} \leq \|e^c(t_*)\|^2 + \frac{1}{2}\int_0^{t_*} |||e^c|||^2 ds \leq \mathrm{e}^{2\lambda t_*}\mathcal{R}(t_*) \leq \mathrm{e}^{2\lambda T}\mathcal{R}(T),$$

with T being the final time. Combining this with (6.48) for $t = T$, we arrive at

$$\|e^c\|^2_* = \|e^c\|^2_{L_\infty(0,T;L_2(\Omega))} + \frac{1}{2}\int_0^{T} |||e^c|||^2 ds \leq 2\mathrm{e}^{2\lambda T}\mathcal{R}(T).$$

Triangle inequality now implies $\|e\|_* \leq \|e^c\|_* + \|u_h^d\|_*$, thereby, concluding

$$\|e\|^2_* \leq 4\mathrm{e}^{2\lambda T}\mathcal{R}(T) + 2\|u_h^d\|^2_*.$$

Lemmas 6.2, 3.14 and 4.2 now give

$$\begin{aligned}\mathcal{R}(T) \leq \Big(\|u_0 - u_h(0)\| + C_0\|\sqrt{\theta\eta\mathbf{h}}[\![u_h(0)]\!]\|\Big)^2 + C\int_0^T \big(\Upsilon^2_{S_1^c}(u_h) + \Upsilon^2_{S_1^d}(u_h)\big)dt \\ + \|\sqrt{\theta\eta\mathbf{h}}[\![\frac{\partial u_h}{\partial t}]\!]\|^2_{\Gamma\setminus\Gamma^{tr}},\end{aligned}$$

while

$$\|u_h^d\|^2_* \leq \|\sqrt{\theta\eta\mathbf{h}}[\![u_h]\!]\|^2_{L_\infty(0,T;L_2(\Omega))} + C\int_0^T \Upsilon^2_{S_1^d}(u_h)dt.$$

The result, therefore, already follows by combining the last three inequalities. □

Remark 6.8. We note that the elemental residual in $\Upsilon_{S_1^c}(u_h)$ is equal to

$$\sum_{K\in\mathcal{T}} \|\mathbf{h}(f - \frac{\partial u_h}{\partial t} + \Delta u_h)\|^2_K,$$

since $g = f - \frac{\partial u_h}{\partial t} + \lambda u_h$. Therefore, the above approach, indeed, results to the expected residuals.

6.3.2 $L_\infty(L_2)$-norm a posteriori error bounds

We now derive a posteriori error bounds for the $L_\infty(L_2)$-norm only, which are expected to be of higher order than the respective $(L_\infty(L_2) + L_2(H^1))$-norm ones derived above. The elliptic reconstruction framework will now play a crucial role

in achieving optimal order a posteriori estimates, just like the classical elliptic projection idea does for the respective a priori error analysis.

Lemma 6.9 ($L_\infty(L_2)$-norm estimate)**.** *For each time T, and for λ as defined above, $s \in (\frac{3}{2}, 2]$ as in* (6.24)*. Then, the following bound holds:*

$$\begin{aligned}\|e\|^2_{L_\infty(0,T;L_2(\Omega))} \leq \mathrm{e}^{\lambda T/2}\Big(\big(\|u_0 - u_h(0)\| + S_1^{L_2}(s, u_h(0))\big)^2 \\ + \int_0^T 8\lambda\big(\Upsilon^2_{S_{1,L_2}}(s, u_h(t)) + \frac{4}{\lambda}\Upsilon^2_{S_{2,L_2}}(s, u_h(t))\big)dt\Big) \\ + 2\max_{0\leq t\leq T} \Upsilon^2_{S_{1,L_2}}(s, u_h(t)),\end{aligned} \tag{6.49}$$

with $\Upsilon_{S_{1,L_2}}$ and $\Upsilon_{S_{2,L_2}}$ as in Lemma 6.5.

Proof. Testing with $v = \rho$ in (6.54), we have

$$\langle\frac{\partial\rho}{\partial t}, \rho\rangle + D(t; \rho, \rho) + \mathcal{M}(u, \rho) - \mathcal{M}(w, \rho) = \lambda\langle\epsilon, \rho\rangle - \langle\frac{\partial\epsilon}{\partial t}, \rho\rangle. \tag{6.50}$$

From (6.2) (with ρ in place of w and a different choice of the parameter in Young's inequality,) and the Cauchy-Schwarz inequality, we have

$$\frac{1}{2}\frac{d}{dt}\|\rho\|^2 + |||\rho|||^2 \leq |||\rho|||^2 + \frac{\lambda}{16}\|\rho\|^2 + 4\lambda\|\epsilon\|^2 + \frac{\lambda}{16}\|\rho\|^2 + \frac{2}{\lambda}\|\frac{\partial\epsilon}{\partial t}\|^2 + \frac{\lambda}{8}\|\rho\|^2,$$

or

$$\frac{d}{dt}\|\rho\|^2 \leq \frac{\lambda}{2}\|\rho\|^2 + 8\lambda\|\epsilon\|^2 + \frac{4}{\lambda}\|\frac{\partial\epsilon}{\partial t}\|^2. \tag{6.51}$$

Integrating for a dummy variable u between 0 and t the time variable and using Gronwall's inequality (2.4), we deduce

$$\|\rho(t)\|^2 \leq \mathrm{e}^{\lambda t/2}\Big(\|\rho(0)\|^2 + \int_0^t \Big(8\lambda\|\epsilon\|^2 + \frac{4}{\lambda}\|\frac{\partial\epsilon}{\partial t}\|^2\Big)du\Big). \tag{6.52}$$

Since $\|w(t)\|$ is assumed to be continuous with respect to t, we can select $t = t_*$ such that $\|\rho(t_*)\| = \|\rho\|_{L_\infty(0,T;L_2(\Omega))}$ in (6.52), to arrive at

$$\|\rho\|^2_{L_\infty(0,T;L_2(\Omega))} \leq \mathrm{e}^{\lambda T/2}\Big(\|\rho(0)\|^2 + \int_0^T \Big(8\lambda\|\epsilon\|^2 + \frac{4}{\lambda}\|\frac{\partial\epsilon}{\partial t}\|^2\Big)du\Big). \tag{6.53}$$

Using Lemma 6.5 and the bounds

$$\|\rho(0)\| = \|u_0 - w(0)\| \leq \|u_0 - u_h(0)\| + \|\epsilon(0)\|,$$

$$\|u-u_h\|^2_{L_\infty(0,T;L_2(\Omega))} \le 2\|\rho\|^2_{L_\infty(0,T;L_2(\Omega))} + 2\|\epsilon\|^2_{L_\infty(0,T;L_2(\Omega))},$$

the result already follows. □

6.4 A posteriori bounds for the fully-discrete case

Let u be the solutions of (2.19) and the sequence and $\{u_h^n\}_n$ be the fully-discrete solution from (2.23) with $u_h^n \in S^n$, $n = 0, 1, \ldots, N$, respectively. Let also $w^n \in \mathcal{H}_0^1$ be the elliptic reconstruction of u_h^n given by (6.1) for $Z_h = u_h^n$. Let u_h and w denote the piecewise linear interpolants with respect to t at the points $\{u_h^n\}_n$ and $\{w^n\}_n$, respectively, viz., for $t \in (t_{n-1}, t_n]$

$$u_h(t) := \ell_{n-1}(t)u_h^{n-1} + \ell_n(t)u_h^n, \qquad w(t) := \ell_{n-1}(t)w^{n-1} + \ell_n(t)w^n,$$

for all $n = 1, \ldots, N$, with $\ell_{n-1}(t) := (t - t_{n-1})/k^n$ and $\ell_n(t) := (t_n - t)/k^n$, noting that

$$\frac{\partial u_h}{\partial t} = \frac{u_h^n - u_h^{n-1}}{k^n}.$$

Setting, as before,

$$e := \rho + \epsilon, \qquad \rho := u - w, \qquad \epsilon := w - u_h,$$

and correspondingly for e^c, ϵ^c and u_h^d, we have from (2.19) for $v \in \mathcal{H}_0^1$,

$$\begin{aligned} &\langle \frac{\partial e}{\partial t}, v\rangle + D(\rho, v) + \lambda\langle \rho, v\rangle \\ &= \langle f, v\rangle - \mathcal{M}(u, v) - \langle \frac{u_h^n - u_h^{n-1}}{k^n}, v\rangle - D(w, v) + \lambda\langle \rho, v\rangle. \end{aligned} \tag{6.54}$$

Now, from the elliptic reconstruction definition, we have

$$\begin{aligned} &D(w, v) + \lambda\langle w, v\rangle + \ell_{n-1}(t)\mathcal{M}(w^{n-1}, v) + \ell_n(t)\mathcal{M}(w^n, v) \\ &= \langle \ell_{n-1}(t)g^{n-1} + \ell_n(t)g^n, v\rangle, \end{aligned} \tag{6.55}$$

from linearity, for

$$g^n = f^n - \frac{u_h^n - u_h^{n-1}}{k^n} + \lambda u_h^n,$$

with $g^n = g(t_n, \cdot)$ and $f^n = f(t_n, \cdot)$. Combining, therefore (6.54) and (6.55), we have the identity

$$\begin{aligned}
&\langle \frac{\partial e}{\partial t}, v\rangle + D(\rho, v) + \lambda\langle \rho, v\rangle \\
&= \langle f, v\rangle - \mathcal{M}(u, v) - \langle \frac{u_h^n - u_h^{n-1}}{k^n}, v\rangle + \lambda\langle u, v\rangle \\
&\quad + \ell_{n-1}(t)\mathcal{M}(w^{n-1}, v) + \ell_n(t)\mathcal{M}(w^n, v) - \langle \ell_{n-1}(t)g^{n-1} + \ell_n(t)g^n, v\rangle \\
&= \lambda\langle e, v\rangle + \langle f - \ell_{n-1}(t)f^{n-1} - \ell_n(t)f^n, v\rangle \\
&\quad + \ell_{n-1}(t)\langle \frac{u_h^{n-1} - u_h^{n-2}}{k^{n-1}} - \frac{u_h^n - u_h^{n-1}}{k^n}, v\rangle \\
&\quad + \Big(\ell_{n-1}(t)\mathcal{M}(w^{n-1}, v) + \ell_n(t)\mathcal{M}(w^n, v) - \mathcal{M}(u, v)\Big) \\
&=: \lambda\langle e, v\rangle + \mathcal{A}(v) + \mathcal{B}(v) + \mathcal{C}(v),
\end{aligned} \tag{6.56}$$

noting the trivial identity $\ell_n(t) = 1 - \ell_{n-1}(t)$ for $t \in (t_{n-1}, t_n]$. We observe that the first arguments in $\lambda\langle e, v\rangle$ and $\mathcal{C}$ are not computable as it stands, so they will have to be estimated using the Lipschitz property of $\mathcal{M}(\cdot, v)$ and compensated on the left-hand side by the choice of $\lambda > 0$ being sufficiently large.

Theorem 6.10 ($(L_\infty(L_2)+L_2(H^1))$-norm estimate)**.** *For every $n = 1, \dots, N$, and λ as defined above, we have*

$$\|e\|_*^2(t_n) \le 4\mathrm{e}^{5\lambda t_n/2}\Upsilon_{fd}^n + 4\max_{1\le j\le n}\|\sqrt{\theta\eta\mathbf{h}_j}[\![u_h^j]\!]\|^2, \tag{6.57}$$

with

$$\Upsilon_{fd}^n := \Upsilon_{ini}^2 + \sum_{j=1}^n k^j\big(C(\Upsilon_{space}^j)^2 + (\Upsilon_{time}^j)^2\big), \tag{6.58}$$

where

$$\begin{aligned}
\Upsilon_{ini} &:= \|u_0 - u_h(0)\| + C_0\|\sqrt{\theta\eta\mathbf{h}}[\![u_h(0)]\!]\|_{\Gamma\setminus\Gamma^{tr}}, \\
\Upsilon_{space}^j &:= \Big(\frac{k^j + k^{j+1}}{k^j}\big(\Upsilon_{S_1^c}^2(u_h^j) + \Upsilon_{S_1^d}^2(u_h^j)\big)\Big)^{1/2}, \\
\Upsilon_{time}^j &:= \Big(\frac{4}{\lambda}\|\frac{u_h^{j-1} - u_h^{j-2}}{k^{j-1}} - \frac{u_h^j - u_h^{j-1}}{k^j}\|^2 + 2|||u_h^j - u_h^{j-1}|||^2 + 2\lambda\|u_h^j - u_h^{j-1}\|^2 \\
&\qquad + \frac{4C_0}{\lambda}\|\sqrt{\theta\eta\mathbf{h}}[\![\frac{u_h^j - u_h^{j-1}}{k^j}]\!]\|_{\Gamma\setminus\Gamma^{tr}}^2 + \frac{4}{\lambda}\|f - \ell_{n-1}(t)f^{n-1} - \ell_n(t)f^n\|^2\Big)^{1/2},
\end{aligned}$$

with $C > 0$ constant depending only on the shape-regularity of the spatial mesh.

Proof. Starting from (6.56), we set $v = e^c$, and we have

$$\begin{aligned} &\frac{1}{2}\frac{d}{dt}\|e^c\|^2 + D(t; e^c, e^c) = \langle \frac{\partial e^c}{\partial t}, e^c\rangle + D(e^c, e^c) \\ &= \lambda\langle \epsilon, e^c\rangle + D(\epsilon^c, e^c) - \langle \frac{\partial u_h^d}{\partial t}, e^c\rangle + \mathcal{A}(e^c) + \mathcal{B}(e^c) + \mathcal{C}(e^c). \end{aligned} \tag{6.59}$$

The first three terms on the right-hand side of the above identity can be estimated in similar fashion to (6.45):

$$\begin{aligned} |\lambda\langle \epsilon, e^c\rangle| &\leq 2\lambda\|\epsilon\|^2 + \frac{\lambda}{8}\|e^c\|^2, \\ |\langle \frac{\partial u_h^d}{\partial t}, e^c\rangle\| &\leq 2\lambda^{-1}\|\frac{\partial u_h^d}{\partial t}\|^2 + \frac{\lambda}{8}\|e^c\|^2, \\ |D(t; \epsilon^c, e^c)| &\leq 2C|||\epsilon^c|||^2 + \frac{1}{8}|||e^c|||^2 \leq 2C|||\epsilon|||^2 + 2C|||u_h^d|||^2 + \frac{1}{8}|||e^c|||^2. \end{aligned} \tag{6.60}$$

For the remaining three terms we work as follows:

$$\begin{aligned} |\mathcal{A}(e^c)| &\leq 2\lambda^{-1}\|f - \ell_{n-1}(t)f^{n-1} - \ell_n(t)f^n\|^2 + \frac{\lambda}{8}\|e^c\|^2, \\ |\mathcal{B}(e^c)| &\leq 2\lambda^{-1}\|\frac{u_h^{n-1} - u_h^{n-2}}{k^{n-1}} - \frac{u_h^n - u_h^{n-1}}{k^n}\|^2 + \frac{\lambda}{8}\|e^c\|^2, \end{aligned}$$

and

$$\begin{aligned} |\mathcal{C}(e^c)| &\leq |\ell_{n-1}(t)\mathcal{M}(w^{n-1}, e^c) + \ell_n(t)\mathcal{M}(w^n, e^c) - \mathcal{M}(u_h, e^c)| \\ &\quad + |\mathcal{M}(u_h, e^c) - \mathcal{M}(u, e^c)| \\ &\leq \ell_{n-1}(t)|\mathcal{M}(w^{n-1}, e^c) - \mathcal{M}(u_h, e^c)| + \ell_n(t)|\mathcal{M}(w^n, e^c) - \mathcal{M}(u_h, e^c)| \\ &\quad + |\mathcal{M}(u_h, e^c) - \mathcal{M}(u, e^c)|, \end{aligned}$$

since $\ell_{n-1} + \ell_n = 1$ and $0 \leq \ell_{n-1}, \ell_n \leq 1$. Working now as in (6.44), and recalling that $\lambda > 16C_{\tilde{p}}^2 C_{trace}^2$, we have

$$\begin{aligned} |\mathcal{M}(w^m, e^c) - \mathcal{M}(u_h, e^c)| &\leq C_{\tilde{p}}\sum_{j=1}^{2}\left(\|(w^m - u_h)|_{\Omega_j}\|_{\Gamma^{tr}}^2 + \|e^c|_{\Omega_j}\|_{\Gamma^{tr}}^2\right) \\ &\leq \frac{1}{4}|||w^m - u_h|||^2 + \frac{\lambda}{4}\|w^m - u_h\|^2 + \frac{1}{4}|||e^c|||^2 + \frac{\lambda}{4}\|e^c\|^2, \end{aligned}$$

for $m = n-1, n$, and

$$\begin{aligned}|\mathcal{M}(u_h, e^c) - \mathcal{M}(u, e^c)| &\leq C_{\tilde{p}} \sum_{j=1}^{2} \left(\|e|_{\Omega_j}\|^2_{\Gamma^{tr}} + \|e^c|_{\Omega_j}\|^2_{\Gamma^{tr}} \right) \\ &\leq 2C_{\tilde{p}} \sum_{j=1}^{2} \left(\|e^c|_{\Omega_j}\|^2_{\Gamma^{tr}} + \|u_h^d|_{\Omega_j}\|^2_{\Gamma^{tr}} \right) \\ &\leq \frac{1}{2}|||u_h^d|||^2 + \frac{\lambda}{2}\|u_h^d\|^2 + \frac{1}{2}|||e^c|||^2 + \frac{\lambda}{2}\|e^c\|^2,\end{aligned}$$

Noting the identity $\frac{1}{2}\frac{d}{dt}\|e^c\|^2 + |||e^c|||^2 = \frac{1}{2}\frac{d}{dt}\|e^c\|^2 + D(t; e^c, e^c)$, integrating the time variable between 0 and t, and combining the above estimates we arrive at

$$\|e^c(t)\|^2 + \frac{1}{4}\int_0^t |||e^c|||^2 ds \leq \frac{5\lambda}{2}\int_0^t \|e^c\|^2 ds + \mathcal{R}_{fd}(t), \tag{6.61}$$

with

$$\begin{aligned}\mathcal{R}_{fd}(t) := \|e^c(0)\|^2 + \int_0^t \Big(&4\lambda\|\epsilon\|^2 + 4C|||\epsilon|||^2 + 4C|||u_h^d|||^2 + \lambda\|u_h^d\|^2 + \frac{4}{\lambda}\|\frac{\partial u_h^d}{\partial t}\|^2 \\ &+ \frac{4}{\lambda}\|\frac{u_h^{n-1} - u_h^{n-2}}{k^{n-1}} - \frac{u_h^n - u_h^{n-1}}{k^n}\|^2 + \frac{4}{\lambda}\|f - \ell_{n-1}(t)f^{n-1} - \ell_n(t)f^n\|^2 \\ &+ \frac{1}{2}\sum_{i=0,1}\Big(|||w^{n-i} - u_h|||^2 + \lambda\|w^{n-i} - u_h\|^2 \Big)\Big) ds.\end{aligned}$$

Using Gronwall inequality (2.4), we deduce, therefore,

$$\|e^c(t)\|^2 + \frac{1}{4}\int_0^t |||e^c|||^2 ds \leq \mathrm{e}^{5\lambda t/2}\mathcal{R}_{fd}(t), \tag{6.62}$$

as before. Working in identical fashion to the semidiscrete case above, we arrive at

$$\|e\|_*^2 \leq 4\mathrm{e}^{5\lambda T/2}\mathcal{R}_{fd}(T) + 2\|u_h^d\|_*^2.$$

Now, setting for brevity $\epsilon^n := \epsilon(t_n)$, $n = 0, 1, \ldots, N$, straightforward calculations reveal the bounds

$$\sum_{i=0,1}\left(|||\epsilon|||^2 + \lambda\|\epsilon\|^2 \right) \leq 2\sum_{i=0,1}\left(|||\epsilon^{n-i}|||^2 + \lambda\|\epsilon^{n-i}\|^2 \right),$$

and

$$\sum_{i=0,1} \left(|||w^{n-i} - u_h|||^2 + \lambda \|w^{n-i} - u_h\|^2 \right) \leq 2 \sum_{i=0,1} \left(|||\epsilon^{n-i}|||^2 + \lambda \|\epsilon^{n-i}\|^2 \right) + 2|||u_h^n - u_h^{n-1}|||^2 + 2\lambda \|u_h^n - u_h^{n-1}\|^2,$$

noting the trivial bound $\ell_{n-1}^2(t) + \ell_n^2(t) \leq 1$. The a posteriori bound now follows by combining the last three estimates, along with Lemmas 6.2, 3.14 and 4.2. □

Remark 6.11. We note that the maximum with respect to t in the $L_\infty(L_2)$-norm can only be attained at one of the time nodes t_n, since it is a linear interpolant with respect to t.

6.4.1 $L_\infty(L_2)$-norm a posteriori bound

The proof of the $L_\infty(L_2)$-norm a posteriori bound for the fully discrete scheme will be split in a number of intermediate results for accessibility.

Lemma 6.12. *For λ as above, we have the bound*

$$\begin{aligned} \frac{d}{dt}\|\rho\|^2 \leq \frac{11\lambda}{8}\|\rho\|^2 + 4\lambda\|\epsilon\|^2 + \frac{16}{\lambda}\|\frac{\partial \epsilon}{\partial t}\|^2 \\ + 4\lambda^{-1}\|f - \ell_{n-1}(t) f^{n-1} - \ell_n(t) f^n\|^2 \\ + 4\lambda^{-1}\|\frac{u_h^{n-1} - u_h^{n-2}}{k^{n-1}} - \frac{u_h^n - u_h^{n-1}}{k^n}\|^2 \\ + \frac{1}{2}|||w^n - w^{n-1}|||^2 + \frac{\lambda}{2}\|w^n - w^{n-1}\|^2. \end{aligned} \tag{6.63}$$

Proof. Setting $v = \rho$ in (6.56), we have

$$\langle \frac{\partial \rho}{\partial t}, \rho \rangle + D(\rho, \rho) = \lambda \langle \epsilon, \rho \rangle + \langle \frac{\partial \epsilon}{\partial t}, \rho \rangle + \mathcal{A}(\rho) + \mathcal{B}(\rho) + \mathcal{C}(\rho). \tag{6.64}$$

Working as before, (6.64) gives

$$\begin{aligned} &\frac{1}{2}\frac{d}{dt}\|\rho\|^2 + |||\rho|||^2 \\ &\leq 4\lambda\|\epsilon\|^2 + \frac{\lambda}{16}\|\rho\|^2 + \frac{2}{\lambda}\|\frac{\partial \epsilon}{\partial t}\|^2 + \frac{\lambda}{8}\|\rho\|^2 \\ &\quad + 2\lambda^{-1}\|f - \ell_{n-1}(t) f^{n-1} - \ell_n(t) f^n\|^2 + \frac{\lambda}{8}\|\rho\|^2 \\ &\quad + 2\lambda^{-1}\|\frac{u_h^{n-1} - u_h^{n-2}}{k^{n-1}} - \frac{u_h^n - u_h^{n-1}}{k^n}\|^2 + \frac{\lambda}{8}\|\rho\|^2 + |\mathcal{C}(\rho)|. \end{aligned} \tag{6.65}$$

To estimate $|\mathcal{C}(\rho)|$ we work as follows:

$$\begin{aligned}|\mathcal{C}(\rho)| &\leq |\ell_{n-1}(t)\mathcal{M}(w^{n-1},\rho)+\ell_n(t)\mathcal{M}(w^n,\rho)-\mathcal{M}(w,\rho)|\\ &\quad+|\mathcal{M}(w,\rho)-\mathcal{M}(u,\rho)|\\ &\leq \ell_{n-1}(t)|\mathcal{M}(w^{n-1},\rho)-\mathcal{M}(w,\rho)|+\ell_n(t)|\mathcal{M}(w^n,\rho)-\mathcal{M}(w,\rho)|\\ &\quad+|\mathcal{M}(w,\rho)-\mathcal{M}(u,\rho)|,\end{aligned}$$

since $\ell_{n-1}(t)+\ell_n(t)=1$ for $t\in(t_{n-1},t_n]$. Working now as above, and recalling that $\lambda>16C_{\tilde{p}}^2C_{trace}^2$, we have

$$\begin{aligned}|\mathcal{M}(w^m,\rho)-\mathcal{M}(w,\rho)| &\leq C_{\tilde{p}}\sum_{j=1}^{2}\left(\|(w^m-w)|_{\Omega_j}\|_{\Gamma^{tr}}^2+\|\rho|_{\Omega_j}\|_{\Gamma^{tr}}^2\right)\\ &\leq C_{\tilde{p}}\sum_{j=1}^{2}\left(\|(w^n-w^{n-1})|_{\Omega_j}\|_{\Gamma^{tr}}^2+\|\rho|_{\Omega_j}\|_{\Gamma^{tr}}^2\right)\\ &\leq \frac{1}{4}|||w^n-w^{n-1}|||^2+\frac{\lambda}{4}\|w^n-w^{n-1}\|^2+\frac{1}{4}|||\rho|||^2+\frac{\lambda}{4}\|\rho\|^2,\end{aligned}$$

for $m=n-1,n$, noting that $w^m-w=\ell_m(w^n-w^{n-1})$. Also,

$$|\mathcal{M}(w,\rho)-\mathcal{M}(u,\rho)|\leq 2C_{\tilde{p}}\sum_{j=1}^{2}\|\rho|_{\Omega_j}\|_{\Gamma^{tr}}^2\leq\frac{1}{2}|||\rho|||^2+\frac{\lambda}{2}\|\rho\|^2.$$

Combining the last three estimates, we arrive at

$$|\mathcal{C}(\rho)|\leq\frac{1}{4}|||w^n-w^{n-1}|||^2+\frac{\lambda}{4}\|w^n-w^{n-1}\|^2+\frac{3}{4}|||\rho|||^2+\frac{3\lambda}{4}\|\rho\|^2.$$

The result now follows by using the last estimate on (6.65). □

Since the terms involving ρ will be treated as above, we turn our attention to the terms involving the difference w^n-w^{n-1}, which as it stands is not computable.

Lemma 6.13. *With $\lambda>0$ as above, we have*

$$\begin{aligned}&\frac{1}{4}|||w^n-w^{n-1}|||^2+\frac{\lambda}{4}\|w^n-w^{n-1}\|^2\\ &\leq 4\lambda^{-1}\|f^n-f^{n-1}\|^2+4\lambda^{-1}\|\frac{u_h^{n-1}-u_h^{n-2}}{k^{n-1}}-\frac{u_h^n-u_h^{n-1}}{k^n}\|^2.\end{aligned}$$

Proof. By definition of the elliptic reconstruction, we have

$$\begin{aligned}&D(w^n-w^{n-1},v)+\lambda\langle w^n-w^{n-1},v\rangle+\mathcal{M}(w^n,v)-\mathcal{M}(w^{n-1},v)\\ &=\langle g^n-g^{n-1},v\rangle,\end{aligned}$$

which, upon setting $v = w^n - w^{n-1}$ and working as before leads to

$$\begin{aligned}&|||w^n - w^{n-1}|||^2 + \lambda\|w^n - w^{n-1}\|^2 - \frac{1}{4}|||w^n - w^{n-1}|||^2 - \frac{\lambda}{4}\|w^n - w^{n-1}\|^2\\ &\leq \frac{1}{\lambda}\|g^n - g^{n-1}\|^2 + \frac{\lambda}{4}\|w^n - w^{n-1}\|^2,\end{aligned}$$

from which the result already follows by replacing the g^m's with their equals. □

We are now ready to state and prove the following a posteriori bound.

Theorem 6.14 ($L_\infty(L_2)$-norm estimate)**.** *For every $n = 1, \ldots, N$, and $\lambda > 0$ as defined above, we have*

$$\|e\|^2_{L_\infty(0,t_n;L_2(\Omega))} \leq 2\mathrm{e}^{11\lambda t_n/8}\Upsilon^n_{fd,L_2} + 4\max_{1\leq j\leq n}\Upsilon^2_{S_1^{L_2}}(s,u_h^j), \tag{6.66}$$

with

$$\Upsilon^n_{fd,L_2} := \Upsilon^2_{ini,L_2} + \sum_{j=1}^{n} k^j\big(C(\Upsilon^j_{space,L_2})^2 + (\Upsilon^j_{time,L_2})^2\big), \tag{6.67}$$

where

$$\begin{aligned}\Upsilon_{ini,L_2} &:= \|u_0 - u_h^0\| + \Upsilon_{S_1^{L_2}}(s,u_h^0),\\ \Upsilon^j_{space,L_2} &:= \Big(4\lambda\frac{k^j + k^{j+1}}{k^j}\Upsilon^2_{S_1^{L_2}}(s,u_h^j) + \frac{16}{\lambda}\hat{\Upsilon}^2_{S_2^{L_2}}(s,\frac{\partial u_h}{\partial t}|_{t_j^-})\Big)^{1/2},\\ \Upsilon^j_{time,L_2} &:= \Big(\frac{8}{\lambda}\|\frac{u_h^{j-1} - u_h^{j-2}}{k^{j-1}} - \frac{u_h^j - u_h^{j-1}}{k^j}\|^2\\ &\qquad + \frac{4}{\lambda}\Big(\|f - \ell_{j-1}(t)f^{j-1} - \ell_j(t)f^j\|^2 + \|f^j - f^{j-1}\|^2\Big)\Big)^{1/2},\end{aligned}$$

with $C > 0$ constant depending only on the shape-regularity of the spatial mesh and $\hat{\Upsilon}_{S_2^{L_2}}$ signifying the $\Upsilon_{S_2^{L_2}}$ of Lemma 6.5 taken on the union mesh *$\hat{\mathcal{T}}^n := \mathcal{T}^{n-1} \cup \mathcal{T}^n$, i.e., the coarsest common refinement of $\mathcal{T}^{n-1}$ and $\mathcal{T}^n$.*

Proof. From Lemmas 6.12 and 6.13, we have, upon integration in the time variable:

$$\|\rho(t_n)\|^2 \leq \frac{11\lambda}{8}\int_0^{t_n}\|\rho\|^2 dt + \mathcal{R}_{fd,L_2}(t_n), \tag{6.68}$$

with

$$\begin{aligned}\mathcal{R}_{fd,L_2}(t_n) :=& \|\rho(0)\|^2 + \int_0^{t_n}\Big(4\lambda\|\epsilon\|^2 + \frac{16}{\lambda}\|\frac{\partial\epsilon}{\partial t}\|^2 + \frac{8}{\lambda}\|\frac{u_h^{n-1} - u_h^{n-2}}{k^{n-1}} - \frac{u_h^n - u_h^{n-1}}{k^n}\|^2\\ &+ 4\lambda^{-1}\Big(\|f - \ell_{n-1}(t)f^{n-1} - \ell_n(t)f^n\|^2 + \|f^n - f^{n-1}\|^2\Big)\Big)dt.\end{aligned}$$

Gronwall's inequality (2.4), thus, implies

$$\|\rho(t_n)\|^2 \leq \mathrm{e}^{11\lambda t_n/8}\mathcal{R}_{fd,L_2}(t_n).$$

Now, setting for brevity $\epsilon^n := \epsilon(t_n)$, $n = 0, 1, \ldots, N$, straightforward calculations reveal the bounds

$$4\lambda\|\epsilon\|^2 + \frac{16}{\lambda}\|\frac{\partial\epsilon}{\partial t}\|^2 \leq 4\lambda \sum_{i=0,1} \|\epsilon^{n-i}\|^2 + \frac{16}{\lambda}\|\frac{\epsilon^n - \epsilon^{n-1}}{k^n}\|^2. \tag{6.69}$$

To further estimate the terms ϵ^{n-i}, $i = 0, 1$, we can use Lemma 6.5. For the last term on the right-hand side of (6.69), we can (essentially) also apply Lemma 6.5 by viewing the linear interpolant ϵ as a continuous function in time whose finite element solution is given by

$$\frac{u_h^n - u_h^{n-1}}{k^n} = \frac{\partial u_h}{\partial t}|_{t_n^-}.$$

Crucially, however, the application of Lemma 6.5 in this case has to take place on the *union mesh* $\hat{\mathcal{T}}^n := \mathcal{T}^{n-1} \cup \mathcal{T}^n$, i.e., the coarsest common refinement of $\mathcal{T}^{n-1}$ and $\mathcal{T}^n$.

The bound now follows by triangle inequality $\|e(t_j)\| \leq \|\rho(t_j)\| + \|\epsilon(t_j)\|$ and Lemma 6.5, noting that a maximum with respect to t can only be achieved at a time-node. □

6.5 Numerical experiments

We present a numerical experiment aiming to investigate the performance of the presented a posteriori bound from Theorem 6.14 for the backward-Euler dG method for the parabolic non-linear interface problem (2.17). To this end, we have extended the implementation of the adaptive algorithm of Metcalfe from [**?**] (see also [23] for another detailed description) based on the `deal.II` finite element library [7] to the present setting of interface problems. Here, we choose $\gamma = 5$ and polynomials of degree $p = 2$.

The adaptive algorithm from [50], starts with an initial uniform mesh in space and with a given initial time step. Starting from a uniform square mesh of 16×16 elements, the algorithm adapts the mesh to improve approximation to the initial

condition using the initial condition estimator Υ_{ini} until some tolerance **intol** is satisfied.

To adapt the timestep k^j, the algorithm bisects a time interval not satisfying a user-defined temporal tolerance $\Upsilon^j_{time} \leq \mathbf{ttol}$, and leaves a time-interval unchanged if $\Upsilon^j_{time} \leq \mathbf{ttol}$.

Once the time-step is adapted, the algorithm performs spatial mesh refinement and coarsening, determined by the space indicator Υ^j_{space} using the user-defined tolerances $\mathbf{stol}^+$ and $\mathbf{stol}^-$, corresponding to refinement and coarsening, respectively. More specifically, we select the elements with the largest local contributions which result to $\Upsilon^j_{space} > \mathbf{stol}^+$ for refinement. The spatial coarsening threshold is set to $\mathbf{stol}^- = 0.001 * \mathbf{stol}^+$; we select the elements with the smallest local contributions which result to $\Upsilon^j_{space} < \mathbf{stol}^-$ for coarsening. The algorithm iterates for each time-step. We refer to [50] for the algorithm's workflow and all implementation details.

6.5.1 Example 1.

We use the adaptive algorithm described above to approximate the solution to the problem (2.17) when $\Omega = (-1,1)^2$, subdivided into two subdomains interfacing at $x = 0$, i.e., $\Omega_1 = (-1,0) \times (-1,1)$, $\Omega_2 = (0,1) \times (-1,1)$, and $T = 1$. The non-homogeneous Dirichlet boundary conditions, the initial condition and the source term f are determined by the exact solution

$$u = \begin{cases} (4x + 4x^2)\, e^{\left(y^2-1\right)^2} cos(t) & \text{in} \quad \Omega_1 \\ (-5x^3 + 4x + 1)\, e^{\left(y^2-1\right)^2} cos(t) & \text{in} \quad \Omega_2; \end{cases}$$

this is is compatible with the linear interface condition (2.5) having permeability $C_{tr} = 4$.

Solution profiles and meshes produced by the adaptive algorithm at the final time $T = 1$ are shown in Figures 6.1 and 6.2, respectively. The meshes generated by the adaptive algorithm clearly show that the error estimator is correctly picking up the solution's features.

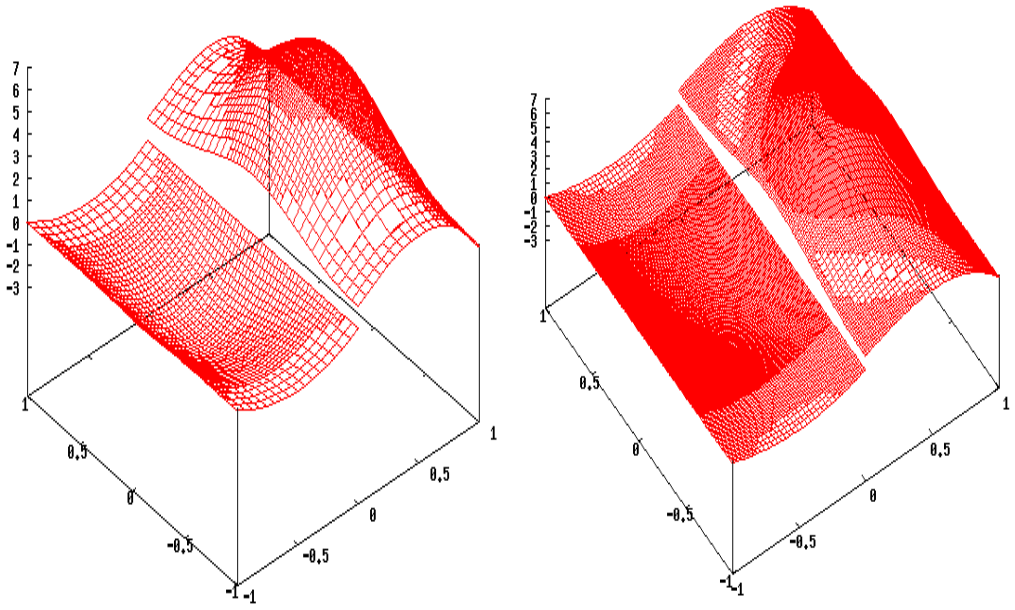

(a) (b)

FIGURE 6.1: Example 1. Final time adaptive solution profiles with $p = 2$ obtained with different values of the spatial refinement tolerance: $\mathbf{stol}^+ = 0.1$ (left) and $\mathbf{stol}^+ = 0.01$ (right).

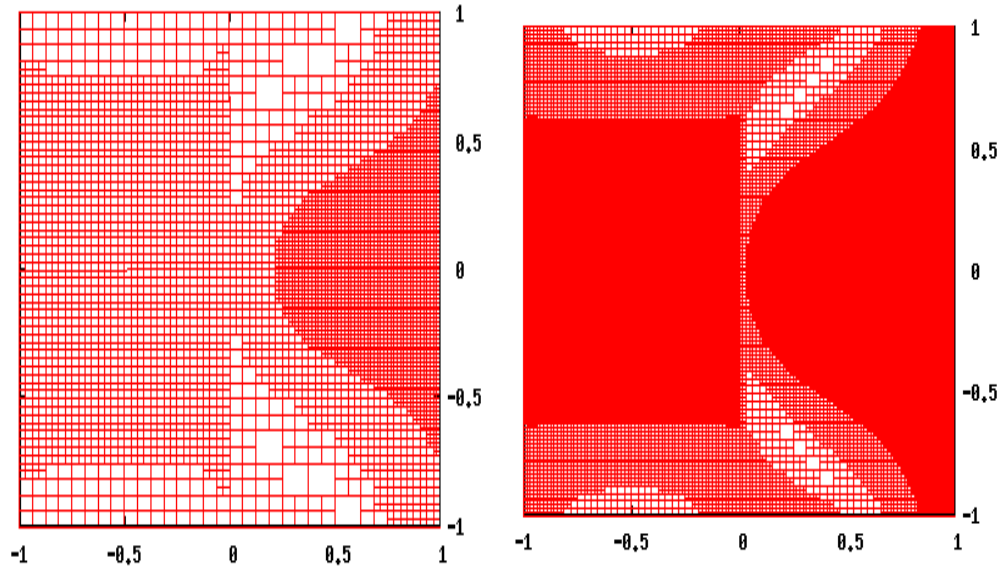

(a) (b)

FIGURE 6.2: Example 1. Meshes corresponding to the solution plots of Figure 6.1.

Chapter 7

Conclusions and Future Work

This thesis is devoted to the development and error analysis of adaptive discontinuous Galerkin methods for the numerical study of elliptic and parabolic interface problem on partition subdomains involving, possibly, curved interfaces and arising in the modelling of mass transfer of solutes through semi-permeable membranes. We presented a *fitted* interior-penalty dG method for an elliptic interface problem involving elements with extremely general curved faces to resolve interface geometry. As such, a key feature of this approach is that *physical coordinate* basis functions, as opposed to standard mapped ones from a reference element, need to be employed. The fitted nature of the discretisation permitted us to prove residual-type a posteriori error bounds for a dG energy norm in standard fashion, after extending standard approximation, inverse and conforming-nonconforming recovery estimates (in the spirit of the important work of Karakashian and Pascal [41]) from the literature. Furthermore, we investigated adaptive algorithms for elliptic interface problems with a focus on addressing some challenges to derive the necessary contraction property which leads to proof of convergence of standard adaptive procedures. Finally, we took the approach one step further to prove a posteriori error estimates for the respective non linear parabolic interface problem in the $L_\infty(L_2)$- and $(L_\infty(L_2) + L_2(H^1))$-norms. The analysis for the parabolic problems is based on the elliptic reconstruction framework of Makridakis and Nochetto [48] although, crucially, a number of challenges had to be overcome due to the non-linearity on the interface condition in the present setting.

Another aim of this work was to investigate the possibility of incorporating fitted, curved elements in adaptive finite element computations. Nonetheless, a number of important challenges remain.

First and foremost, the mesh design for curved elements is not treated in standard mesh generators. This creates a number of practical issues, such as the representation of curves at the algorithmic level and, crucially for us, the refinement of curved elements, which remains largely open. We remark that for the convergence result presented in Chapter 5 we assumed that a "good" bisection refinement strategy is available which results to refined meshes with the same geometric properties for the curved elements. It is not clear at this point how to construct refinement strategies that guarantee these required geometric properties, which are in turn needed for the a posteriori bounds to hold.

Second, it would be very interesting to extend the results from this work to the case of unfitted meshes, which are widely accepted as more practical, especially in the context of temporally moving interfaces. The geometry variational crime present in unfitted approximations of the interface poses a number of difficulties (mentioned in the Introduction) in proving rigorous a posteriori bounds for such methods.

Another interesting direction would be the extension of the analysis to higher order time-stepping methods such as Crank-Nicolson (see Akrivis, Makridakis and Nochetto [5] and the recent work of Bänsch, Karakatsani and Makridakis [8]).

Bibliography

[1] Robert A. Adams and John J. F. Fournier. *Sobolev spaces*, volume 140 of *Pure and Applied Mathematics (Amsterdam)*. Elsevier/Academic Press, Amsterdam, second edition, 2003.

[2] Slimane Adjerid, Joseph E. Flaherty, and Ivo Babuška. A posteriori error estimation for the finite element method-of-lines solution of parabolic problems. *Math. Models Methods Appl. Sci.*, 9(2):261–286, 1999.

[3] Shmuel Agmon. *Lectures on elliptic boundary value problems*, volume 369. American Mathematical Soc., 2010.

[4] Mark Ainsworth and Richard Rankin. Computable error bounds for finite element approximation on non-polygonal domains, 2012.

[5] Georgios Akrivis, Charalambos Makridakis, and Ricardo H. Nochetto. A posteriori error estimates for the Crank-Nicolson method for parabolic equations. *Math. Comp.*, 75(254):511–531, 2006.

[6] Georgios Akrivis, Charalambos Makridakis, and Ricardo H. Nochetto. Optimal order a posteriori error estimates for a class of Runge-Kutta and Galerkin methods. *Numer. Math.*, 114(1):133–160, 2009.

[7] Wolfgang Bangerth, Ralf Hartmann, and Guido Kanschat. deal. iiâĂŤa general-purpose object-oriented finite element library. *ACM Transactions on Mathematical Software (TOMS)*, 33(4):24, 2007.

[8] E. Bänsch, F. Karakatsani, and Ch. Makridakis. A posteriori error control for fully discrete Crank-Nicolson schemes. *SIAM J. Numer. Anal.*, 50(6):2845–2872, 2012.

[9] Peter Bastian and Christian Engwer. An unfitted finite element method using discontinuous Galerkin. *Internat. J. Numer. Methods Engrg.*, 79(12):1557–1576, 2009.

[10] Roland Becker, Erik Burman, and Peter Hansbo. A hierarchical NXFEM for fictitious domain simulations. *Internat. J. Numer. Methods Engrg.*, 86(4-5):549–559, 2011.

[11] Andrea Bonito and Ricardo H Nochetto. Quasi-optimal convergence rate of an adaptive discontinuous galerkin method. *SIAM Journal on Numerical Analysis*, 48(2):734–771, 2010.

[12] Susanne Brenner and Ridgway Scott. *The mathematical theory of finite element methods*, volume 15. Springer Science & Business Media, 2007.

[13] Susanne C. Brenner and L. Ridgway Scott. *The mathematical theory of finite element methods*, volume 15 of *Texts in Applied Mathematics*. Springer, New York, third edition, 2008.

[14] Erik Burman, Susanne Claus, Peter Hansbo, Mats G. Larson, and André Massing. CutFEM: discretizing geometry and partial differential equations. *Internat. J. Numer. Methods Engrg.*, 104(7):472–501, 2015.

[15] Erik Burman and Peter Hansbo. Fictitious domain finite element methods using cut elements: I. A stabilized Lagrange multiplier method. *Comput. Methods Appl. Mech. Engrg.*, 199(41-44):2680–2686, 2010.

[16] Erik Burman and Peter Hansbo. Interior-penalty-stabilized Lagrange multiplier methods for the finite-element solution of elliptic interface problems. *IMA J. Numer. Anal.*, 30(3):870–885, 2010.

[17] Francesco Calabrò and Paolo Zunino. Analysis of parabolic problems on partitioned domains with nonlinear conditions at the interface. Application to mass transfer through semi-permeable membranes. *Math. Models Methods Appl. Sci.*, 16(4):479–501, 2006.

[18] A. Cangiani, E. H. Georgoulis, and P. Houston. hp-version discontinuous galerkin methods on polygonal and polyhedral meshes. *Mathematical Models and Methods in Applied Sciences*, 24(10):2009–2041, 2014.

[19] A. Cangiani and R. Natalini. A spatial model of cellular molecular trafficking including active transport along microtubules. *J. Theoret. Biol.*, 267(4):614–625, 2010.

[20] Andrea Cangiani, Emmanuil H. Georgoulis, and Max Jensen. Discontinuous Galerkin Methods for Mass Transfer through Semipermeable Membranes. *SIAM J. Numer. Anal.*, 51(5):2911–2934, 2013.

[21] Andrea Cangiani, Emmanuil H. Georgoulis, and Max Jensen. Discontinuous Galerkin methods for fast reactive mass transfer through semi-permeable membranes. *Appl. Numer. Math.*, 104:3–14, 2016.

[22] Andrea Cangiani, Emmanuil H Georgoulis, and Stephen Metcalfe. An a posteriori error estimator for discontinuous galerkin methods for non-stationary convection-diffusion problems. *arXiv preprint arXiv:1211.3632*, 2012.

[23] Andrea Cangiani, Emmanuil H. Georgoulis, and Stephen Metcalfe. Adaptive discontinuous Galerkin methods for nonstationary convection-diffusion problems. *IMA J. Numer. Anal.*, 34(4):1578–1597, 2014.

[24] Carsten Carstensen, Wenbin Liu, and Ningning Yan. A posteriori error estimates for finite element approximation of parabolic p-Laplacian. *SIAM J. Numer. Anal.*, 43(6):2294–2319, 2006.

[25] J. Manuel Cascon, Christian Kreuzer, Ricardo H. Nochetto, and Kunibert G. Siebert. Quasi-optimal convergence rate for an adaptive finite element method. *SIAM J. Numer. Anal.*, 46(5):2524–2550, 2008.

[26] Alan Demlow, Omar Lakkis, and Charalambos Makridakis. A posteriori error estimates in the maximum norm for parabolic problems. *SIAM J. Numer. Anal.*, 47(3):2157–2176, 2009.

[27] W. Dörfler and M. Rumpf. An adaptive strategy for elliptic problems including a posteriori controlled boundary approximation. *Math. Comp.*, 67(224):1361–1382, 1998.

[28] Willy Dörfler. A convergent adaptive algorithm for Poisson's equation. *SIAM J. Numer. Anal.*, 33(3):1106–1124, 1996.

[29] Jim Douglas, Jr. and Todd Dupont. Galerkin methods for parabolic equations with nonlinear boundary conditions. *Numer. Math.*, 20:213–237, 1972/73.

[30] Kenneth Eriksson and Claes Johnson. Adaptive finite element methods for parabolic problems. IV. Nonlinear problems. *SIAM J. Numer. Anal.*, 32(6):1729–1749, 1995.

[31] Xiaobing Feng and Ohannes A. Karakashian. Two-level additive Schwarz methods for a discontinuous Galerkin approximation of second order elliptic problems. *SIAM J. Numer. Anal.*, 39(4):1343–1365 (electronic), 2001.

[32] Emmanuil H. Georgoulis. Inverse-type estimates on *hp*-finite element spaces and applications. *Math. Comp.*, 77(261):201–219 (electronic), 2008.

[33] Emmanuil H. Georgoulis, Omar Lakkis, and Juha M. Virtanen. A posteriori error control for discontinuous Galerkin methods for parabolic problems. *SIAM J. Numer. Anal.*, 49(2):427–458, 2011.

[34] Thirupathi Gudi. A new error analysis for discontinuous finite element methods for linear elliptic problems. *Mathematics of Computation*, 79(272):2169–2189, 2010.

[35] Grégory Guyomarc'h, Chang-Ock Lee, and Kiwan Jeon. A discontinuous Galerkin method for elliptic interface problems with application to electroporation. *Comm. Numer. Methods Engrg.*, 25(10):991–1008, 2009.

[36] Johnny Guzmán, Manuel Sásnchez-Uribe, and Markus Sarkis. On the accuracy of finite element approximations to a class of interface problems. *preprint.*

[37] Anita Hansbo and Peter Hansbo. An unfitted finite element method, based on Nitsche's method, for elliptic interface problems. *Comput. Methods Appl. Mech. Engrg.*, 191(47-48):5537–5552, 2002.

[38] Dan Henry and Daniel Bauman Henry. *Geometric theory of semilinear parabolic equations*, volume 840. Springer-Verlag New York, 1981.

[39] R. H. W. Hoppe, G. Kanschat, and T. Warburton. Convergence analysis of an adaptive interior penalty discontinuous Galerkin method. *SIAM J. Numer. Anal.*, 47(1):534–550, 2008/09.

[40] R. H. W. Hoppe and N. Sharma. Convergence analysis of an adaptive interior penalty discontinuous Galerkin method for the Helmholtz equation. *IMA J. Numer. Anal.*, 33(3):898–921, 2013.

[41] Ohannes A. Karakashian and Frederic Pascal. A posteriori error estimates for a discontinuous Galerkin approximation of second-order elliptic problems. *SIAM J. Numer. Anal.*, 41(6):2374–2399 (electronic), 2003.

[42] Ohannes A. Karakashian and Frederic Pascal. Convergence of adaptive discontinuous Galerkin approximations of second-order elliptic problems. *SIAM J. Numer. Anal.*, 45(2):641–665 (electronic), 2007.

[43] Natalia Kopteva and Torsten Linss. Maximum norm a posteriori error estimation for parabolic problems using elliptic reconstructions. *SIAM J. Numer. Anal.*, 51(3):1494–1524, 2013.

[44] Omar Lakkis and Charalambos Makridakis. Elliptic reconstruction and a posteriori error estimates for fully discrete linear parabolic problems. *Math. Comp.*, 75(256):1627–1658, 2006.

[45] Randall J Leveque and Zhilin Li. The immersed interface method for elliptic equations with discontinuous coefficients and singular sources. *SIAM Journal on Numerical Analysis*, 31(4):1019–1044, 1994.

[46] Zhilin Li. The immersed interface method using a finite element formulation. *Appl. Numer. Math.*, 27(3):253–267, 1998.

[47] Charalambos Makridakis. Space and time reconstructions in a posteriori analysis of evolution problems. In *ESAIM Proceedings. Vol. 21 (2007) [Journées d'Analyse Fonctionnelle et Numérique en l'honneur de Michel Crouzeix]*, volume 21 of *ESAIM Proc.*, pages 31–44. EDP Sci., Les Ulis, 2007.

[48] Charalambos Makridakis and Ricardo H. Nochetto. Elliptic reconstruction and a posteriori error estimates for parabolic problems. *SIAM J. Numer. Anal.*, 41(4):1585–1594, 2003.

[49] André Massing, Mats G. Larson, and Anders Logg. Efficient implementation of finite element methods on nonmatching and overlapping meshes in three dimensions. *SIAM J. Sci. Comput.*, 35(1):C23–C47, 2013.

[50] Stephen Metcalfe. Adaptive discontinuous Galerkin methods for nonlinear parabolic problems. *PHD Thesis, University of Leicester*, 2015.

[51] Peter K. Moore. A posteriori error estimation with finite element semi- and fully discrete methods for nonlinear parabolic equations in one space dimension. *SIAM J. Numer. Anal.*, 31(1):149–169, 1994.

[52] Pedro Morin, Ricardo H. Nochetto, and Kunibert G. Siebert. Data oscillation and convergence of adaptive FEM. *SIAM J. Numer. Anal.*, 38(2):466–488 (electronic), 2000.

[53] Serge Nicaise and Sarah Cochez-Dhondt. Adaptive finite element methods for elliptic problems: abstract framework and applications. *M2AN Math. Model. Numer. Anal.*, 44(3):485–508, 2010.

[54] Charles S. Peskin. The immersed boundary method. *Acta Numer.*, 11:479–517, 2002.

[55] Daniel Peterseim. Composite finite elements for elliptic interface problems. *Math. Comp.*, 83(290):2657–2674, 2014.

[56] Marco Picasso. Adaptive finite elements for a linear parabolic problem. *Comput. Methods Appl. Mech. Engrg.*, 167(3-4):223–237, 1998.

[57] Huafei Sun and David L. Darmofal. An adaptive simplex cut-cell method for high-order discontinuous Galerkin discretizations of elliptic interface problems and conjugate heat transfer problems. *J. Comput. Phys.*, 278:445–468, 2014.

[58] Vidar Thomée and Lars Wahlbin. On Galerkin methods in semilinear parabolic problems. *SIAM J. Numer. Anal.*, 12:378–389, 1975.

[59] R. Verfürth. A posteriori error estimates for finite element discretizations of the heat equation. *Calcolo*, 40(3):195–212, 2003.

[60] Rüdiger Verfürth. A posteriori error estimation and adaptive mesh-refinement techniques. *Journal of Computational and Applied Mathematics*, 50(1):67–83, 1994.

[61] Weiying Zheng and He Qi. On Friedrichs-Poincaré-type inequalities. *J. Math. Anal. Appl.*, 304(2):542–551, 2005.